UNIVERSITY OF CALIFORNIA, SAN DIEGO
SAN DIEGO STATE UNIVERSITY

Reactions of Stannylamines and Anionic Main Group Metal Halides: A Mild Route to Novel Main Group Metal-Nitrogen Compounds

A dissertation submitted in partial satisfaction of the

requirements for the degree Doctor of Philosophy in

Chemistry

by

Robert James Wilson Jr.

Committee in charge:

University of California, San Diego

Professor Seth M. Cohen
Professor Joanna McKittrick
Professor Yitzhak Tor

San Diego State University

Professor Miriam V. Bennett, Chair
Professor Carl J. Carrano
Professor Anca M. Segall

2013

The Dissertation of Robert James Wilson Jr. is approved, and it is acceptable in quality and form for publication on microfilm and electronically:

_____

_____

_____

_____

_____

_____

Chair

University of California, San Diego

San Diego State University

2013

DEDICATION

This dissertation is dedicated to the memory of my late father and grandfather

Robert J. Wilson Sr. and DeWitt C. Wilson

who inspired me and still inspire me to know and achieve more

and to my young nephews

Charles R. Ellison and Silas H. Johnston

for whom I wish to leave the world a better place than I found it

TABLE OF CONTENTS

LIST OF TABLES

LIST OF FIGURES

LIST OF SCHEMES

ACKNOWLEDGEMENTS

First and foremost I need to thank my advisor, Miriam Bennett, for guiding me on my journey through graduate school. I was the first to join the lab and have had the unique experience of watching it grow from being just myself and Miriam, to being a functional and mature research group. Most of all I appreciate that she has always held me and my work to high standards, not letting me slip when grad school or life was wearing me down. I also want to thank Laurence Beauvais, who allowed me to raid his lab, pick his brain, and TA in his classes for many years.

I truly believe that the Chemistry Departments of both SDSU and UCSD have some of the best Professors that I've had the pleasure of learning from. Carl Carrano, Miriam Bennett, Yitzak Tor, Josh Figueroa, Cliff Kubiak, and many others made returning to academics after three years a joy instead of a chore.

Many of the students in this department provided me with research (or just plain emotional) support. Derek Butler let me bug him nearly constantly about X-ray issues. Jean Werle, Jason Jones, Michelle Beoris, Mike Nguyen, and Rob Gilley, are all undergrads that have passed through our group and have helped me out with chemistry and made the lab a great place to work. Savannah DeLorenzo, Nobuyuki Yamamoto, and Aaron Nash have been awesome to work with and have helped me so much over the last few months as I've gone into dissertation writing mode. All the people in this department who make life better, Caline Abadjian, Derek Brown, Madhura Rane, Hai Tran, Casey Larson, Gulin Erdogan, Melinda Pope, and so many others.

I also want to thank my patient and loving girlfriend Melissa Lokensgard for helping me keep my sanity, tolerating my stress, and making me believe that I could get it done. Also thanks to my parents, Susan and Jim Johnston, and Kandy Musselman, and my siblings, Natalie Ellison and Brady Johnston, for being so supportive through my decade plus of higher education.

Chapter 2 contains material that has been published. Wilson, Robert J.; Jones, Jason R.; Bennett, Miriam V. "Unprecedented gallium-nitrogen anions: synthesis and characterization of $[(Cl_3Ga)_3N]^{3-}$ and $[(Cl_3Ga)_2NSnMe_3]^{2-}$" *Chem. Commun.* **2013**, *49*, 5049-5051.

Chapter 3 contains material which is being prepared for submission. Wilson, R. J.; Bennett, M. V. "The Highest Nuclearity Indium-Nitrogen Compound: $[In_6(NSnMe_3)_5Cl_9]^{1-}$" *Manuscript in preparation.*

Chapter 4 contains material which is being prepared for submission. Wilson, Robert J.; Beoris, Michelle R.; Bennett, Miriam V. "Unique Gallium-Tin Nitrogen Compounds Via Dehalostannylation: Pathways to Small Molecules and Oligomers" *Manuscript in preparation.*

Chapter 5 contains material which is being prepared for submission. Yamamoto, Nobuyuki; Gilley, Robert N.; Wilson, Robert J.; Bennett, Miriam V. "Unprecedented Octanuclear Heterobimetallic-Nitrogen Compounds: Synthesis and Dehalostannylation of $[Bi_4N_4(SnMe_3)_4Cl_6]^{2-}$ to Afford $[Bi_4N_4(GaCl_3)_4]\cdot 6MeCN$" *Manuscript in preparation.*

VITA

2003-2004	Undergraduate research assistant, Advisor: Dr. Derek Gragson California Polytechnic State University, San Luis Obispo
2004	Bachelor of Science California Polytechnic State University, San Luis Obispo
2005-2007	Chemist, Frazee Paint and Wallcoverings
2007-2013	Research Assistant, Advisor: Dr. Miriam Bennett San Diego State University
2013	Doctor of Philosophy University of California, San Diego San Diego State University

Publications

Wilson, R. J.; Jones, J. R.; Bennett, M. V. "Unprecedented gallium–nitrogen anions: synthesis and characterization of $[(Cl_3Ga)_3N]^{3-}$ and $[(Cl_3Ga)_2NSnMe_3]^{2-}$" *Chem. Commun.* **2013**, *49*, 5049-5051

Presentations

Wilson, R. J.; Beoris, M. R.; Bennett, M. V. "Self assembly of group-III tin nitride clusters: The first anionic ammonia and ammonium analogs" 241st ACS National Meeting & Exposition; Anaheim, CA; March 2011

Wilson, R. J.; Beoris, M. R.; Jones, J. R.; Bennett, M. V. "Anionic Molecules Containing Gallium and Indium Bound to Nitrogen: Potential Precursors to GaN and InN Materials" Gordon Research Seminar: Inorganic Chemistry; University of New England, Biddeford, ME; June 2012

Wilson, R. J.; Bennett, M. V. "Toward a family of gallium and indium nitride containing molecules" 238th ACS National Meeting; Washington, DC; August 2009

Awards

Achievement Rewards for College Scientists (ARCS) Scholar
2008-2009, 2009-2010, 2010-2011, 2011-2012, 2012-2013

SDSU Student Research Symposium President's Award, 2011

Major Fields of Study

Major Field: Chemistry (Inorganic)

Studies in Inorganic Synthesis
Professor Miriam Bennett

ABSTRACT OF THE DISSERTATION

Reactions of Stannylamines and Anionic Main Group Metal Halides: A Mild Route to Novel Main Group Metal-Nitrogen Compounds

by

Robert James Wilson Jr.

Doctor of Philosophy in Chemistry

University of California, San Diego, 2013

San Diego State University, 2013

Professor Miriam V. Bennett, Chair

This dissertation details the syntheses and structures of novel main group metal nitrogen compounds which are accessed through reaction of stannylamines with anionic metal halides. A brief review of nitrogen compounds of the group 13 metals is presented in Chapter 1, focusing on their synthesis, structure, and application as precursors to nitride semiconductors.

Chapter 2 focuses on the synthesis of unassociated μ_3-nitrogen compounds of gallium. Reaction of $[GaCl_4]^-$ salts with $(Me_3Sn)_3N$ afforded the novel salts $(Me_4N)_2[(X_3Ga)_2NSnMe_3]$ and $(Ph_4P)_2[(X_3Ga)_2NSnMe_3]$ (X = Cl, Br). These are the first reported species containing a $Ga_2(\mu_3\text{-}N)Sn$ core and were shown to decompose at 150 °C in the solid state with the release of Me_3SnCl. Reaction of $(Me_4N)[GaCl_4]$ with

$Cl_3Ga{\cdot}N(SnMe_3)_3$ afforded $(Me_4N)_3[(Cl_3Ga)_3N]$, the first reported molecule in which nitrogen is ligated solely by gallium atoms.

Chapter 3 focuses on the synthesis and characterization of $[(ClIn)_6(NSnMe_3)_5(\mu\text{-}Cl)_3]^-$. This anion, with its In_6N_5 core, is the highest nuclearity indium–nitrogen cluster or cage compound yet characterized. Molecules with preformed indium–nitrogen bonds are of interest as low temperature precursors to indium nitride semiconductors. Metal–nitrogen clusters, which in a sense are small fragments of the bulk nitrides, could potentially act as nucleation sites in colloidal nanoparticle synthesis. Mass spectrometry and NMR data for $[(ClIn)_6(NSnMe_3)_5(\mu\text{-}Cl)_3]^-$ indicates some stability in solution while solid state reactions show decomposition at 150 °C with the release of Me_3SnCl.

Chapter 4 discusses the synthesis of μ_4-nitrogen compounds of gallium. Reaction of $[MCl_4]^-$ salts with $Cl_3M{\cdot}N(SnMe_3)_3$ afforded the anions $[(Cl_3M)_2N(SnMe_3)_2]^-$ (M = Ga, In). These molecules join the small family of μ_4-nitrides of the *p*-block metals of which only 16 examples had been previously identified. Additionally $[(Cl_3Ga)_2N(SnMe_3)_2]^-$ is the first species with a Ga_2NSn_2 core. Elimination of $[Me_3SnX_2]^-$ (X = Cl, Br) from highly concentrated reactions of $[GaCl_4]^-$ and $(Me_3Sn)_3N$ was exploited to produce the polynuclear clusters, $[(Cl_2GaNSnMe_3)_3(SnMe_2Cl)]^{2-}$ and $[Ga_3(NSnMe_3)_3(SnMe_2)MeBr_5]^-$. These clusters provide crystallographic evidence for methyl–halogen exchange in the $[GaCl_4]^-/(Me_3Sn)_3N$ system.

Finally Chapter 5 discusses the application of methods described in chapters 2-4 to the synthesis of bismuth–nitrogen clusters. Reaction of $[Bi_2Cl_9]^{3-}$ with $(Me_3Sn)_3N$ afforded the anion $[Bi_4(NSnMe_3)_4(\mu\text{-}Cl)_6]^{2-}$ which has a Bi_4N_4 cubane core structure. This molecule is only the second such Bi_4N_4 cubane, and is the first example of a bismuth–nitrogen compound in which nitrogen is bonded only to metals.

Appendix A details the structures of 7 previously unreported $[Me_3SnX_2]^-$ (X = Cl, Br) salts characterized during the course of our research. Appendix B details the syntheses of metal halide salts used as reactants in this work.

Chapter 1: Nitrogen Containing Compounds of Gallium and Indium: Synthesis, Structure, and Application

Background: Gallium and Indium Nitride Materials

Group 13 Metal Nitride Materials

For the 21st century synthetic chemist the motivation for seeking a new molecule or material lies in its potential direct or predicted downstream application. For the chemist of the early 20th century this goal was often superseded by far more fundamental questions: could elements be combined in ratios predicted from Mendeleev's periodic table (only three decades old at the turn of the century) to form stable compounds? What are the properties of these new materials? Initial synthetic exploration of gallium and indium nitride was carried out for just this purpose. In 1910 it was reported that a nitride of indium was formed from the discharge of an electric arc through a mixture of liquid nitrogen and liquid argon using indium electrodes.[1] The product was a poorly characterized unstable black powder. By the 1930's synthesis of gallium nitride (GaN) and indium nitride (InN) in sufficient quantity and purity for elemental analysis, reactivity studies (with acids, bases, and oxygen), and crystallographic characterization, had been achieved. GaN was synthesized by the reaction of the pure metal with gaseous ammonia at high temperatures (900-1000 °C) (Scheme 1.1a).[2] InN was produced from the decomposition of ammonium hexafluoroindate at 600 °C (Scheme 1.1b).[3]

$$2Ga(s) + 2NH_3(g) \xrightarrow[900\text{-}1200\ ^\circ C]{} 2GaN(s) + 3H_2(g) \quad \text{(a)}$$

$$(NH_4)_3InF_6(s) \xrightarrow[600\ ^\circ C]{} InN(s) + N_2(g) + 3F_2(g) + 6H_2(g) \quad \text{(b)}$$

Scheme 1.1. High temperature synthesis of GaN and InN.

Both compounds were found to crystalize in the hexagonal wurtzite, or zinc sulfide, structure (in wurtzite type materials cations and anions occupy tetrahedral holes with a coordination number of four).[4,5] Both materials were also found to be chemically resistant to dilute acids and bases and thermally stable up to at least 600 °C. In the following decades variations on the syntheses of these materials were explored for the purpose of providing higher quality products to improve characterization. These reactions included metal chlorides with ammonia to eliminate HCl (Scheme 1.2a),[6] gallium phosphide (GaP) with ammonia to eliminate elemental phosphorous and hydrogen gas (Scheme 1.2b),[7] and indium oxide with ammonia to eliminate water (Scheme 1.2c).[8]

$$MCl_3 + NH_3 \xrightarrow[M = Ga,\ In]{600\text{-}1000\ ^\circ C} MN + 3HCl \quad \text{(a)}$$

$$4GaP + 4NH_3 \xrightarrow[1000\ ^\circ C]{} 4GaN + P_4 + 6H_2 \quad \text{(b)}$$

$$In_2O_3 + NH_3 \xrightarrow[600\ ^\circ C]{} InN + H_2O \quad \text{(c)}$$

Scheme 1.2. Alternate early syntheses of GaN and InN.

Interest in semiconducting materials capable of visible light emission began to blossom after World War II. In the simplest sense, a semiconductor is a material in which energy input can excite electrons from a non-conducting valence state to a conducting excited state. The difference in energy between these two states is known as the "band gap". When a valence electron is excited a separation of charge carriers (electrons and holes) occurs. Recombination of these carriers may produce radiation, the wavelength of which depends on the band gap.[9] Research into these materials in the late 1950's and early 1960's lead to the first light emitting diodes (LEDs) based on gallium arsenide (GaAs).[10] It was quickly understood that emission based on electron-hole recombination in direct band gap semiconductors was efficient enough for use in LASERs. The successful fabrication of high efficiency light emitting devices incentivized the production of new materials and the revisiting of known materials to analyze their optical properties. Thus reports of experiments to determine the band gap of GaN and InN began to appear in the literature.[11,12,13,14,15]

For many years high-brightness LEDs were limited to the red–yellow region of the visible spectrum because of a lack of bright and robust blue–green emitting semiconductors.[16] This deficiency hampered the commercialization of LED based lighting. Gallium rich gallium–indium nitride alloys ($Ga_{1-x}In_xN$) possessed a desirable mix of properties, such as wide band gaps and thermal stability.[17] GaN has a reported band gap of 3.45 eV and emits light at a wavelength of 360 nm, just inside of the near ultraviolet region.[18] The band gap of InN was the subject of controversy until the early 2000s when improved film growth techniques allowed for proper characterization. The

band gap of InN is now assigned as 0.64 eV with emission of the pure material occurring at ~1900 nm (in the near infrared region).[19] In theory, LEDs constructed from $Ga_{1-x}In_xN$ semiconductor alloys could emit light across the entire visible region by varying the stoichiometric ratio of gallium to indium. In practice most $Ga_{1-x}In_xN$ devices are gallium-rich and emit between 400-530 nm due to a drop-off in quantum efficiency at higher In:Ga ratios.[19] It would be difficult to understate the importance of this material. When the first high quality $Ga_{1-x}In_xN$ device was produced in the early 1990s[20] it provided the blue-green emission necessary to complete the color space of modern LEDs (and thus make white light), leading to a technological revolution in solid state lighting (Figure 1.1a). Efficient radiative recombination coupled with high resistance to thermal and chemical degradation make modern inorganic LEDs brighter, longer lasting, and cheaper to operate than other technologies (Figure 1.1b).

(a)

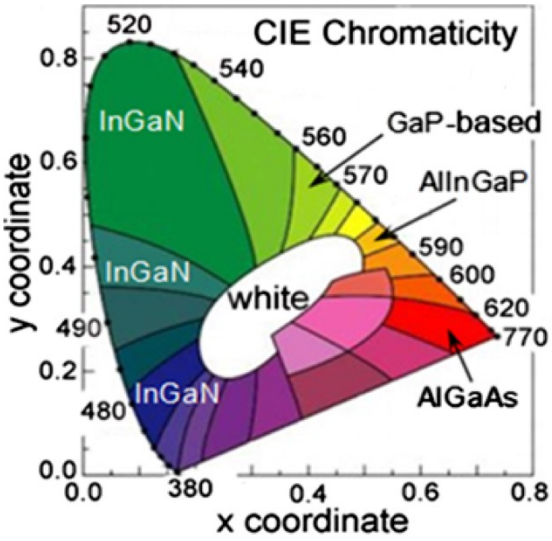

(b)

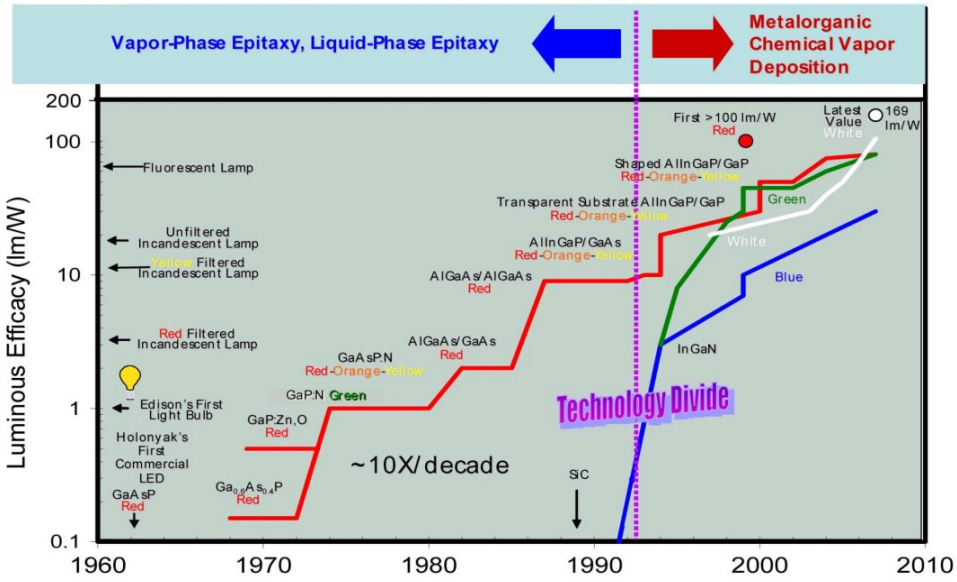

Figure 1.1. (a) The CIE chromaticity diagram showing the relative positions of modern LED materials in terms of their emission wavelength.[19] (b) The progress in brightness and color of LED's.[21]

New potential applications are emerging for GaN and InN materials with the advent of nanometer scale semiconductors. Crystalline semiconductor particles in the nanometer size regime can exhibit "quantum confinement" in which electronic properties become size dependent.[22] Size tunable absorption and emission may lead to GaInN and InN becoming important in the longer wavelengths of the visible spectrum. This in turn could lead to GaN and InN nanomaterials finding applications in photovoltaics, white LED's, and infrared photodetectors.[23] Colloidal nanoparticles may find use in low cost solution based device fabrication, such as ink-jet printing, spin coating or dip coating.[24]

The importance of GaN and InN materials has motivated significant effort in the synthesis of molecular nitrogen compounds of gallium and indium. Much of the research in this field has focused on compounds that could serve as single source precursors to GaN and InN films made by vapor deposition techniques.[25] Recent advances have yielded a wide variety of GaN and InN nanomaterial morphologies, including nanowires,[26] nanorods,[27] nanobelts,[28] and colloidal[29-31] and surface[23] quantum dots. With this in mind, the synthetic inorganic chemist continues to serve a vital role in the making of novel compounds to investigate as precursors or model intermediates to GaN and InN materials. Outlined below is a brief review of the synthesis and structure of nitrogen containing compound of gallium and indium. The remainder of this work is concerned with our efforts and achievements in the synthesis of new gallium and indium nitrogen compounds from stannylamine precursors.

Molecular Gallium and Indium Nitrogen Compounds

Classifications of *p*-Block Metal Nitrogen Compounds

Significant structural variation is observed in group 13 metal–nitrogen (M–N) compounds. For the purpose of this thesis we will define six classes of M–N compounds and will focus on those containing *p*-block M–N bonds (M = Al, Ga, In, Tl, Sn, Pb, Bi). These classifications are as follows (R = any non-metal or metalloid): **amines** result from the coordination of a Lewis basic R_3N to a Lewis acidic metal center; **amides** consist of an R_2N^- fragment bound to one or more metal atoms; **imides** are formed from the coordination of an RN^{2-} fragment by one, two, or three metal atoms; **nitrides** consist of a naked N^{3-} anion coordinated only by metal atoms; two other related types of compounds are **hydrazides**, formed from fragments containing an N–N bond (e.g. $R_2N–NR^{1-}$ or $R_2N–N^{2-}$), and **azides**, formed from N_3^- fragments. The coordination spheres of these molecule types are shown in Figure 1.2.

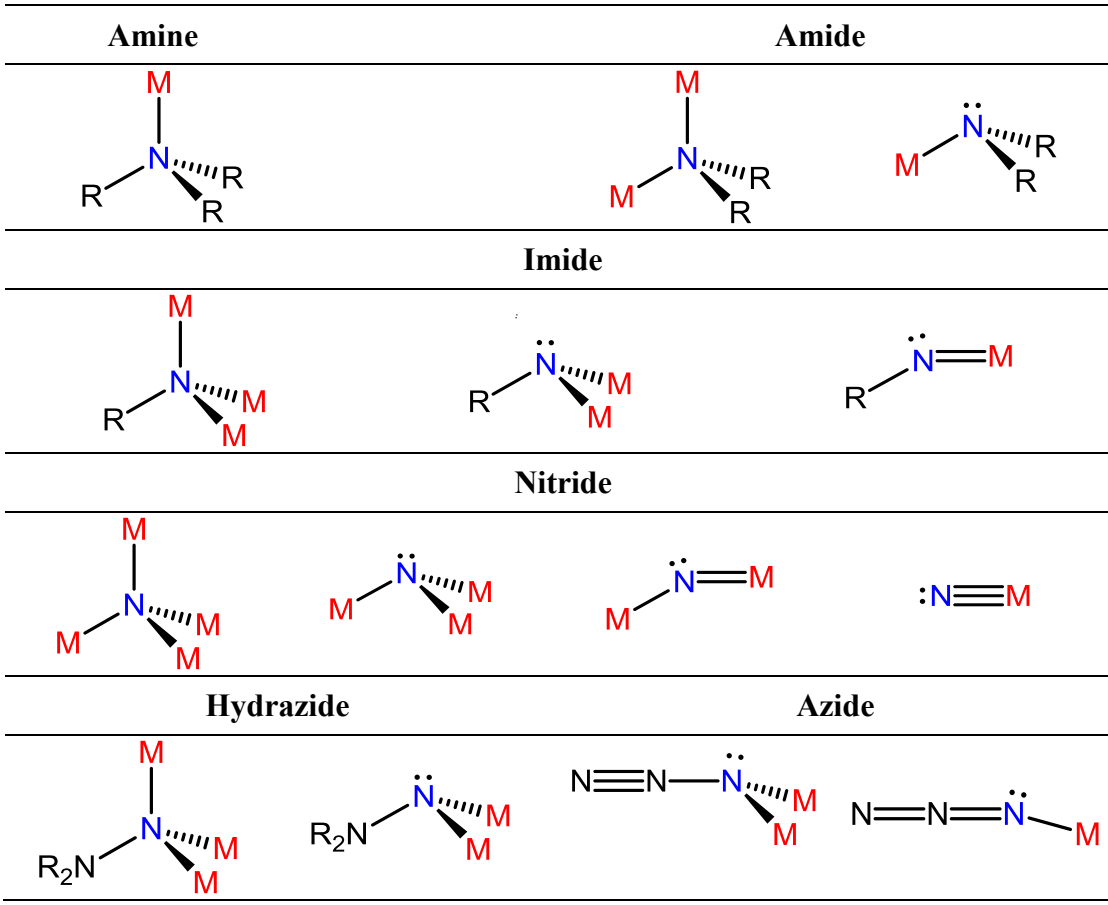

Figure 1.2. Nitrogen atom coordination spheres for different classes of metal–nitrogen (M–N) compounds, where M = any metal, and R = any non-metal or metalloid.

Bonding in Group 13 Metal Nitrogen Compounds

Neutral compounds of the group 13 elements, with their sub-octet of only six valence electrons and an unoccupied non-bonding valence orbital, are prototypical Lewis acids. Neutral compounds of nitrogen, with their occupied non-bonding valence orbital, are prototypical Lewis bases. The reactivity and structure of group 13 (Al, Ga, In) metal–nitrogen compounds are dominated by the simple Lewis acid-base interaction between nitrogen's lone pair and the unoccupied *p*-orbital on the metal. Amines will form zwitterionic Lewis adducts with neutral group 13 compounds. Group 13 metal amido and imido compounds have a tendency to oligomerize via intermolecular M–N coordination. This oligomerization leads to a variety of cluster motifs; most notably, amides tend to form dimers with an M_2N_2 rhomboid core (Figure 1.3a), and imides often form tetramers with an M_4N_4 cubane structure (Figure 1.3b). However, many decades of research have produced oligomeric structures of varying geometries containing 2-8 metal atoms. Some of the core structures that have been observed in these compounds are shown in Figure 1.4. Several monomeric amides and imides have also been synthesized. However, the use of sterically bulky ligands is generally necessary to prevent oligomerization.

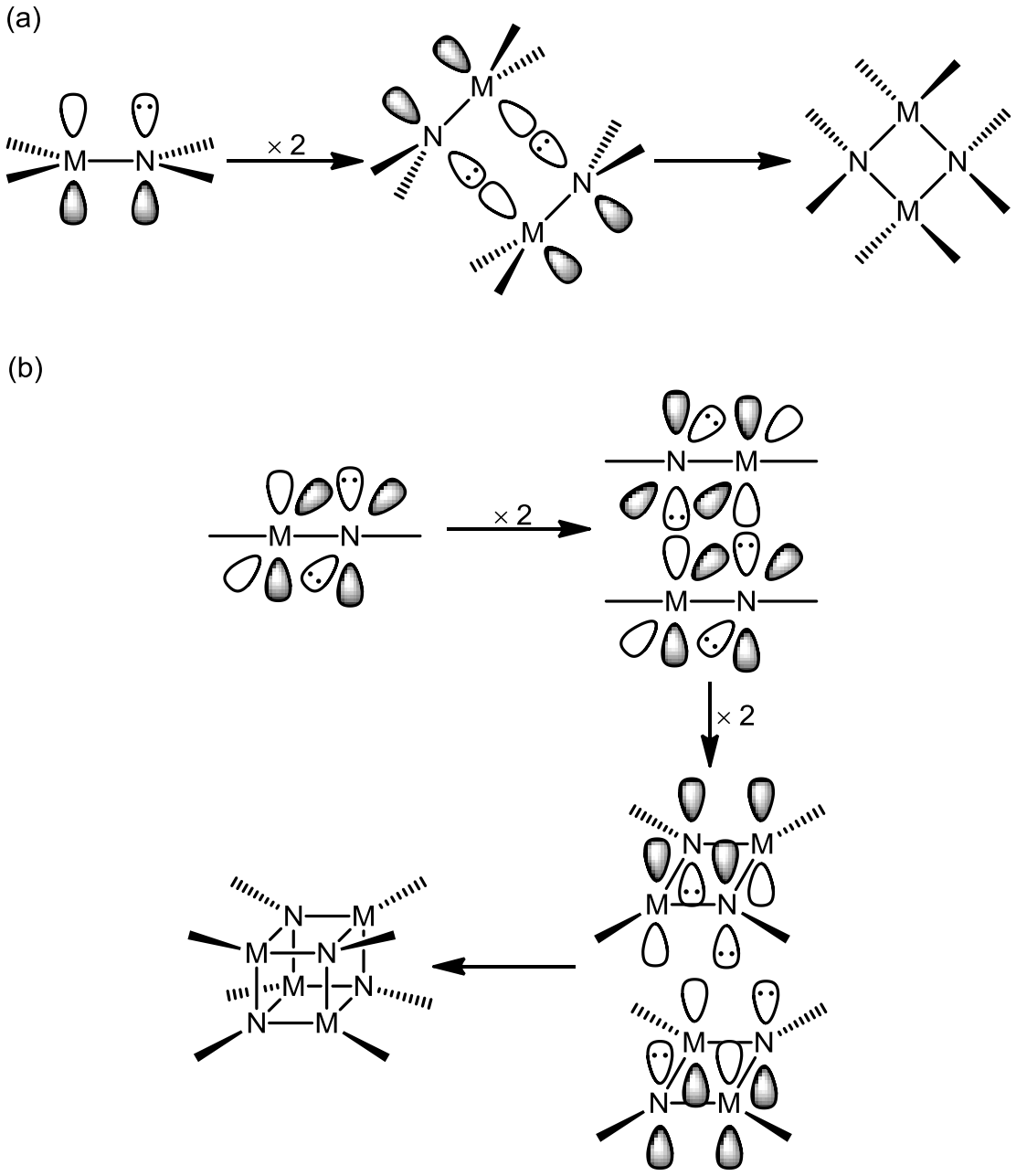

Figure 1.3. Formation of group 13 metal (a) amide dimers and (b) imide tetramers.

Dimer[a,b,c]	Trimer[a,b]	Broken Cube[c]
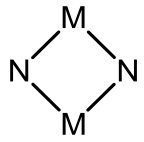	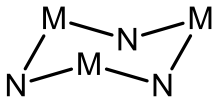	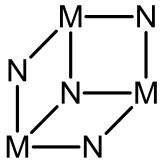
Cubane[a,b,c]	**Ladder[a,c]**	**Adamantane[a,b]**
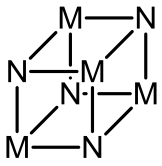	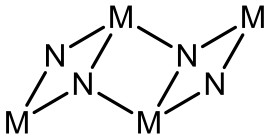	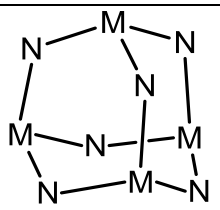
Hexagonal Prism[a,b]	**Double Adamantane[b]**	**Octamer[a,b]**
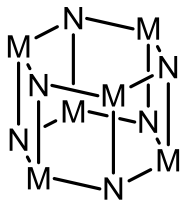	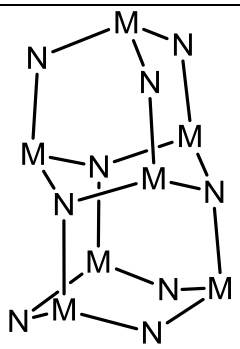	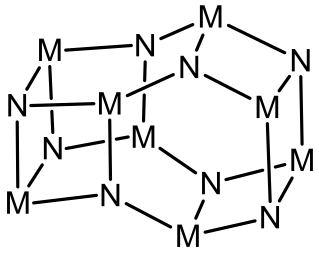

[a] M = Al. [b] M = Ga. [c] M = In

Figure 1.4. Some M–N core structures observed for group 13 metal amides and imides.

Metal Amine Adducts.

The earliest work on organometallic gallium–nitrogen (Ga–N) and indium–nitrogen (In–N) compounds focused on the properties of simple amine adducts of MR_3 (M = Ga, In; R = H, Me, Et). Trimethylgallium amine ($Me_3Ga{\cdot}NH_3$) was first isolated as a white moisture sensitive solid via a substitution reaction with trimethylgallium etherate in liquid ammonia.[32] The trimethyl and triethylamine adducts were isolated a decade later.[33] Early studies sought to use the interactions of amines with alkylated group 13 compounds in order to establish their trend as Lewis acceptors. It was established that aluminum was the strongest Lewis acid, followed by gallium and boron, then indium and thallium (B < Al > Ga > In > Tl).[34,35,36]

In these studies of amino adducts of gallium and indium it was often noted that trimethylgallium and trimethylindium adducts with dimethylamine, methylamine, or ammonia ($Me_3M{\cdot}N(H)R_2$; M = Ga, In; R = H, Me), decomposed with the concomitant elimination of methane.[34,35] It was proposed that formation of the corresponding amide dimers, $[Me_2MNR_2]_2$, was occurring (which would be later borne out by X-ray diffraction studies, *vide infra*). Kinetic studies of $Me_3Al{\cdot}NH_3$ in the gas phase suggested that decomposition occurs via a unimolecular pathway. The monomeric amides produced by this decomposition associates into dimers at equilibrium (Figure 1.5).[37] Conclusions could not be drawn about the decomposition mechanism of the Ga and In congeners (in the gas phase) due to reversible adduct formation-dissociation. Volatile adducts of group 13 metals have been studied as potential single source precursors in vapor phase syntheses of nitride semiconductors.[38,39,40]

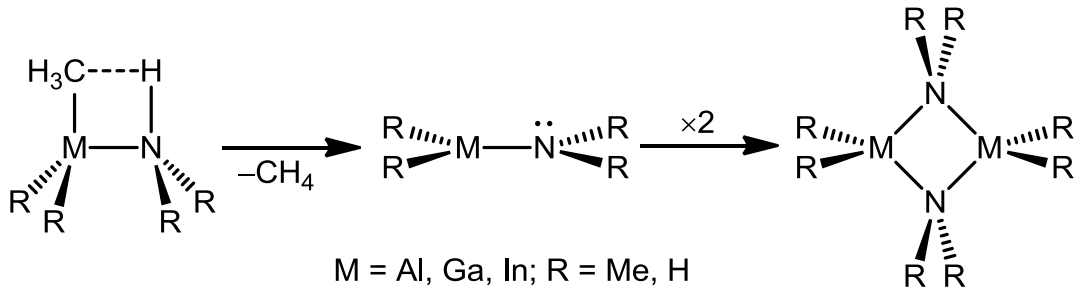

Figure 1.5. Unimolecular decomposition and dimerization of group 13 amine adducts.

Metal Amides and Imides

A variety of techniques have been employed to affect the formation of M–N bonds (M = Ga and In) over the preceding four decades. Five of these will be discussed here: alkane elimination, dehalosilylation, lithium halide salt elimination, alkylstannyl elimination, and oxidative addition. The generalized reactions are shown in Scheme 1.3a-e.

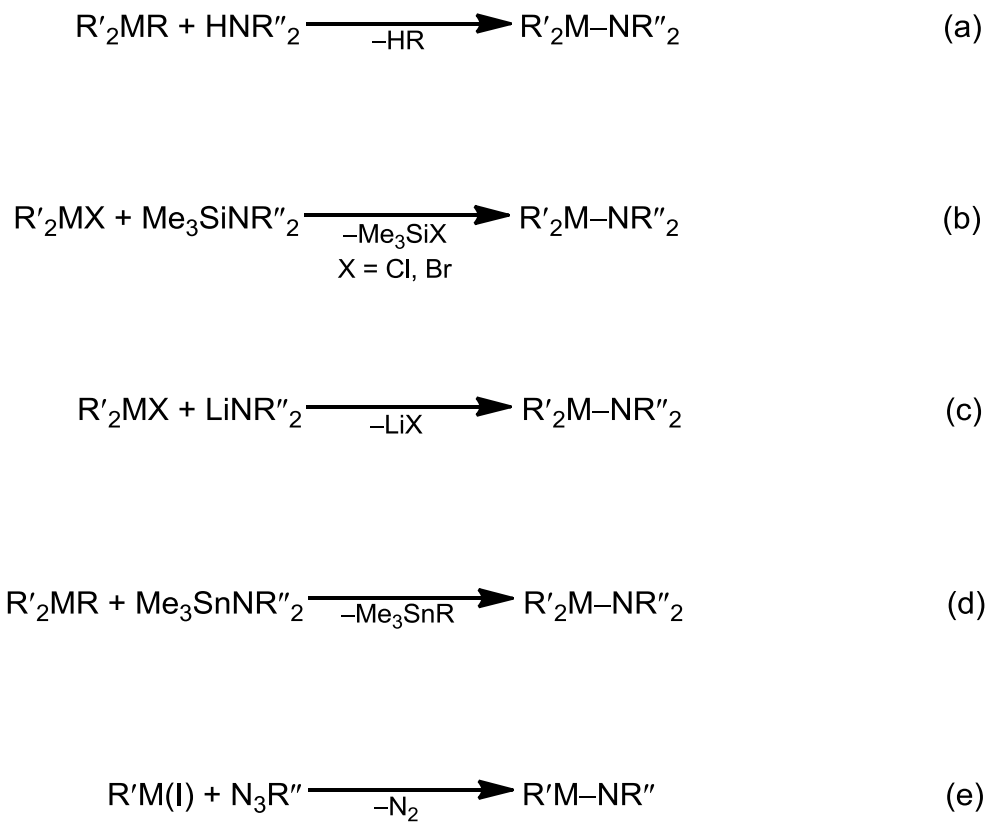

Scheme 1.3. General M–N bond formation reactions (M = Ga, In): (a) alkane elimination, (b) dehalosilylation, (c) Lithium halide salt elimination (transmetallation), (d) alkylstannyl elimination, (e) oxidative addition.

Alkane Elimination

Group 13 metal amides were first noted as the byproducts in the decomposition of alkyl metal amine adducts with the concomitant loss of a volatile alkane (*vide supra*).[34,35,41] These compounds were not structurally characterized but were postulated to be dimers based on stoichiometry (molar quantity of methane eliminated). This prediction was born out when thermolysis of the dimethylamine adduct, $Me_3In{\cdot}NMe_2H$, afforded the neutral dimer, $[Me_2InNMe_2]_2$ (Scheme 1.4a).[42] The structure consists of a planar rhomboid In_2N_2 core with near 90° angles (N–In–N 86°, In–N–In 94°).

Intermolecular thermolysis reactions have also been exploited to synthesize Ga and In amides. When N-methylaniline ($C_6H_5N(H)Me$) is reacted with MMe_3 (M = Ga, In) in a sealed tube at elevated temperatures a stoichiometric amount of methane is given off. Purification of the products by sublimation affords the dimeric amides $[Me_2MN(Me)Ph]_2$ (M = Ga, In) (Scheme 1.4b).[43] In the solid state this dimer also consists of a planar M_2N_2 rhomboid core with the phenyl rings in the trans positions and rotated perpendicular to the plane of the four member ring. In solution this dimer displayed cis-trans isomerization which varied with the polarity of the solvent. This data led the authors to suggest a stepwise formation of the dimer rather than a concerted cycloaddition reaction.

Many group 13 metal imide cage compounds have been obtained through thermolysis of amine or amide precursors with concomitant alkane elimination. Roesky reported the synthesis of tetrameric imides, $[MeMN(C_6F_5)]_4$ (M = Ga, In),

from the thermolysis of Ga and In pentafluorophenyl amide dimers at 200 °C for 1-3 hours followed by subsequent recrystallization from hexane (Scheme 1.4c).[44] The products were shown by X-ray diffraction to have a cubane type structure. High temperature decomposition of the amine adduct, $Me_3Ga{\cdot}N(Me)H_2$, resulted in formation of the octamer, $[(Me_2GaNMe)_2(MeGaNMe)_6]$ (Scheme 1.4d).[45]

Alkane elimination reactions provide a synthetic route to a wide variety of group 13 amide and imide structural types. However, these reactions often require significant heating and structural outcomes can be difficult to predict.

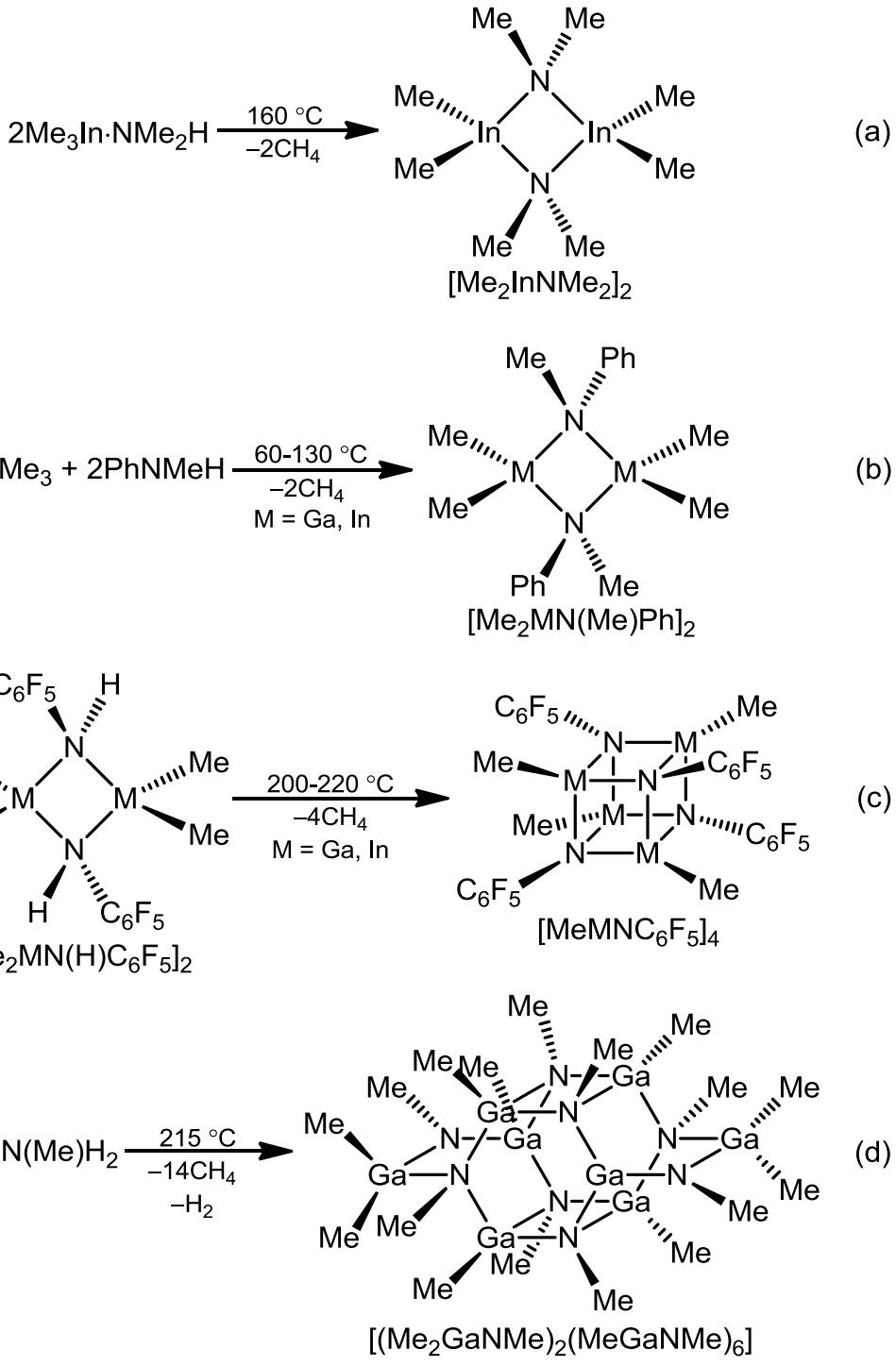

Scheme 1.4. Synthesis of gallium and indium amides (a, b) and imides (c, d) by thermolysis/alkane elimination.

Dehalosilylation

Alkane elimination reactions often require high temperature solvent-less reaction conditions. A milder solution synthesis based on dehalosilylation takes advantage of the relatively strong Si–X (X = Cl, Br) bond to drive amide formation.[46,47,48] In a typical synthesis, bis(trimethylsilyl)amine is combined with a gallium di- or tri-halide and refluxed in diethylether (Et_2O) for several hours. Removal of the solvent followed by recrystallization from Et_2O affords the trans dimeric amide (Scheme 1.5).

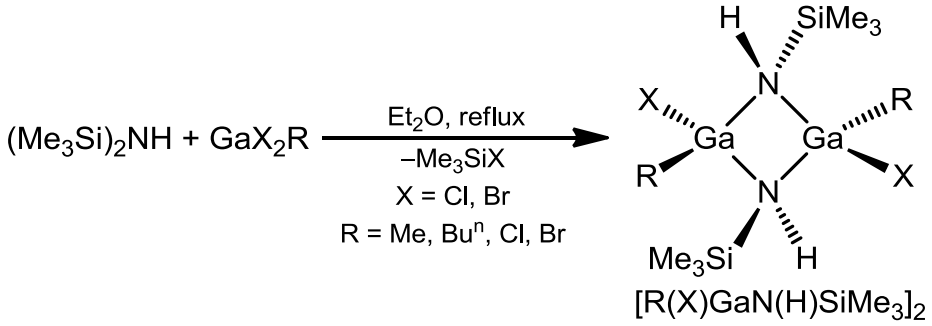

Scheme 1.5. The general synthesis of gallium amide dimers by dehalosilylation.

Interestingly, when bis(dialkylamino)dimethylsilanes are reacted with $GaCl_3$ dehalosilylation and dimer formation do not occur as expected. Instead the reaction of $GaCl_3$ with bis(dimethylamino)dimethylsilane results in adduct formation; However, reaction with bis(diethlyamino)dimethylsilane does result in non-stoichiometric dehalosilylation followed by disproportionation to afford an anionic digallium amide (Scheme 1.6).[49] Few such anionic group 13 amides were isolated prior to the present work (see chapter 4).

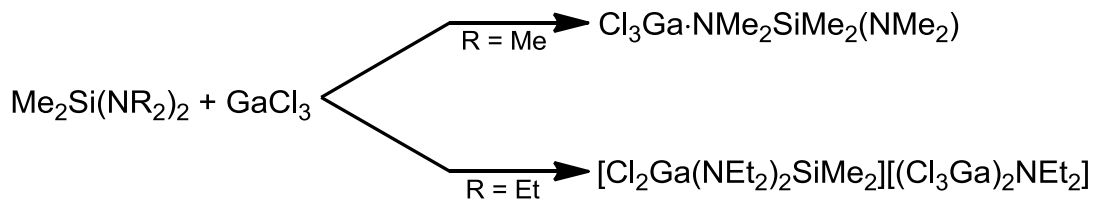

Scheme 1.6. Reaction of bis(dialkylamino)dimethylsilanes with $GaCl_3$.

Lithium Halide Salt Elimination (Transmetallation)

One of the most prolific methods used in the synthesis of group 13 metal amides and imides is alkali salt elimination (sometimes referred to metathesis or transmetallation reactions). This method involves metathesis between an amido lithium salt and a metal halide (generally chloride). Precipitation of insoluble lithium salts drives the reaction forward. Salt elimination reactions can provide high selectivity at low reaction temperatures but have the disadvantage that lithium reagents are reactive and often pyrophoric.

Many conventional dimeric monoamides have been synthesized by this method. As an example, reaction of dimethyl indium chloride and lithium dialkyl or disilyl amides in diethylether affords $[Me_2InNR_2]_2$ (R = Et, Pr^i, $SiMe_3$) (Scheme 1.7).[50] The solvent was removed *in vacuo* and the product extracted from the Li salts with pentane.

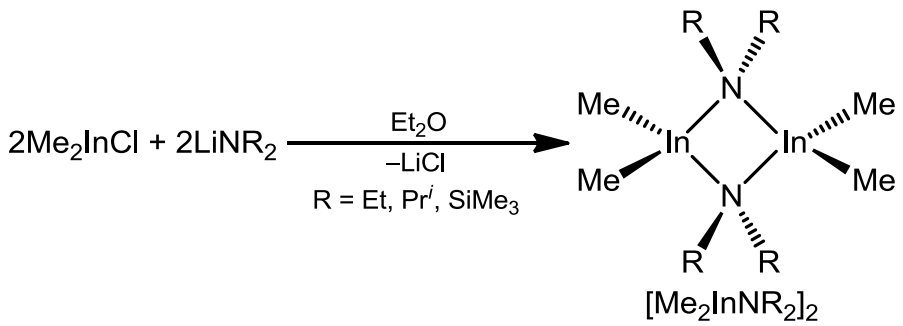

Scheme 1.7. The synthesis of a dimeric monoamide by lithium chloride elimination.

Lithium salt elimination has been the method of choice employed in the synthesis of mono-, di-, and tri-substituted monomeric amides. Bis(*tert*-butyl)gallium chloride may be reacted with lithium 1-adamantyltriphenylsilylamide to yield $(Bu^t)_2GaN(Ad)SiMe_3$ (Ad = 1-adamantyl) (Scheme 1.8a).[51] The diamide, $ArIn(N(SiMe_3)_2)_2$ (Ar = 2,4,6-$Bu^t_3C_6H_2$), is isolated from the reaction of 2,4,6-*tert*-butylphenylindium dichloride and two equivalents of lithium bis(trimethylsilyl)amide (Scheme 1.8b).[52] Lastly, the reaction of indium trichloride with three equivalents of lithium bis(cyclohexyl)amide produces the triamide, $In(NCy_2)_3$ (Cy = Cyclohexyl) (Scheme 1.8c).[53] Note that in all cases the use of considerable steric bulk was required to prevent oligomerization.

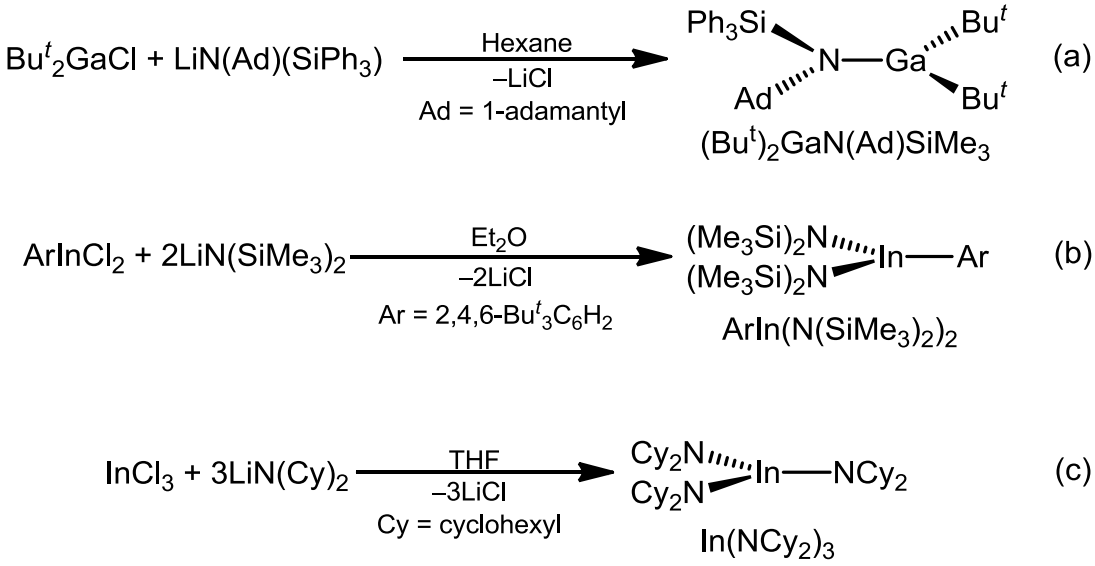

Scheme 1.8. The synthesis of Ga and In mono-, di-, and tri-amides.

This method has been employed in the synthesis of Ga and In oligomeric imides. Generally the products of these reactions are tetrameric and have a cubane structure. In one example indium trihalides were reacted with two equivalents of lithium *tert*-butylamide in THF at room temperature for 40 hours to afford the tetramers, $[XInNBu^t]_4$ (X = Cl, Br, I) (Scheme 1.9a).[54] Presumably this reaction takes place via a dimeric amide intermediate, $[X_2InN(H)Bu^t]_2$, followed by deprotonation of this dimer with an extra equivalent of $LiN(H)Bu^t$ to form the tetramer. This mechanism may be justified by a second example in which a gallium amide dimer, $[Br_2GaN(H)SiMe_3]_2$, is deprotanated with lithium methanide in diethylether to form the tetramer, $[MeGaNSiMe_3]_4$ (Scheme 1.9b).[55]

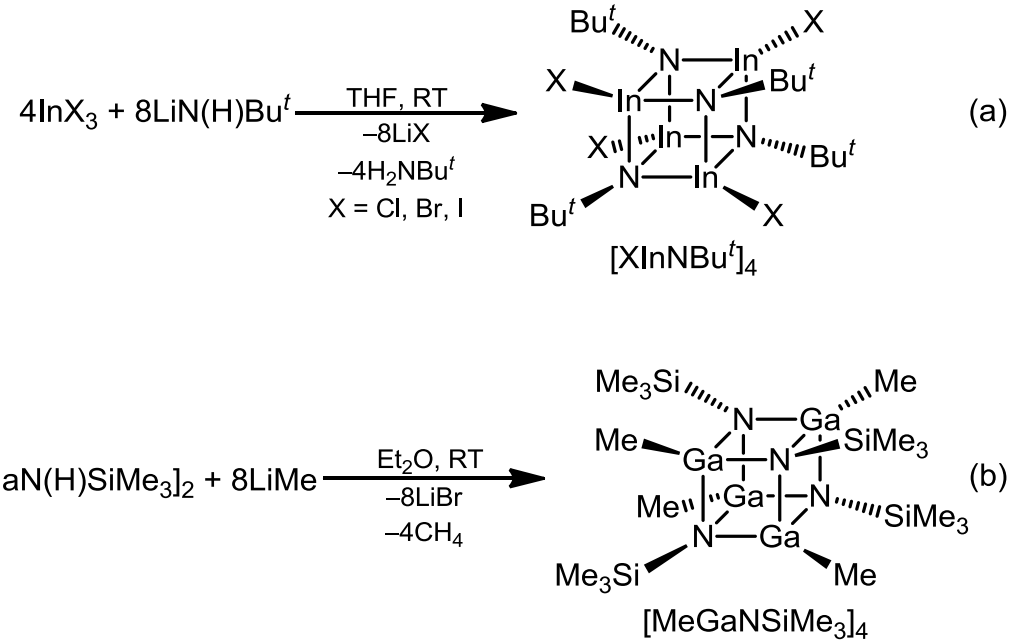

Scheme 1.9. Examples of Ga and In imide tetramers formed by alkali salt elimination reactions.

Alkylstannyl Elimination

Less common, but pertinent to the research presented here, is the synthesis of Ga and In amides via alkylstannyl elimination. These reactions entail metathesis of a metal alkyl and a stannyl-amine or amide with the concomitant elimination of $R'SnR_3$ (R, R′ = alkyl group). This reaction was observed when studying the group 13 metal adducts, $Me_3M{\cdot}N(SnMe_3)_3$ (M = Al, Ga, In).[56] When the authors reacted R_2InCl (R = Me, Et) and $(Me_3Sn)_3N$ in diethyl ether they isolated and structurally characterized the amide dimer, $[R(Cl)InN(SnMe_3)_2]_2$, instead of the expected amine adduct (Scheme 1.10a). A more deliberate study of gallium amides synthesized by this method was carried out by Nutt, et al.[57] Homoleptic trialkyl gallium compounds were reacted with

mono and bis(trimethyl)stannylamines without solvent (Scheme 1.10b). The volatile components were collected and confirmed to be the expected biproducts ($SnMe_4$ and $EtSnMe_3$) by ^1H NMR.

Thermolysis of the gallium-stannyl imide dimer, $[Me_2GaN(Bu^i)SnMe_3]_2$, in an evacuated tube at 160 °C for three hours affords the hexamer, $[MeGaNBu^i]_6$, and $SnMe_4$ (Scheme 1.10c).[58] X-ray diffraction revealed that $[MeGaNBu^i]_6$ has a hexagonal prismatic structure.

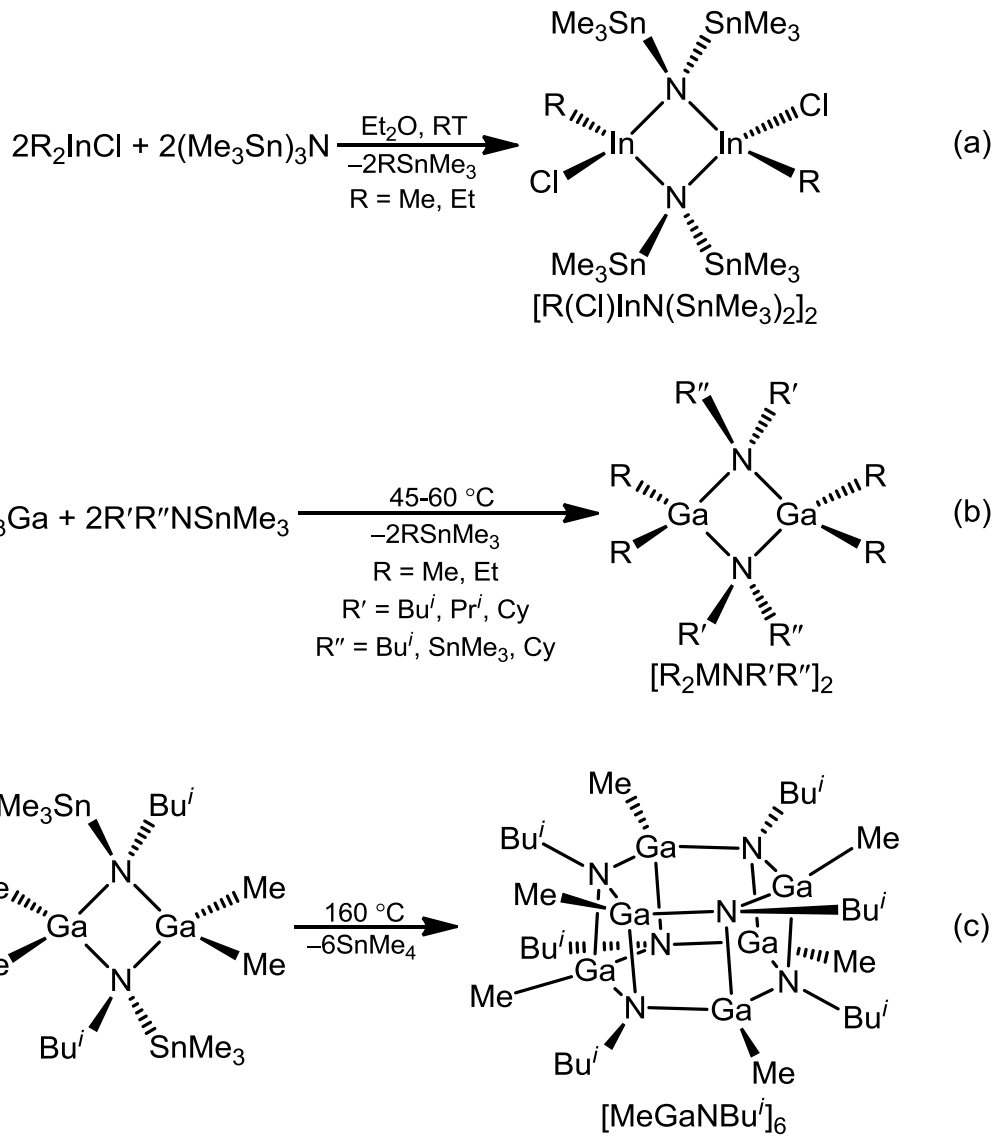

Scheme 1.10. The synthesis of Ga and In monoamide dimers via alkylstannyl elimination.

Oxidative Addition

There are two possible forms of unassociated (monomeric) Ga and In imides. The RN^{2-} fragment may form a double bond with one metal atom or sigma bonds with two metal atoms (Figure 1.6).

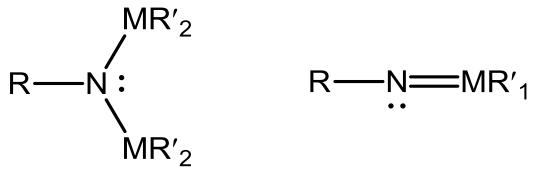

Figure 1.6. Generalized forms of unassociated (monomeric) Ga and In imides.

Significant steric bulk and low reaction temperatures are necessary to prevent oligomerization to the 4-coodinate imides. This has been achieved in both cases via oxidative addition reactions between formal Ga(I) compounds and arylazides with elimination of N_2. Power, et al, reacted terphenylazides with M(I) (M = Al, Ga) β-ketiminate monomers[59] and terphenyl M(I) dimers (M = Ga, In; shown below)[60] with arylazides to afford 2-coordinate monomeric imides (Scheme 1.11a). These molecules have formal M=N double bonds and display a bent conformation at both the metal and nitrogen centers. A 3-coordinate gallium imide dimer was isolated by Jutzi from the reaction of the half sandwich Cp*Ga(I) complex with 2,6,-dimethylphenylazide (Scheme 1.11b).[61] These low coordinate gallium and indium nitrogen compounds are of interest for comparison with computational studies of multiple bonding in heavier main group elements; however, they are of limited utility as precursors to functional materials due to the large organic groups required to stabilize them.

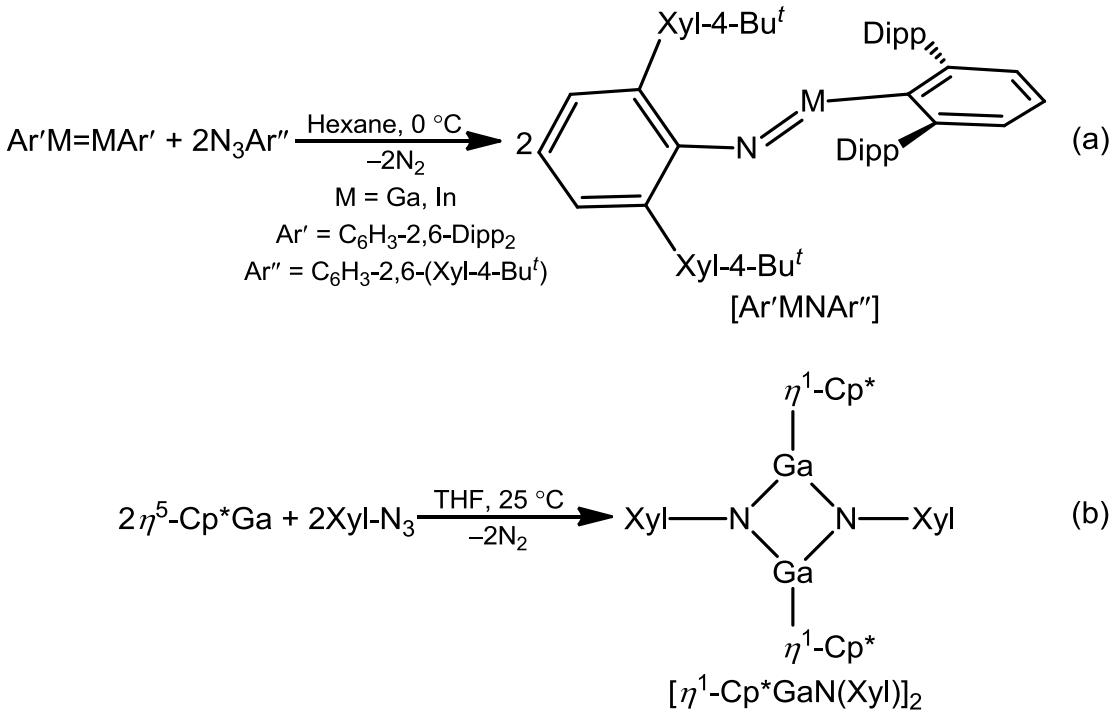

Scheme 1.11. Examples of syntheses of unassociated (monomeric) Ga and In imides.

Hydrazides and Azides of Ga and In

Close cousins of metal amides and imides are the group 13 metal hydrazides and azides. Hydrazides are derivatives of hydrazine, N_2H_4, which contains an N–N single bond. Thus metal hydrazides have varying forms, such as: $R_2N–NRM$, $R_2N–NM_2$, $MRN–NM_2$, and $M_2N–NM_2$. Like the corresponding amides and imides, group 13 hydrazides may be synthesized by alkane or salt elimination.[62] Hydrazine derivatives contain two adjacent Lewis basic nitrogen centers and thus a variety of binding modes are observed in these compounds (Figure 1.7). Thermolysis of hydrazides and hydrazine adducts has produced complex cage compounds, including one in which an $[N–N]^{4–}$ fragment is coordinated by 6 gallium atoms.[63] Gallium hydrazide cage compounds have been investigated as possible intermediates in the formation of GaN.[64]

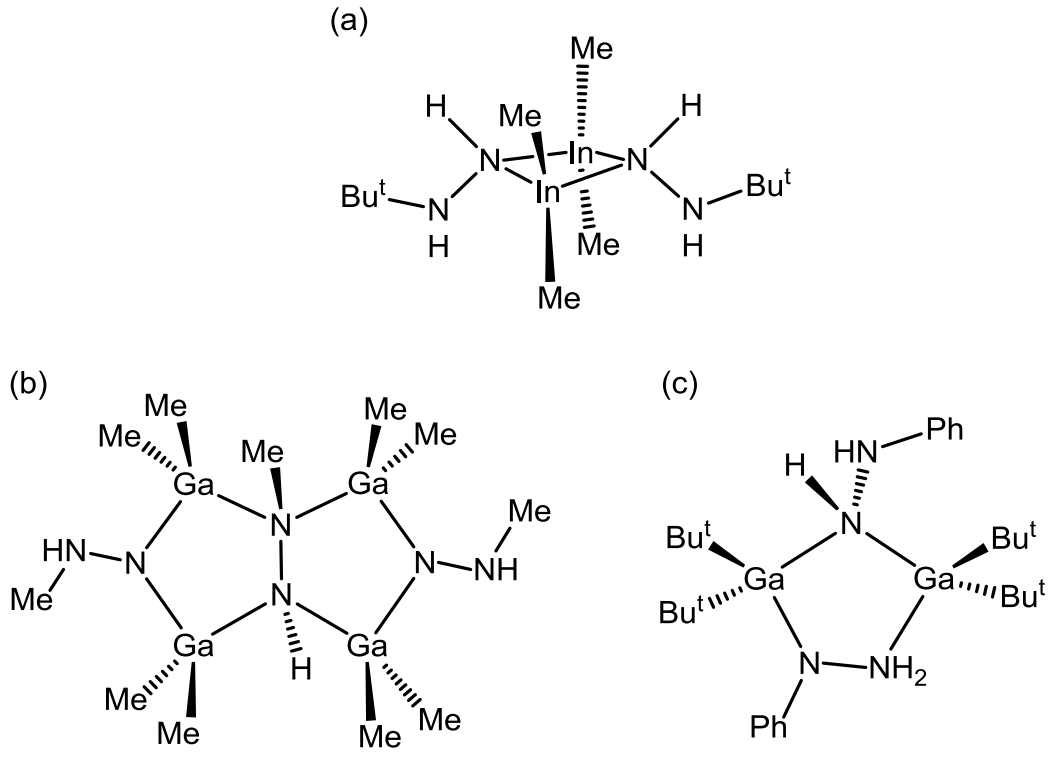

Figure 1.7. Examples of hydrazide coordination: (a) N–NM_2,[65] (b) M_2N–NM_2,[66] (c) MN–NM.[67]

Group 13 metal azides consist of an N^{3-} fragment bound to one metal atom or bridging two metal atoms through one of the terminal nitrogens. A multitude of syntheses of these compounds have been reported. Salt, alkyl, and silyl halide elimination are common.[68] Azides decompose to form N_2 gas and a nitrene intermediate. Because this pathway could lead the formation of MN from MN_3, volatile group 13 metal azides have been investigated as possible single molecule precursors to the respective nitrides in vapor deposition processes.[69]

Metal Nitrides of Gallium and Indium: The Missing Functional Group.

While the chemistry of Ga and In metal amines, amides, imides, hydrazides, and azides has been well explored, the corresponding nitrides (N^{3-} fragment coordinated only by Ga and In) are absent from the literature. There are six possible metal nitride coordination modes excluding purely geometric differences (e.g. trigonal planar versus T-shaped) (Figure 1.8).

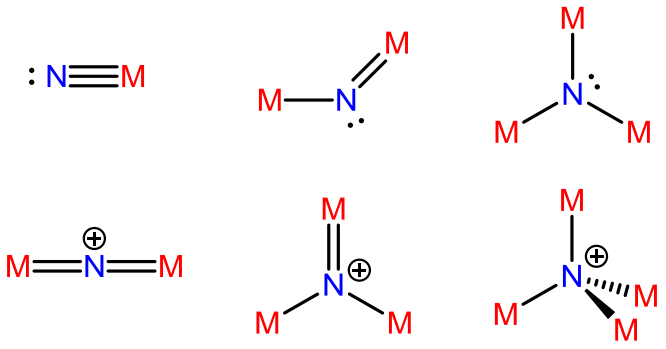

Figure 1.8. Possible coordination modes of metal nitrides.

While all of these coordination modes have been documented for transition metal nitrides only three and four coordinate single bond modes have been observed for nitrides of the *p*-block metals (Al, Ga, In, Tl, Sn, Pb, Bi). Most of these consist of monomeric[70,71,72,73] and oligomeric[74,75,76] Sn–N compounds.

Several adducts of the form $X_2RM{\cdot}N(SnMe_3)_3$ (M = Al, Ga, In; X = Me, Cl, Br; R = Me, Cl, Br) have been characterized.[56,77] These compounds are synthesized by the simple mixing of Et_2O solutions of MX_2R and $(Me_3Sn)_3N$. The pyrolysis of these products was investigated (*vide infra*). Their precursor chemistry is of interest because

the volatile byproducts of pyrolysis ($SnMe_4$ and Me_3SnX) may be removed *in vacuo* leaving only MN.[78]

The only group 13 metal nitride yet characterized (prior to the current work) is an aluminum nitride dimer with an Al–NAl_2N–Al planar rhomboid core.[79] It was synthesized via an oxidative addition reaction between $[Cp^*Al]_4$ and trimethylsilylazide (Scheme 1.12). The steric bulk of the substituents prevents further dimerization to a cubane structure with an $Al_4(N–Al)_4$ core.

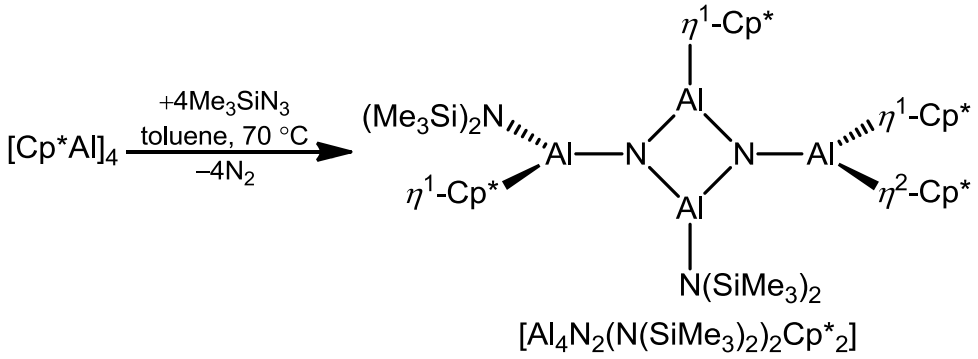

Scheme 1.12. The synthesis of an aluminum nitride dimer.

Molecular nitrides such as the example shown in Scheme 1.12 are of interest as possible intermediates in the formation of MN materials. Chapter 2 details our success in accessing a molecular nitride of Ga using $Cl_3Ga{\cdot}N(SnMe_3)_3$ as a nitrogen source.

Single Source Precursors to GaN and InN

Traditional methods of GaN and InN film growth by metal-organic chemical vapor deposition (MOCVD) involved reaction of MMe_3 (M = Ga, In) with NH_3. Activation of the ammonia N–H bond requires temperatures in excess of 900 °C. Such high growth temperatures can lead to thermal stresses in the film, defect accumulation, and N_2 dissociation.[80] Temperatures in this range are particularly problematic for InN which begins to decompose between 600-650 °C. Pressurization with N_2 is often needed to prevent dissociation of the films. Thus, activated nitrogen species with preformed M–N bonds are attractive candidates as precursors for materials synthesis at lower temperatures.

Reaction of $GaMe_3$ with NH_3 first produces the adduct, $Me_3Ga{\cdot}NH_3$, which decomposes upon further heating to form the trimeric amide, $[Me_2GaNH_2]_3$.[81] Thus, oligomeric amides are intermediates in the growth of GaN by MOCVD. Low pressure MOCVD of the trimeric amide, $[Et_2GaNH_2]_3$, was shown to produce GaN films at 650 °C.[82] A pyrolysis study of the dimeric Ga silylamide, $[Cl_2GaN(H)SiMe_3]_2$, showed that the formation of low quality GaN occurred with the loss of Me_3SiCl.[83] The adducts, $Cl_2MeM{\cdot}N(SnMe_3)_3$ (M = Al, Ga) and $X_3M{\cdot}N(SnMe_3)_3$ (X = Cl, Br; M = Al, Ga, In), contain no N–H bonds. Pyrolysis of these compounds proceeds with the elimination of $SnMe_4$ and Me_3SnX between 100-350 °C. Polycrystalline AlN, GaN, and InN were identified by powder X-ray diffraction (PXRD) after annealing at 650 °C for 1-2 hours.

Colloidal GaN nanoparticles with an average diameter of 30(12) Å were produced from the thermal decomposition of $[Ga(NH)_{3/2}]_n$ in trioctylamine/hexadecylamine (TOA/HDA) at 360°C. The particles exhibited quantum confinement but had low crystallinity and high polydispersity.[29] Pyrolysis of the dimeric Ga amide, $[Ga(NMe_2)_3]_2$, afforded colloidal GaN nanoparticles with an average diameter of 24(4) Å. However, these particles suffered from low crystallinity as well.

Both Ga and In azides have been investigated as precursors to GaN and InN by MOCVD. Growth of crystalline InN was achieved at temperatures of 300-450 °C using the monoazide precursor, $[N_3In((CH_2)_3NMe_2)]$.[84] Vapor deposition of the dimeric amido-azide, $[N_3(Me_2N)GaNMe_2]_2$, produced amorphous GaN at 250 °C and crystalline GaN at 580 °C with little carbon impurity.[80] A variety of other Ga azides have been investigated as vapor deposition precursors to GaN.[40,85,86] Ga azides have also been used as precursors in the solution phase synthesis of colloidal GaN.[30,87]

Relatively unexplored is the use of larger inorganic clusters as precursors to GaN and InN. Clusters containing only Ga–N, In–N, and other weak M–N bonds are interesting as precursor for low temperature film and solution nitride syntheses. Such clusters are also interesting as model intermediates in the formation of nitride materials. Indeed, clusters of up to 8 repeating units have been found during AlN formation.[88] Inorganic clusters, which are essentially small fragments of the bulk material, may also provide nucleation sites in colloidal syntheses. Transition metal–main group element clusters, such as $[M_{10}Se_4(SPh)_{16}]^{4-}$, have been used as

effective precursors in the synthesis of colloidal II-VI (CdSe, CdS, ZnSe, ZnS) nanoparticles.[89,90] By extension, exploration of group 13 metal–nitrogen cluster chemistry may provide insight into material formation and new routes to low temperature colloidal syntheses of GaN and InN.

The chemistry presented in this thesis details our exploration of the reactions of stannylamines with anionic Ga, In, and Bi halides. These reactions have produced novel compounds and clusters containing only M–N bonds. Their syntheses, structures, properties, and outlooks, are presented herein.

References

(1) Fischer, F.; Schroter, F. *Ber. Dtsch. Chem. Ges.* **1910**, *43*, 1465.

(2) Johnson, W. C.; Parsons, J. B.; Crew, M. C. *J. Phys. Chem.* **1932**, *36*, 2651.

(3) Hahn, H.; Juza, R. *Z. Anorg. Allg. Chem.* **1940**, *244*, 111.

(4) Juza, R.; Hahn, H. *Z. Anorg. Allg. Chem.* **1938**, *239*, 282.

(5) Lirman, J. V.; Zhdanov, H. S. *Acta Physicochim. URSS* **1937**, *6*, 306.

(6) Renner, T. *Z. Anorg. Allg. Chem.* **1958**, *298*, 22.

(7) Addamiano, A. *J. Electrochem. Soc.* **1961**, *108*, 1072.

(8) Samsonov, G. V.; Lyutaya, M. D. *Zh. Prikl. Khim. (S.-Peterburg, Russ. Fed.)* **1963**, *36*, 1416.

(9) Garlick, G. F. J. *Rep. Progr. Phys.* **1967**, *30*, 491.

(10) Rediker, R. H. *IEEE J. Quantum Electron.* **1987**, *QE-23*, 692.

(11) Kauer, E.; Rabenau, A. *Z. Naturforsch.* **1957**, *12a*, 942.

(12) Grimmeiss, H. G.; Koelmans, H. *Z. Naturforsch.* **1959**, *14a*, 264.

(13) Grimmeiss, H. G.; Groth, R.; Maak, J. *Z. Naturforsch.* **1960**, *15a*, 799.

(14) Lorenz, M. R.; Binkowski, B. B. *J. Electrochem. Soc.* **1962**, *109*, 24.

(15) Sclar, N. *J. Appl. Phys.* **1962**, *33*, 2999.

(16) Ponce, F. A.; Bour, D. P. *Nature (London)* **1997**, *386*, 351.

(17) Morkoç, H.; Mohammad, S. N. *Science* **1995**, *267*, 51.

(18) Muth, J. F.; Lee, J. H.; Shmagin, I. K.; Kolbas, R. M.; Casey, H. C., Jr.; Keller, B. P.; Mishra, U. K.; DenBaars, S. P. *Appl. Phys. Lett.* **1997**, *71*, 2572.

(19) Wu, J. *J. Appl. Phys.* **2009**, *106*, 011101/1.

(20) Nakamura, S.; Mukai, T.; Senoh, M. *Appl. Phys. Lett.* **1994**, *64*, 1687.

(21) Dupuis, R. D.; Krames, M. R. *J. Lightwave Technol.* **2008**, *26*, 1154.

(22) Lannoo, M.; Delerue, C.; Allan, G. *J. Lumin.* **1996**, *70*, 170.

(23) Weng, G. E.; Ling, A. K.; Lv, X. Q.; Zhang, J. Y.; Zhang, B. P. *Nano-Micro Lett.* **2011**, *3*, 200.

(24) Talapin, D. V.; Lee, J.-S.; Kovalenko, M. V.; Shevchenko, E. V. *Chem. Rev. (Washington, DC, U. S.)* **2010**, *110*, 389.

(25) Malik, M. A.; Afzaal, M.; O'Brien, P. *Chem. Rev. (Washington, DC, U. S.)* **2010**, *110*, 4417.

(26) Calarco, R. *Materials* **2012**, *5*, 2137.

(27) Shen, C. H.; Chen, H. Y.; Lin, H. W.; Gwo, S.; Klochikhin, A. A.; Davydov, V. Y. *Appl. Phys. Lett.* **2006**, *88*, 253104.

(28) Hu, M. S.; Wang, W. M.; Chen, T. T.; Hong, L. S.; Chen, C. W.; Chen, C. C.; Chen, Y. F.; Chen, K. H.; Chen, L. C. *Adv. Funct. Mater.* **2006**, *16*, 537.

(29) Micic, O. I.; Ahrenkiel, S. P.; Bertram, D.; Nozik, A. J. *Appl. Phys. Lett.* **1999**, *75*, 478.

(30) Manz, A.; Birkner, A.; Kolbe, M.; Fischer, R. A. *Adv. Mater. (Weinheim, Ger.)* **2000**, *12*, 569.

(31) Greenberg, M. R.; Chen, W.; Pulford, B. N.; Smolyakov, G. A.; Jiang, Y.-B.; Bunge, S. D.; Boyle, T. J.; Osinski, M. *Proc. SPIE-Int. Soc. Opt. Eng.* **2005**, *5705*, 68.

(32) Kraus, C. A.; Toonder, F. E. *Proc. Natl. Acad. Sci. U. S. A.* **1933**, *19*, 292.

(33) Wiberg, E.; Johannsen, T.; Stecher, O. *Z. Anorg. Allg. Chem.* **1943**, *251*, 114.

(34) Coates, G. E. *J. Chem. Soc.* **1951**, 2003.

(35) Coates, G. E.; Whitcombe, R. A. *J. Chem. Soc.* **1956**, 3351.

(36) Stone, F. G. A. *Chem. Rev. (Washington, DC, U. S.)* **1958**, *58*, 101.

(37) Creighton, J. R.; Wang, G. T. *J. Phys. Chem. A* **2005**, *109*, 10554.

(38) Bradley, D. C.; Faktor, M. M.; Scott, M.; White, E. A. D. *J. Cryst. Growth* **1986**, *75*, 101.

(39) Bradley, D. C.; Faktor, M. M.; Frigo, D. M.; Smith, L. M. *J. Cryst. Growth* **1988**, *92*, 37.

(40) Jones, A. C.; Whitehouse, C. R.; Roberts, J. S. *Chem. Vap. Deposition* **1995**, *1*, 65.

(41) Greenwood, N. N.; Ross, E. J. F.; Storr, A. *J. Chem. Soc. A* **1966**, 706.

(42) Mertz, K.; Schwarz, W.; Eberwein, B.; Weidlein, J.; Hess, H.; Hausen, H. D. *Z. Anorg. Allg. Chem.* **1977**, *429*, 99.

(43) Beachley, O. T., Jr.; Bueno, C.; Churchill, M. R.; Hallock, R. B.; Simmons, R. G. *Inorg. Chem.* **1981**, *20*, 2423.

(44) Belgardt, T.; Roesky, H. W.; Noltemeyer, M.; Schmidt, H. G. *Angew. Chem.* **1993**, *105*, 1101.

(45) Amirkhalili, S.; Hitchcock, P. B.; Smith, J. D. *J. Chem. Soc., Dalton Trans.* **1979**, 1206.

(46) Nutt, W. R.; Stimson, R. E.; Leopold, M. F.; Rubin, B. H. *Inorg. Chem.* **1982**, *21*, 1909.

(47) Nutt, W. R.; Anderson, J. A.; Odom, J. D.; Williamson, M. M.; Rubin, B. H. *Inorg. Chem.* **1985**, *24*, 159.

(48) Nutt, W. R.; Blanton, J. S.; Kroh, F. O.; Odom, J. D. *Inorg. Chem.* **1989**, *28*, 2224.

(49) Nutt, W. R.; Blanton, J. S.; Boccanfuso, A. M.; Silks, L. A., III; Garber, A. R.; Odom, J. D. *Inorg. Chem.* **1991**, *30*, 4136.

(50) Aitchison, K. A.; Backer-Dirks, J. D. J.; Bradley, D. C.; Faktor, M. M.; Frigo, D. M.; Hursthouse, M. B.; Hussain, B.; Short, R. L. *J. Organomet. Chem.* **1989**, *366*, 11.

(51) Waggoner, K. M.; Ruhlandt-Senge, K.; Wehmschulte, R. J.; He, X.; Olmstead, M. M.; Power, P. P. *Inorg. Chem.* **1993**, *32*, 2557.

(52) Leung, W.-P.; Chan, C. M. Y.; Wu, B.-M.; Mak, T. C. W. *Organometallics* **1996**, *15*, 5179.

(53) Pauls, J.; Chitsaz, S.; Neumüller, B. *Z. Anorg. Allg. Chem.* **2001**, *627*, 1723.

(54) Grabowy, T.; Merzweiler, K. *Z. Anorg. Allg. Chem.* **2000**, *626*, 736.

(55) Kuehner, S.; Kuhnle, R.; Hausen, H. D.; Weidlein, J. *Z. Anorg. Allg. Chem.* **1997**, *623*, 25.

(56) Hillwig, R.; Harms, K.; Dehnicke, K. *J. Organomet. Chem.* **1995**, *501*, 327.

(57) Nutt, W. R.; Murray, K. J.; Gulick, J. M.; Odom, J. D.; Ding, Y.; Lebioda, L. *Organometallics* **1996**, *15*, 1728.

(58) Schmid, K.; Niemeyer, M.; Weidlein, J. *Z. Anorg. Allg. Chem.* **1999**, *625*, 186.

(59) Hardman, N. J.; Cui, C.; Roesky, H. W.; Fink, W. H.; Power, P. P. *Angew. Chem., Int. Ed.* **2001**, *40*, 2172.

(60) Wright, R. J.; Phillips, A. D.; Allen, T. L.; Fink, W. H.; Power, P. P. *J. Am. Chem. Soc.* **2003**, *125*, 1694.

(61) Jutzi, P.; Neumann, B.; Reumann, G.; Stammler, H.-G. *Organometallics* **1999**, *18*, 2037.

(62) Uhl, W. *Struct. Bonding (Berlin, Ger.)* **2003**, *105*, 41.

(63) Uhl, W.; Rezaeirad, B.; Layh, M.; Hagemeier, E.; Wuerthwein, E.-U.; Ghavtadze, N.; Kuzu, I. *Chem.--Eur. J.* **2010**, *16*, 12195.

(64) Uhl, W.; Abel, T.; Hagemeier, E.; Hepp, A.; Layh, M.; Rezaeirad, B.; Luftmann, H. *Inorg. Chem.* **2011**, *50*, 325.

(65) Uhl, W.; Emden, C. H.; Massa, W. *J. Organomet. Chem.* **2006**, *691*, 1382.

(66) Uhl, W.; Abel, T.; Hepp, A.; Grimme, S.; Steinmetz, M. *Eur. J. Inorg. Chem.* **2008**, 543.

(67) Uhl, W.; Emden, C. H. *J. Organomet. Chem.* **2005**, *690*, 1529.

(68) Muller, J. *Coord. Chem. Rev.* **2002**, *235*, 105.

(69) Devi, A.; Schmid, R.; Muller, J.; Fischer, R. A. *Top. Organomet. Chem.* **2005**, *9*, 49.

(70) Kober, C.; Kroner, J.; Storch, W. *Angew. Chem. Int. Ed., Engl.* **1993**, *32*, 1608.

(71) Appel, A.; Kober, C.; Neumann, C.; Noeth, H.; Schmidt, M.; Storch, W. *Chem. Ber.* **1996**, *129*, 175.

(72) Driess, M.; Monse, C.; Merz, K.; van Wullen, C. *Angew. Chem., Int. Ed.* **2000**, *39*, 3684.

(73) Pi, C.; Elguero, J.; Wan, L.; Alkorta, I.; Zheng, W.; Weng, L.; Chen, Z.; Wu, L. *Chem.--Eur. J.* **2009**, *15*, 6581.

(74) Bettenhausen, R.; Milius, W.; Schnick, W. *Chem.--Eur. J.* **1997**, *3*, 1337.

(75) Kober, C.; Noth, H.; Storch, W. *Chem. Ber./Recl.* **1997**, *130*, 765.

(76) Eichler, J. F.; Just, O.; Rees, W. S., Jr. *Inorg. Chem.* **2006**, *45*, 6706.

(77) Cheng, Q. M.; Stark, O.; Merz, K.; Winter, M.; Fischer, R. A. *J. Chem. Soc., Dalton Trans.* **2002**, 2933.

(78) Cheng, Q. M.; Stark, O.; Stowasser, F.; Wohlfart, A.; Fischer, R. A. *J. Mater. Chem.* **2002**, *12*, 2470.

(79) Schulz, S.; Häming, L.; Herbst-Irmer, R.; Roesky, H. W.; Sheldrick, G. M. *Angewandte Chemie International Edition in English* **1994**, *33*, 969.

(80) Neumayer, D. A.; Ekerdt, J. G. *Chem. Mater.* **1996**, *8*, 9.

(81) Almond, M. J.; Drew, M. G. B.; Jenkins, C. E.; Rice, D. A. *J. Chem. Soc., Dalton Trans.* **1992**, 5.

(82) Park, H. S.; Waezsada, S. D.; Cowley, A. H.; Roesky, H. W. *Chem. Mater.* **1998**, *10*, 2251.

(83) Carmalt, C. J.; Mileham, J. D.; White, A. J. P.; Williams, D. J. *Dalton Trans.* **2003**, 4255.

(84) Fischer, R. A.; Sussek, H.; Miehr, A.; Pritzkow, H.; Herdtweck, E. *J. Organomet. Chem.* **1997**, *548*, 73.

(85) Devi, A.; Rogge, W.; Wohlfart, A.; Hipler, F.; Becker, H. W.; Fischer, R. A. *Chem. Vap. Deposition* **2000**, *6*, 245.

(86) Khanderi, J.; Wohlfart, A.; Parala, H.; Devi, A.; Hambrock, J.; Birkner, A.; Fischer, R. A. *J. Mater. Chem.* **2003**, *13*, 1438.

(87) Winkler, H.; Devi, A.; Manz, A.; Wohlfahrt, A.; Rogge, W.; Fischer, R. A. *Phys. Status Solidi A* **2000**, *177*, 27.

(88) Egashira, Y.; Kim, H.-J.; Komiyama, H. *J. Am. Ceram. Soc.* **1994**, *77*, 2009.

(89) Cumberland, S. L.; Hanif, K. M.; Javier, A.; Khitrov, G. A.; Strouse, G. F.; Woessner, S. M.; Yun, C. S. *Chem. Mater.* **2002**, *14*, 1576.

(90) Archer, P. I.; Santangelo, S. A.; Gamelin, D. R. *J. Am. Chem. Soc.* **2007**, *129*, 9808.

Chapter 2: Synthesis and Structure of Anionic Gallium and Gallium–Tin μ_3–Nitrogen Compounds

Introduction

As stated in the previous chapter molecular nitrides of the *p*-block metals are exceedingly rare and are mostly limited to neutral tin–nitrogen (Sn–N) compounds with the exception of one homometallic aluminum nitride dimer.[1] The successful isolation of a group 13 metal nitride would generally require bulky substituents on the metal to provide kinetic stabilization of the product, an appropriate N^{3-} source, and stable leaving groups. Many candidates for N^{3-} sources, such as lithium nitride, are highly reactive and difficult to manipulate with standard wet chemical techniques. Tris(trimethylstannyl)amine, $(Me_3Sn)_3N$, has been reacted with transition metal halides to afford molecular transition metal nitrides with the concomitant elimination of Me_3SnX (X =Cl, Br). Reaction of $[Cp^*TaCl_4]$ with $(Me_3Sn)_3N$ in a 1:1 ratio in toluene yielded the tantalum nitride heterocycle, $[Cp^*(Cl)TaN]_3$, in a 67% yield (Scheme 2.1a).[2] When $(Me_3Sn)_3N$ is reacted with $[FeCl_4]^-$ in MeCN the anionic clusters, $[Fe_4N_2Cl_{10}]^{4-}$ and $[Fe_{10}N_8X_{12}]^{5-}$ (X = Cl, Br), are formed (Scheme 2.1b-c).[3]

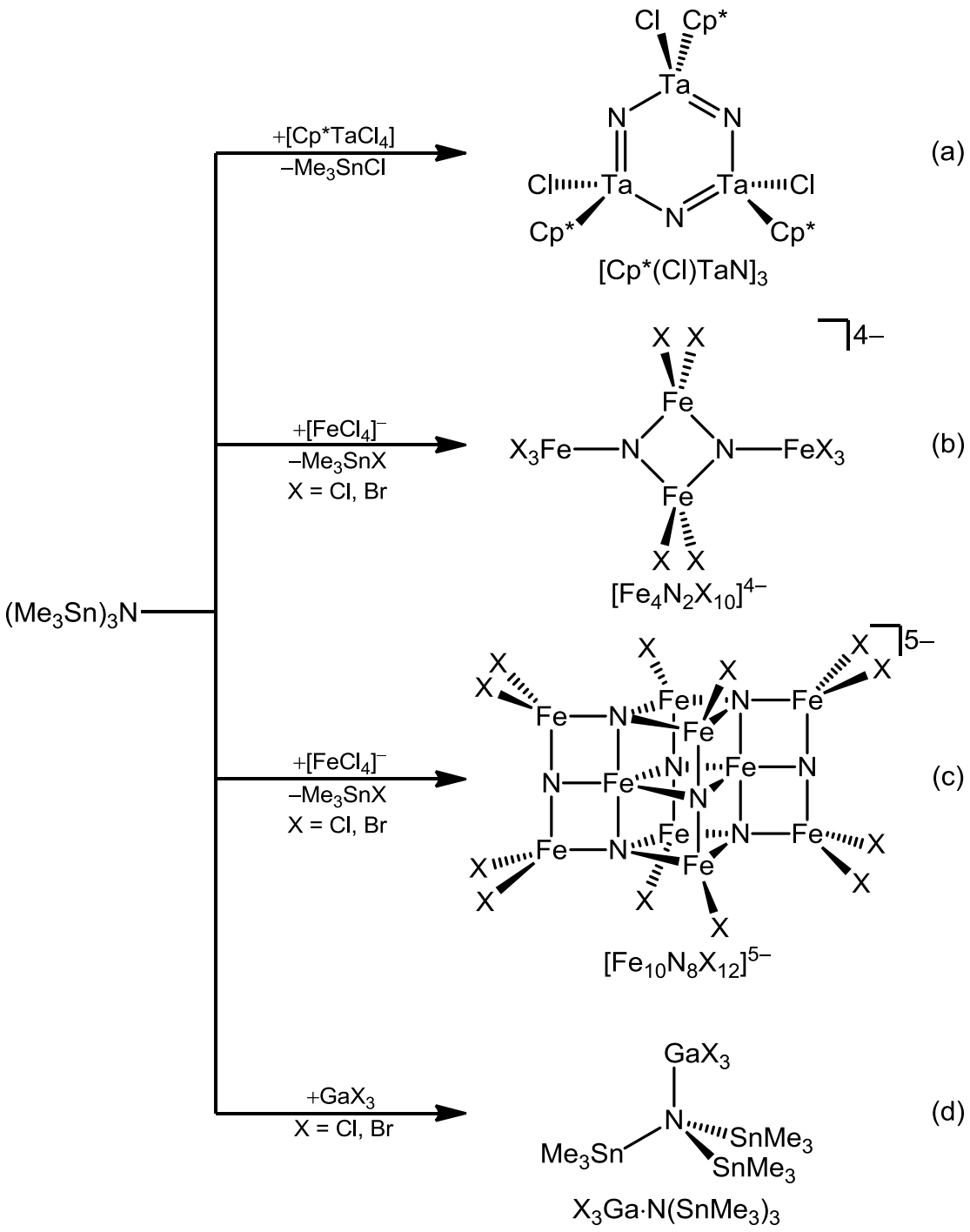

Scheme 2.1. Reactions of anionic transition metal halides and neutral gallium halides with $(Me_3Sn)_3N$.

Previous research has shown that reaction of neutral GaX_3 (X = Cl, Br) with $(Me_3Sn)_3N$ in Et_2O affords the adducts, $X_3Ga{\cdot}N(SnMe_3)_3$ (Scheme 2.1d).[4] No crystallographic evidence of Sn–N bond cleavage was observed, although NMR spectra of these adducts indicate some bond cleavage may occur when dissolved in polar solvents. We hypothesized that $[GaX_4]^-$ (X = Cl, Br), as an X^- donor, could affect complete dehalostannylation of $(Me_3Sn)_3N$ to form molecular gallium μ_3–nitride. Additionally the formation of anionic products provides kinetic stabilization via Coulombic repulsion and thus negates the use of bulky organic substituents. Products of such reactions, with preformed Ga–N bonds, would be of interest as potential precursors or as model intermediates to the formation of GaN materials.

Three reaction pathways are possible for the formation of a μ_3–nitride of gallium from $[GaX_4]^-$ (X = Cl, Br) and $(Me_3Sn)_3N$ (Scheme 2.2). In the first step of all three pathways a single Sn–N bond is cleaved to form the monomeric anion, $[X_3GaN(SnMe_3)_2]^-$. This anion may then dimerize to form $[X_2GaNSnMe_3]_2^{2-}$, which may then be attacked by additional $[GaX_4]^-$ to give the dimeric nitride, $[Ga_4N_2X_{10}]^{4-}$ (Scheme 2.2a). This same molecule may be formed by an alternate pathway in which the initial anion, $[X_3GaN(SnMe_3)_2]^-$, has a second Sn–N bond cleaved to form $[(X_3Ga)_2NSnMe_3]^{2-}$, which itself may dimerize to form $[Ga_4N_2X_{10}]^{4-}$ (Scheme 2.2b). Lastly, $(Me_3Sn)_3N$, may react with 3 equivalents of $[GaX_4]^-$ successively to afford the monomeric nitride, $[(X_3Ga)_3N]^{3-}$ (Scheme 2.2c).

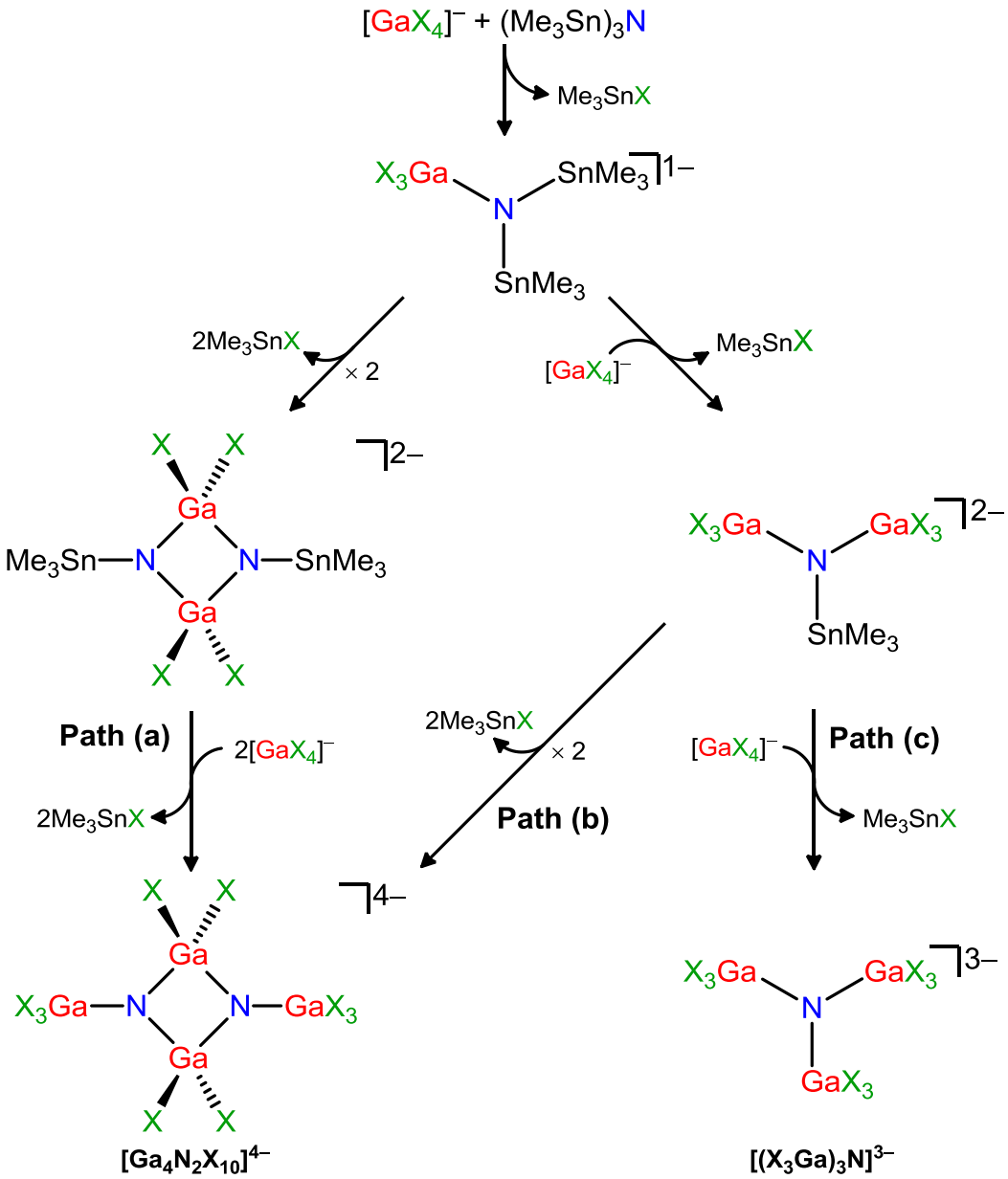

Scheme 2.2. Possible reaction pathways to a gallium μ_3–nitride.

This chapter describes our investigations of room temperature reactions of $[GaX_4]^-$ (X = Cl, Br) salts with $(Me_3Sn)_3N$ in tetrahydrofuran (THF). When these reactants are combined in a 2:1 ratio, the monomeric (unassociated) gallium/tin μ_3–nitrides, $(Me_4N)_2[(X_3Ga)_2NSnMe_3]$ (X = Cl (**1**), Br (**2**)) and $(Ph_4P)_2[(X_3Ga)_2NSnMe_3]$ (X = Cl (**3**), Br (**4**)), are formed. Combining $(Me_4N)[GaCl_4]$ and $(Me_3Sn)_3N$ in a 3:1 ratio in acetonitrile (MeCN) afforded crystals of $(Me_4N)_3[(Cl_3Ga)_3N]$ (**5**). However, it was found that **5** was best obtained by reaction of $(Me_4N)[GaCl_4]$ with $Cl_3Ga{\cdot}N(SnMe_3)_3$ in THF at 50 °C. The anion of **5** is the first compound in which a μ_3-N atom is ligated solely by Ga; thus it is the first characterized gallium nitride molecule. The general syntheses of **1-5** are shown in Scheme 2.3. The isolation of these compounds supports μ_3–nitride formation by path (c) (Scheme 2.2). Dimerization of **1-4** (path (b)) was not directly observed, however, formation of Me_3SnCl occurs when these compounds are dissolved in MeCN. Some evidence for path (a) is observed in this system under highly concentrated conditions (See Chapter 4). Compounds **1-5** have been characterized by single crystal X-ray diffraction, elemental analysis, diffuse reflectance UV-Vis spectroscopy, and nuclear magnetic resonance spectroscopy (NMR). The isolation these species shows that dehalostannylation of $(Me_3Sn)_3N$ by $[GaX_4]^-$ can occur under mild conditions to form unprecedented Ga–N compounds.

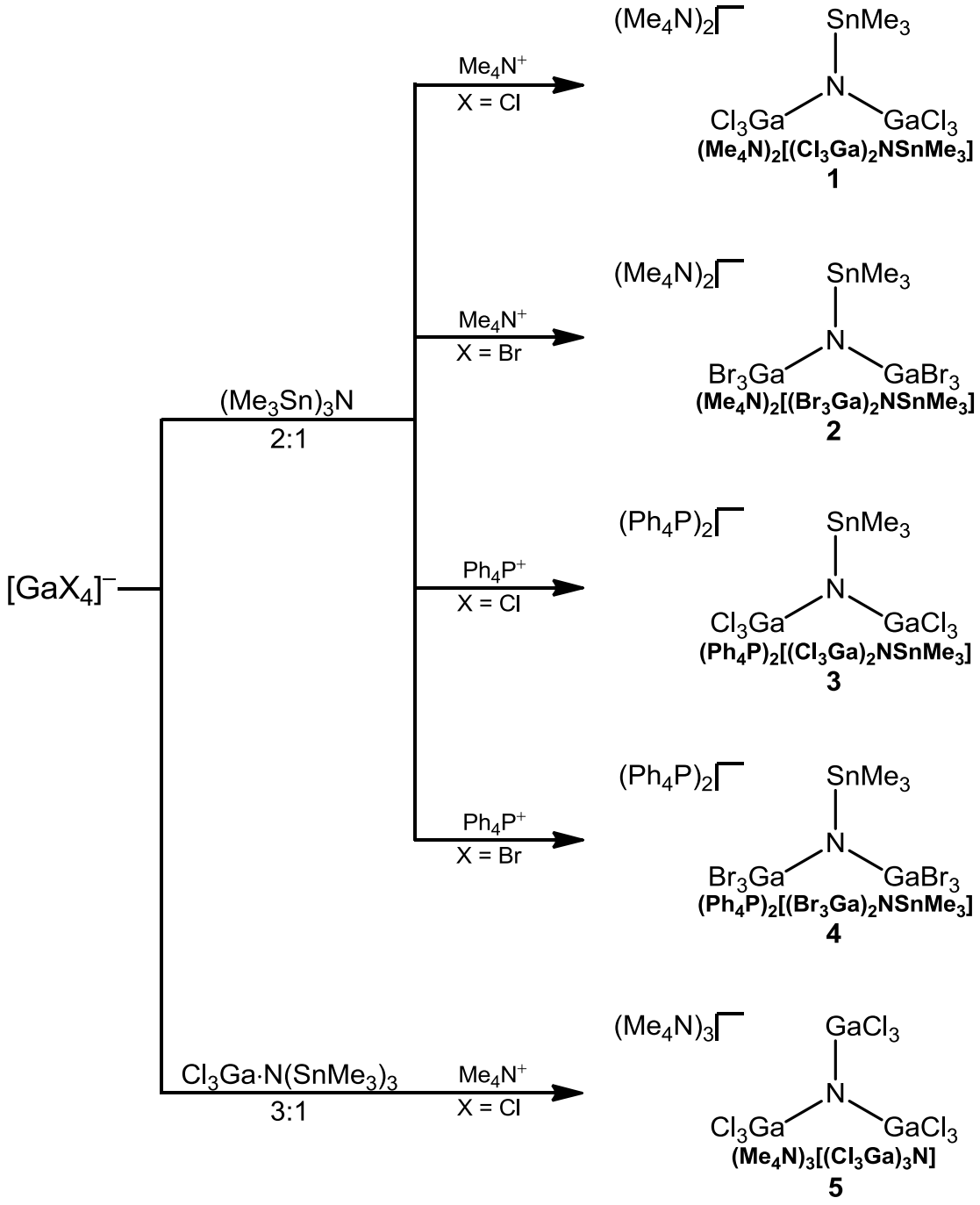

Scheme 2.3. General scheme for the syntheses of $(Me_4N)_2[(X_3Ga)_2NSnMe_3]$ (X = Cl (1), Br (2)), $(Ph_4P)_2[(X_3Ga)_2NSnMe_3]$ (X = Cl (3), Br (4)), and $(Me_4N)_3[(Cl_3Ga)_3N]$ (5).

Experimental

Preparation of Compounds

All manipulations were carried out under a pure dinitrogen atmosphere using standard Schlenk and glove-box techniques. Anhydrous tetrahydrofuran (THF), purchased from EMD, diethylether (Et_2O), purchased from EMD, and acetonitrile (MeCN), purchased from Burdick and Jackson, were stored over activated 4 Å molecular sieves under a pure dinitrogen atmosphere. The compounds $(Me_3Sn)_3N$[5] and $Cl_3Ga{\cdot}N(SnMe_3)_3$[4] were prepare according to the literature procedures. Syntheses of salts of $[GaX_4]^{1-}$ are outlined in appendix B. Elemental analysis of **5** and **4** was performed at Columbia Analytics Laboratory in Tucson, AZ, and analysis of **1**, was performed at the Mikroanalytisches Laboratorium Kolbe, Mülheim an der Ruhr, Germany.

$(Me_4N)_2[(Cl_3Ga)_2NSnMe_3]$ (1). A solution of $(Me_4N)[GaCl_4]$ (0.48 g, 1.7 mmol) in 13 mL of THF was added to a solution of $(Me_3Sn)_3N$ (0.43 g, 0.84 mmol) in 5.0 mL of THF. Small white crystals began to form within 1 min of mixing the reactants. The reaction mixture was allowed to stand for 24 h. After this time the crystals were collected by filtration, washed with successive aliquots of THF (5 × 3 mL) and Et_2O (4 × 3 mL), and dried *in vacuo* to afford 0.45 g (0.67 mmol, 79%) of **1** as a white crystalline solid. ^{1}H NMR (CD_3CN): δ 0.28 ppm (s) ($J_{^1H\text{-}^{117/119}Sn}$ = 58 Hz). Diffuse reflectance spectrum: λ_{max} (nm) 248. Anal. calcd for $C_{11}H_{33}Cl_6Ga_2N_3Sn$: C,

19.48; H, 4.90; Cl, 31.36; Ga, 20.56; N, 6.20; Sn, 17.50. Found: C, 19.56; H, 4.91; Cl, 31.23; Ga, 20.84; N, 5.93; Sn, 17.53.

$(Me_4N)_2[(Br_3Ga)_2NSnMe_3]$ (2). A solution of $(Me_4N)[GaBr_4]$ (0.54 g, 1.2 mmol) in 6 mL of THF was added to a solution of $(Me_3Sn)_3N$ (0.31 g, 0.62 mmol) in 5 mL of THF. A white crystalline precipitate began forming immediately. The mixture was allowed to stand for 24 h, after which the solid portion was collected by vacuum filtration and washed with successive aliquots of THF (3 x 3 mL) and Et_2O (3 x 3 mL) to yield 0.46 g (0.48 mmol, 83%) of **2**. Anal. calcd for $C_{11}H_{33}Br_6Ga_2N_3Sn$: C, 13.98; H, 3.52; N, 4.45. Found: C, 13.52; H, 3.36; N, 2.86. Note: the low value for N may be due to partial hydrolysis of the product as well as difficulties in purifying $(Me_4N)[GaBr_4]$.

$(Ph_4P)_2[(Cl_3Ga)_2NSnMe_3]$ (3). A solution of $(Me_3Sn)_3N$ (0.51 g, 1.0 mmol) in 4.1 mL of THF was added to solid $(Ph_4P)[GaCl_4]$ (1.13 g, 2.05 mmol) and stirred overnight to afford an amber colored solution. Diffusion Et_2O into this solution resulted in the precipitation of cream colored crystals. The crystals were collected on a fritted glass filter and washed with successive aliquots of THF (5 × 5 mL) and Et_2O (5 × 5 mL) to afford 0.51 g (0.43 mmol, 43 %) of **3**. ^{1}H NMR (CD_3CN): δ 0.25 ppm (s) ($J_{^1H\text{-}^{117/119}Sn}$ = 58 Hz).

$(Ph_4P)_2[(Br_3Ga)_2NSnMe_3]$ (4). A solution of $(Ph_4P)[GaBr_4]$ (0.22 g, 0.30 mmol) in 4 mL of THF was added to 0.076 g (0.15 mmol) of $(Me_3Sn)_3N$, dissolved in 2 mL of THF, and stirred overnight. Vapor diffusion of Et_2O into this solution produced colorless plate-like crystals. The crystals were collected and washed with successive aliquots of THF (4 x 6 mL) and Et_2O (2 x 3 mL) to afford 0.071 g (0.048 mmol, 32%) of **4**. Anal. calcd for $C_{51}H_{49}Br_6Ga_2N_1P_2Sn_1$: C, 41.52; H, 3.35; N, 0.95. Found: C, 41.17; H, 3.53; N, 0.79.

$(Me_4N)_3[(Cl_3Ga)_3N]$. (5). A solution of $(Me_4N)[GaCl_4]$ (1.57 g, 5.49 mmol) in 10 mL of THF was added to a solution of $Cl_3Ga{\cdot}N(SnMe_3)_3$ (1.25 g, 1.84 mmol) in 45 mL of THF. The resultant colorless solution was refluxed for 2 h under flowing N_2 yielding a white precipitate. This was collected by vacuum filtration, washed with THF (3 × 5 mL) and Et_2O (3 × 5 mL), and dried *in vacuo* to afford 0.79 g of a white solid. The solid was dissolved in 250 mL of MeCN and filtered through celite. Vapor diffusion of THF into the filtrate afforded small triangular crystals which were collected by vacuum filtration, washed with successive aliquots of THF (5 × 3 mL) and Et_2O (4 × 3 mL), and dried *in vacuo* to afford 0.14 g, (0.18 mmol, 10%) of **5** as a white crystalline solid. Diffuse reflectance spectrum: λ_{max} 240 nm. Anal. calcd for $C_{12}H_{36}Cl_9Ga_3N_4$: C, 18.85; H, 4.75; N, 7.33. Found: C, 19.04; H, 4.39; N, 6.89.

X-ray Structure Determination

Crystals were coated in Paratone oil and mounted by mean of a glass capillary fiber on a Bruker APEX-II CCD area detector instrument operated by the APEX software package. Data reduction was performed by SAINT, absorption correction was applied using SADABS, and the space group was assigned using XPREP. The structures **1**, **2**, **4**, and **5** were solved by direct methods while **3** was solved using a Patterson map. The structures were refined against all data by full-matrix least squares on F_2. OLEX2[6] was used to calculate a solvent accessible void of 122 Å^3 in **3** containing 31 electrons which were masked for further refinement. Hydrogen atoms were attached at idealized positions on carbon atoms and were refined as riding atoms with uniform isotropic thermal parameters. Structure solutions, refinements, graphics and report generation were performed using SHELXTL,[7] OLEX2,[6] and Mercury.[8]

Other Physical Measurements

The solid state electronic reflectance spectra were recorded on a JASCO V-670 UV-Vis spectrophotometer fitted with an integrating sphere. NMR spectra were collected on a Varian Inova 400 MHz instrument at 30 °C with chemical shifts referenced to the signal of residual protons in the deuterated solvent. Infrared spectroscopy was performed on a Perkin-Elmer RX I spectrometer equipped with an attenuated total reflectance accessory.

Table 2.1. Crystallographic data for $(Me_4N)_2[(X_3Ga)_2NSnMe_3]$ (X = Cl (1), Br (2)) and, $(Ph_4P)_2[(X_3Ga)_2NSnMe_3]$ (X = Cl (3), Br (4)).

	1	**2**	**3**	**4**
formula	$C_{11}H_{33}Cl_6Ga_2N_3Sn$	$C_{11}H_{33}Br_6Ga_2N_3Sn$	$C_{51}H_{49}Cl_6Ga_2NP_2Sn$	$C_{51}H_{49}Br_6Ga_2NP_2Sn$
form. weight	678.23	944.99	1208.68	1475.44
cryst. syst.	orthorhombic	Orthorhombic	triclinic	Monoclinic
space group	$P2_12_12_1$	$P2_12_12_1$	$P\bar{1}$	$P2_1/n$
a, Å	11.5910(4)	11.8437(19)	10.2618(8)	10.4631(15)
b, Å	14.2637(5)	14.624(2)	12.9934(10)	27.952(4)
c, Å	15.6726(6)	15.780(2)	22.7874(17)	18.082(3)
α, deg	90	90	74.003(3)	90
β, deg	90	90	78.952(4)	95.458(7)
γ, deg	90	90	70.872(4)	90
V, Å^3	2591.16(16)	2733.0(7)	2742.2(4)	5264.4(14)
Z	4	4	2	4
ρ_{calc}, g/cm^3	1.739	2.297	1.464	1.862
2θ range, deg	2.19 to 31.00	3.8 to 68.66	3.4 to 58.26	1.46 to 31.51
GOF (F^2)	1.04	1.044	1.098	1.004
R_1/wR_2, %	2.67/5.23	2.23/3.61	4.04/10.66	3.66/7.37
largest peak/ hole (e$^-$/Å^3)	0.796 and -0.482	0.78/-0.65	1.70/-1.13	2.500/-1.496
Flack x parameter	0.003(8)	0.004(4)		

Table 2.2. Crystallographic data for $(Me_4N)_3[(Cl_3Ga)_3N]$ (5).

	5
formula	$C_{12}H_{36}Cl_9Ga_3N_4$
form. weight	764.66
cryst. syst.	rhombohedral
space group	*R*3
a, Å	10.7081(18)
b, Å	10.7081(18)
c, Å	22.379(4)
α, deg	90
β, deg	90
γ, deg	120
V, Å^3	2222.3(7)
Z	3
ρ_{calc}, g/cm^3	1.714
2θ range, deg	2.38 to 30.48
GOF (F^2)	1.018
R_1/wR_2, %	3.34/6.44
largest peak/hole (e$^-$/Å^3)	0.331/-0.235
Flack *x* parameter	-0.004(12)

Results and Discussion

Synthesis of (1)-(4)

Addition of THF solutions of $(Me_4N)[GaCl_4]$ and $(Me_3Sn)_3N$ in a 2:1 ratio results in the immediate precipitation of colorless crystals of $(Me_4N)_2[(Cl_3Ga)_2NSnMe_3]$ (**1**) in 79% yield. By the same procedure $(Me_4N)[GaBr_4]$ may be reacted with $(Me_3Sn)_3N$ in THF to afford $(Me_4N)_2[(Br_3Ga)_2NSnMe_3]$ (**2**). An excellent solid state structure of **2** was obtained, however, a low value for N in the elemental analysis indicates an impure bulk product. A low N value may indicate possible hydrolysis of the product. Additionally, removal of bromine impurities from $(Me_4N)[GaBr_4]$ was often problematic.

Combining THF solutions of $(Ph_4P)[GaX_4]$ (X= Cl, Br) and $(Me_3Sn)_3N$ does not result in the precipitation of any products or byproducts; however, vapor diffusion of Et_2O into a concentrated THF solution of these reactants (in a 2:1 ratio) yields $(Ph_4P)_2[(X_3Ga)_2NSnMe_3]$ (X= Cl (**3**), Br (**4**)) along with some contamination with $(Ph_4P)[GaX_4]$. The salt $(Ph_4P)[GaX_4]$ is easily washed away with THF to afford **3** and **4** in a 30-45% yield. The general reaction for the formation of $[(X_3Ga)_2NSnMe_3]^{2-}$ is shown in Scheme 2.4.

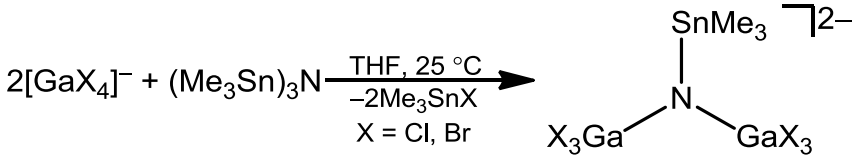

Scheme 2.4. General reaction for the synthesis of the anion of salts $(Me_4N)_2[(X_3Ga)_2NSnMe_3]$ (X = Cl (1), Br (2)) and, $(Ph_4P)_2[(X_3Ga)_2NSnMe_3]$ (X = Cl (3), Br (4)).

Properties of (1)-(4)

The salts **1**-**4** are all soluble in MeCN. Proton NMR shows a broad peak between 0.25 and 0.28 ppm with a proton–tin coupling of $J_{^1H\text{-}^{117/119}Sn} = 58$ Hz (The ^{117}Sn and ^{119}Sn satellites are merged due to peak broadening). This peak may be attributed to the $SnMe_3$ protons of the anion. Over several days in CD_3CN the anion decomposes to $Me_3SnCl/[Me_3SnCl_2]^{1-}$ and an unidentified product characterized by a peak at 0.29 ppm ($J_{^1H\text{-}^{117}Sn}$ = 57 Hz, $J_{^1H\text{-}^{119}Sn}$ = 59 Hz). The byproduct, $(Me_3Sn)_3C–C{\equiv}N$, would result from deprotonation of the solvent by the anion. This molecule has been previously synthesized and was reported to have an ^1H NMR chemical shift of 0.23 ppm and proton–tin coupling constants of $J_{^1H\text{-}^{117}Sn} = 53$ Hz and $J_{^1H\text{-}^{119}Sn} = 55$ Hz.[9] Thus the unidentified peak at 0.29 ppm cannot be positively attributed to deprotonation of the solvent. However, the recurrence of this resonance in several different reaction systems during the course of our research implies that it is characteristic of a decomposition product containing only Sn and no other metal atoms. When **2** is subjected to mild heating (50 °C) in CD_3CN a peak at –0.34 ppm

appears in the ^{1}H NMR spectrum (Figure 2.1). This may indicate methyl migration to gallium metal. Evidence for room temperature methyl–halogen exchange in this system is presented in Chapter 4. Methyl–halogen exchange in the presence of $GaCl_3$ has been previously documented for aminostibanes.[10]

The solid state electronic spectrum of **1** reveals a characteristic intense absorption at 248 nm which decays rapidly upon exposure to air (Figure 2.2). To examine the susceptibility of **1** to hydrolysis a solution in CD_3CN was stirred in air. A white precipitate formed almost immediately. The ^{1}H NMR spectrum of the remaining solution gave only a signal for $[Me_3SnCl_2]^{1-}$. The infrared spectrum on the white precipitate contained a broad IR band at 3385 cm^{-1} which may be assigned to the O–H stretching of water molecules in the precipitate (Figure 2.3). The bands at 3140 and 3048 cm^{-1} may arise from O–H stretching of hydroxyl groups bound to gallium. Similar features have been observed in the IR spectrum of GaO(OH) precipitated from aqueous gallium chloride.[11] In that report broad IR bands at 3403 cm^{-1}, 3243 cm^{-1}, and a shoulder at 2990 cm^{-1} were observed and assigned as stated. A previously reported band characteristic of Sn–O–H deformation at 917 cm^{-1} was not observed.[5] Thus from the evidence we infer that the anion of **1** is highly susceptible to hydrolysis with attack occurring preferentially at the gallium sites.

When **1** was heated to 150 °C in an evacuated glass tube small colorless crystals formed on the side of the glass. X-ray diffraction revealed these to be $[Me_3Sn(NMe_3)(\mu\text{-}Cl)SnMe_3Cl]$ (Figure 2.4). This compound is composed of Me_3SnCl and Me_3SnNMe_3 moieties connected by a μ_2-Cl (Sn–Cl–Sn ~121°). The NMe_3 moiety

most likely is a byproduct of Me_4N^+ decomposition. Thus both the anion and the cation decompose with the formation of volatile byproducts (NMe_3 and Me_3SnCl) at relatively low temperatures. Similar behavior was observed for the adduct, $Cl_3Ga{\cdot}(SnMe_3)_3$, which decomposes with the elimination of Me_3SnCl below 200 °C.[12]

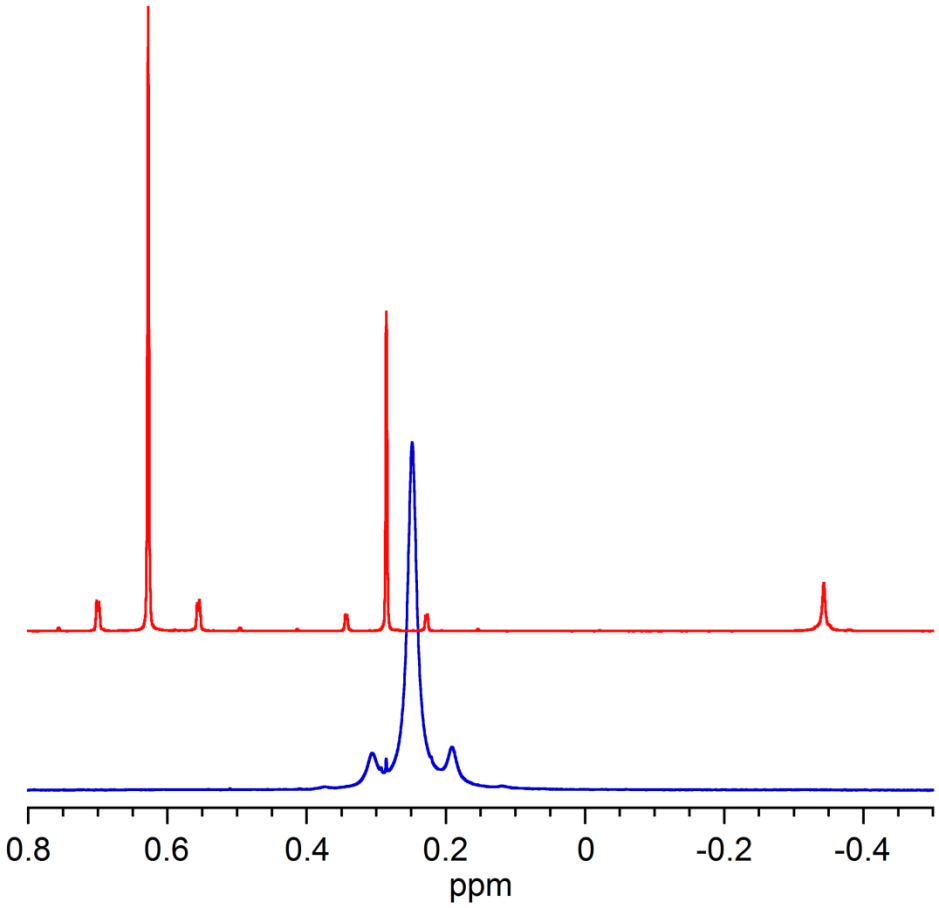

Figure 2.1. ^{1}H NMR (CD_3CN) of $(Ph_4P)_2[(Cl_3Ga)_2NSnMe_3]$ (2) before (blue) and after (red) heating at 50 °C for 48 h.

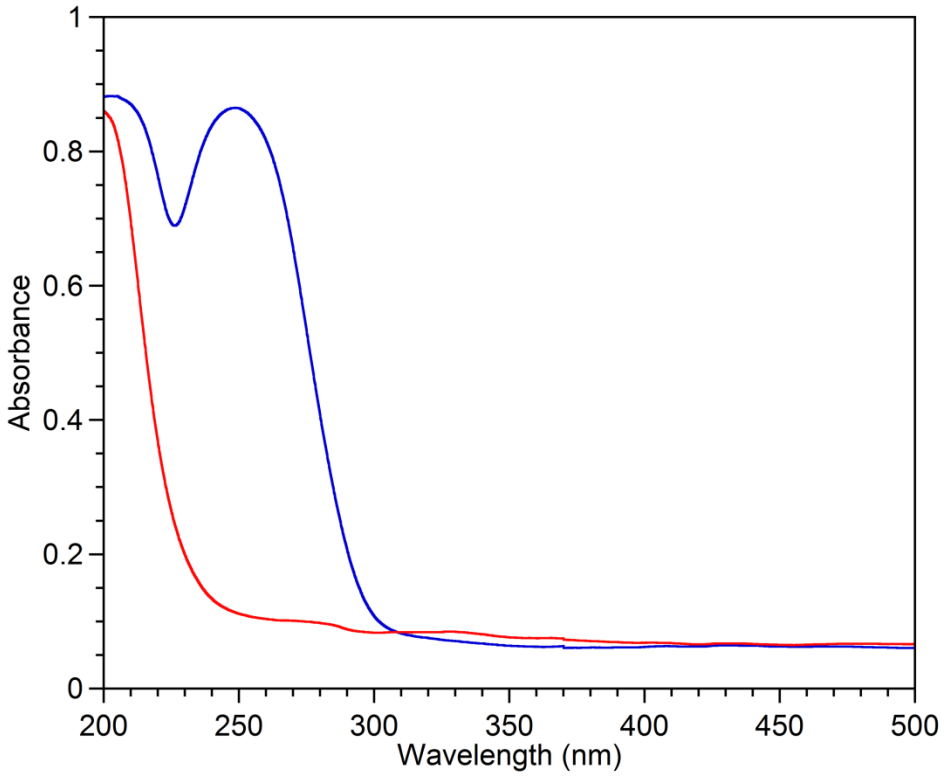

Figure 2.2. Diffuse reflectance UV-Vis spectrum of $(Me_4N)_2[(Cl_3Ga)_2NSnMe_3]$ (1) before (blue) and after (red) air exposure.

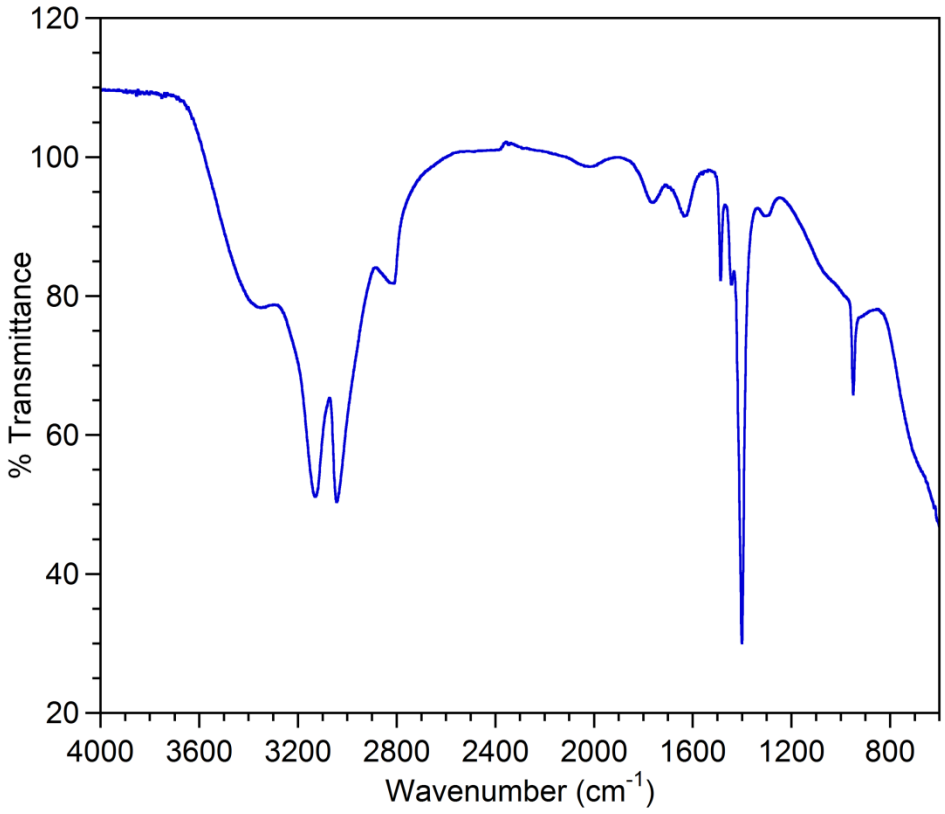

Figure 2.3. IR spectrum of the decomposition product of $(Me_4N)_2[(Cl_3Ga)_2NSnMe_3]$ (1) in air.

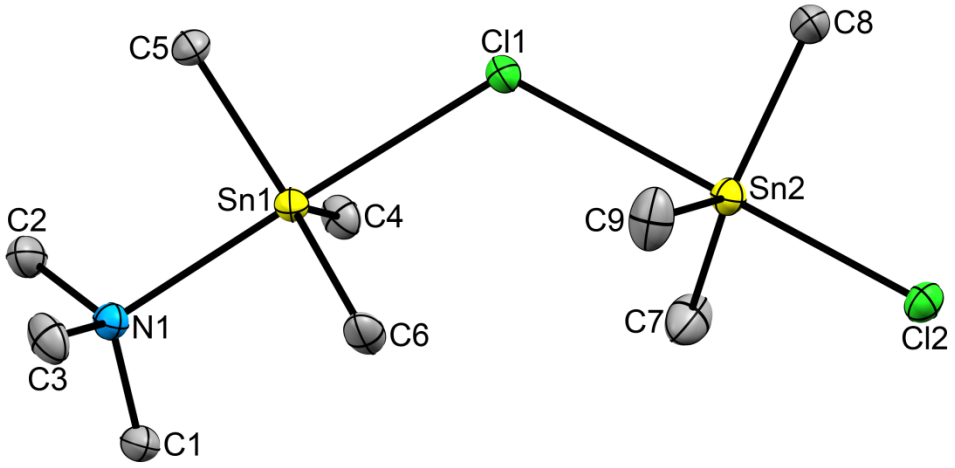

Figure 2.4. The crystal structure of [$Me_3Sn(NMe_3)(\mu$-Cl)$SnMe_3Cl$] with thermal ellipsoids set at 50% probability. Hydrogen atoms have been omitted for clarity.

Table 2.3. Crystallographic data and selected mean bond lengths (Å) and angles (°) for [$Me_3Sn(NMe_3)(\mu$-Cl)$SnMe_3Cl$].

	[$Me_3Sn(NMe_3)(\mu$-Cl)$SnMe_3Cl$]		
formula	$C_9H_{27}Cl_2NSn_2$	Sn1–Cl1	2.7502(4)
form. weight	457.6	Sn2–Cl1	2.8955(5)
cryst. syst.	monoclinic	Sn2–Cl2	2.4989(5)
space group	Cc	Sn1–N1	2.3651(14)
a, Å	7.0313(6)	N–C (mean)	1.483(7)
b, Å	12.6126(12)	Sn–C (mean)	2.129(3)
c, Å	19.5100(18)		
α, deg	90	Sn1–Cl1–Sn2	120.956(15)
β, deg	93.166(4)	Cl1–Sn2–Cl2	178.761(14)
γ, deg	90	Cl1–Sn2– N1	177.58(4)
V, Å^3	1727.6(3)	C–N–C (mean)	108.9(3)
Z	8	C–Sn–C (mean)	120(2)
ρ_{calc}, g/cm^3	3.519	C–Sn1–N1 (mean)	92.6(8)
2θ range, deg	4.18 to 72.74	C–Sn1–Cl1 (mean)	87(2)
GOF (F^2)	1.023	C–Sn2–Cl1 (mean)	86(2)
R_1/wR_2, %	1.89/3.63	C–Sn2–Cl2 (mean)	94(1)
largest peak/hole (e$^-$/Å^3)	0.61/-0.45		

Structures of (1)-(4)

The salts **1**-**4** were characterized by single crystal X-ray diffraction. Salts $(Me_4N)_2[(Cl_3Ga)_2NSnMe_3]$ (**1**) and $(Me_4N)_2[(Br_3Ga)_2NSnMe_3]$ (**2**) are isostructural and crystallize in the orthorhombic, non-centrosymmetric, space group $P2_12_12_1$. The Flack *x* parameters of 0.003(8) and 0.004(4) respectively indicate the absence of racemic twinning. The salts $(Ph_4P)_2[(Cl_3Ga)_2NSnMe_3]$ (**3**) and $(Ph_4P)_2[(Br_3Ga)_2NSnMe_3]$ (**4**) are not isostructural. **3** crystallizes in the triclinic space group $P\bar{1}$ while **4** crystallizes in the monoclinic space group $P2_1/n$. This is a result of **3** having crystallized with a disordered molecule in the asymmetric unit which may be assigned as THF. The ^{1}H NMR spectrum shows that **3** is contaminated with slightly less than one equivalent of THF. Excessive disorder prevented successful modeling of this molecule. Using OLEX2[6] it was calculated that **3** has a solvent accessible void of 122 Å^3 containing 31 electrons (40 e^- expected for THF) which were masked for structure refinement. The structure of **4** contains no solvent accessible voids and has a smaller formula unit volume than its chloride analog.

The anions of **1**-**4** consist of a μ_3-N atom bonded to two GaX_3 moieties and one $SnMe_3$ (Figure 2.5). When crystallized as the Me_4N^+ salts (**1**, **2**) the anion deviates slightly from planarity. The sum of the M–N–M bond angles is 346.9° in **1** and 346.0° in **2** (idealized trigonal pyramid = 328.5°, trigonal planar = 360°) with the central N atom deviating from the mean Ga–Sn–Ga plane by 0.405 Å in **1** and 0.422 Å in **2**. This differs from previously characterized nitrogen compounds of the heavier group 14-15 elements, such as $(Me_3Sn)_3N$,[13] $(Me_2As)_3N$,[14] and $(Me_2Sb)_3N$,[15] which are all

essentially planar. Conversely, when crystallized as the Ph_4P^+ salts (**3**, **4**) the anions more closely approach planar. The sum of the M–N–M bond angles is 359.4° in **3** and 352.9° in **4** with the central N atom deviating from the mean Ga–Sn–Ga plane by 0.080 Å in **3** and 0.297 Å in **4**. The slight difference in conformation may be due to crystal packing forces. In **1** and **2** Me_4N^+ is in closer contact with the anion than Ph_4P^+ is in **3** and **4**. The μ_3-N atom in **2** (N1) is 2.85 Å from the nearest hydrogen atom (H11c) whereas in **4**, N1 is 3.25 Å from the closest hydrogen atom (H44). Potentially then the increase in the pyramidal geometry of the anions of the Me_4N^+ salts (**1**,**2**) may be due to slight stabilization arising from weak cation-anion interaction.

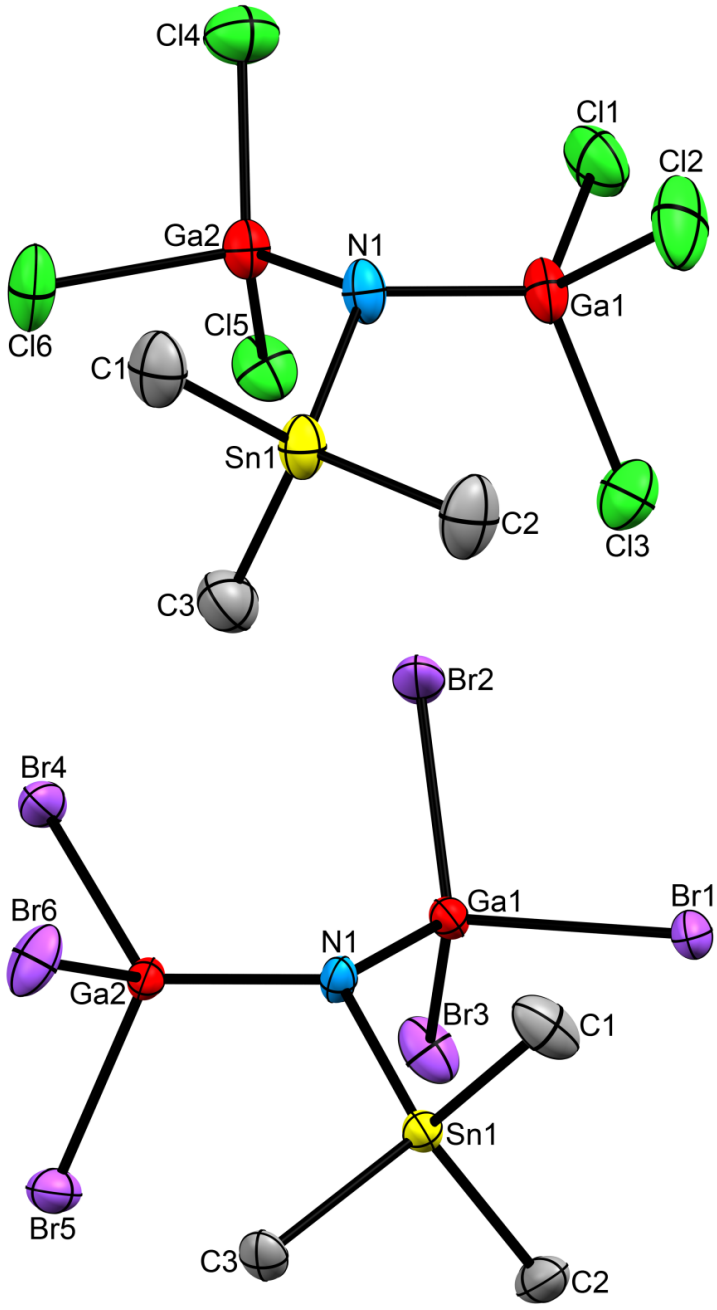

Figure 2.5. The structures of the anions of $(Me_4N)_2[(Cl_3Ga)_2NSnMe_3]$ (1) (top) and $(Ph_4P)_2[(Br_3Ga)_2NSnMe_3]$ (4) (bottom) with thermal ellipsoids drawn at 50% probability. The cations and hydrogen atoms have been omitted for clarity.

Table 2.4. Selected mean bond lengths (Å) and angles (°) for $(Me_4N)_2[(X_3Ga)_2NSnMe_3]$ (X = Cl (1), Br (2)) and, $(Ph_4P)_2[(X_3Ga)_2NSnMe_3]$ (X = Cl (3), Br (4)).

	1	2	3	4
Sn–N	2.060(2)	2.076(2)	2.050(3)	2.064(2)
Ga–N	1.844(5)	1.853(3)	1.828(6)	1.847(4)
Sn–C	2.136(2)	2.152(4)	2.143(6)	2.142(9)
Ga–Cl	2.220(14)		2.212(16)	
Ga–Br		2.381(16)		2.369(13)
Ga–N–Ga	116.7(1)	115.6(1)	127.0(2)	119.1(1)
Ga–N–Sn	115.1(4)	115.2(3)	116.2(7)	116.9(1)
C–Sn–C	111(4)	111(5)	110(3)	109(4)
N–Sn–C	108(2)	108(2)	109(1)	110(2)
Cl–Ga–Cl	104(2)		104(1)	
Br–Ga–Br		104(1)		104(1)
N–Ga–Cl	115(2)		115(4)	
N–Ga–Br		114(2)		114(3)

The Sn–N bond lengths in **1**-**4** range from 2.050(3) to 2.076(2) Å, similar to those in the parent compound $(Me_3Sn)_3N$ (2.04(3) Å).[13] There appears to be a slight increase in the Sn–N bond lengths of the Br analogs (**2**, **4**), but it is too slight to attribute it to sterics or electronics. The Ga–N bond lengths in **1**-**4** range from 1.828(6) Å in **3** to 1.853(3) Å in **2**. This is comparable to the shortest Ga–N bond lengths in monomeric gallium amides. For example the diazabutadiene chelated gallium bis(silyl)amide, $[(Bu^t\text{-DAB})(I)GaN(SiMe_3)_2]$,[16] and the base stabilized gallium bis(silyl)amide, $[(quin)Cl_2GaN(SiMe_3)_2]$,[17] have Ga–N distances of 1.868(2) Å and 1.866(2) Å respectively. Like the anions of **1**-**4**, these examples have $R_3Ga–NR_2$ cores. Monomeric amides with $R_2Ga–NR_2$ planar cores may exhibit short Ga–N bond lengths, in part because of slight π-interaction of the N lone pair with the Ga p_z orbital. The monomeric amides, $[(Tripp)_2GaN(H)Dipp]$[18] and $[Mes^*_2GaN(H)Ph]$,[19] have Ga–N bond lengths of 1.85(1) Å and 1.832(3) Å. These values are comparable to those found in **1**-**4**, likely reflecting the highly ionic nature of the M–N bonds in these compounds.

The mean Ga–Cl bond lengths in **1** and **3** are 2.22(1) Å and 2.21(2) Å respectively. The Ga–Br bond lengths in **2** and **4** are 2.38(2) Å and 2.37(1) Å respectively. These bond distances are longer than those in $(Bu^n_4N)[GaX_4]$[20] (X = Cl, 2.169(6) Å; X = Br, 2.31(1) Å) and in the stannylamine adducts $X_3Ga{\cdot}N(SnMe_3)_3$[4] (X = Cl, 2.184(6) Å; X = Br, 2.34(1) Å).

The anions in **1**-**4** contain a μ_3-N^{3-} fragment bound only to group 13-14 metals and can be thought of as mixed main-group metal nitrides. A search of the Cambridge

structural database reveals that only six such compounds have been characterized, five of which are tin–nitrogen compounds[13,21,22], and one of which is a dimeric aluminum nitride (discussed in Chapter 1).[1] Compare this to the analogous μ_3-O^{2-} metal oxides of which there are over 800 examples. The anions in **1**-**4** may also be viewed as tin analogs of gallium imides. A search of the Cambridge Structural Database[23] (v. 5.34) for compounds containing Ga_2NR fragments returns only 7 examples, all of which are associated as dimers or higher oligomers. Thus **1**-**4** are unique as the first monomeric compounds of this structural type.

Synthesis of (5)

Initial attempts at the complete dehalostannylation of $(Me_3Sn)_3N$ via direct reaction with $[GaCl_4]^-$ were met with some success. ^1H NMR of a 3:1 solution of $(Me_4N)[GaCl_4]$ and $(Me_3Sn)_3N$ in CD_3CN shows no free $(Me_3Sn)_3N$ within minutes of the reactants being mixed. Me_3SnCl was the predominant byproduct of this reaction as well as an unidentified compound characterized by a resonance at 0.28 ppm ($J_{^1H-^{119}Sn}$ = 59 Hz). After sitting overnight, it was noted that small colorless crystals had formed in the NMR tube. Analysis of these crystals by X-ray diffraction revealed them to be $(Me_4N)_3[(Cl_3Ga)_3N]$, (**5**). However the data was not publication quality and we were unable to obtain a bulk sample from this synthesis. One potential issue is the deprotonation of MeCN and concomitant formation of $(Me_3Sn)_3CCN$. The reported ^1H NMR resonance of $(Me_3Sn)_3CCN$ (CD_3CN) is 0.23 ppm ($J_{^1H-^{119}Sn}$ = 55 Hz).[9] Thus we cannot unambiguously identify this species in our reaction; however, we have managed to crystalized $(Me_3Sn)_3CCN$ from a reaction of $(Pr^n_4N)[GaCl_4]$ and $(Me_3Sn)_3N$ in the presence of excess $(Pr^n_4N)Cl$. We identified a different ^1H NMR shift (0.29 ppm) than the literature value, but found that our recorded Sn–H coupling ($J_{^1H-^{119}Sn}$ = 55 Hz) agreed with the reported value.

Fortuitously it was found that the Lewis adduct, $Cl_3Ga{\cdot}N(SnMe_3)_3$, when reacted with excess $(Me_4N)[GaCl_4]$ provided an alternate route to **5**. When refluxed this reaction produces an amorphous white precipitate. Dissolution of this precipitate in MeCN followed by vapor diffusion with THF afforded colorless triangular crystals of **5** in a 10% yield.

Properties of (5)

The solid state electronic spectrum of **5** contains an intense absorption in the UV region with a maximum at 240 nm (Figure 2.6). Exposure to air leads to a rapid decay of this peak, similar to the behavior observed for compound **1**. ^{1}H NMR of the amorphous intermediate that was isolated from the initial reaction of $(Me_4N)[GaCl_4]$ and $Cl_3Ga{\cdot}N(SnMe_3)_3$ showed only trace amounts of $SnMe_3$ moieties to be present. The solid state electronic spectrum of this intermediate contains a peak at 240 nm (Figure 2.7). It is inferred from this that **5** is present in the intermediate prior to crystallization from acetonitrile.

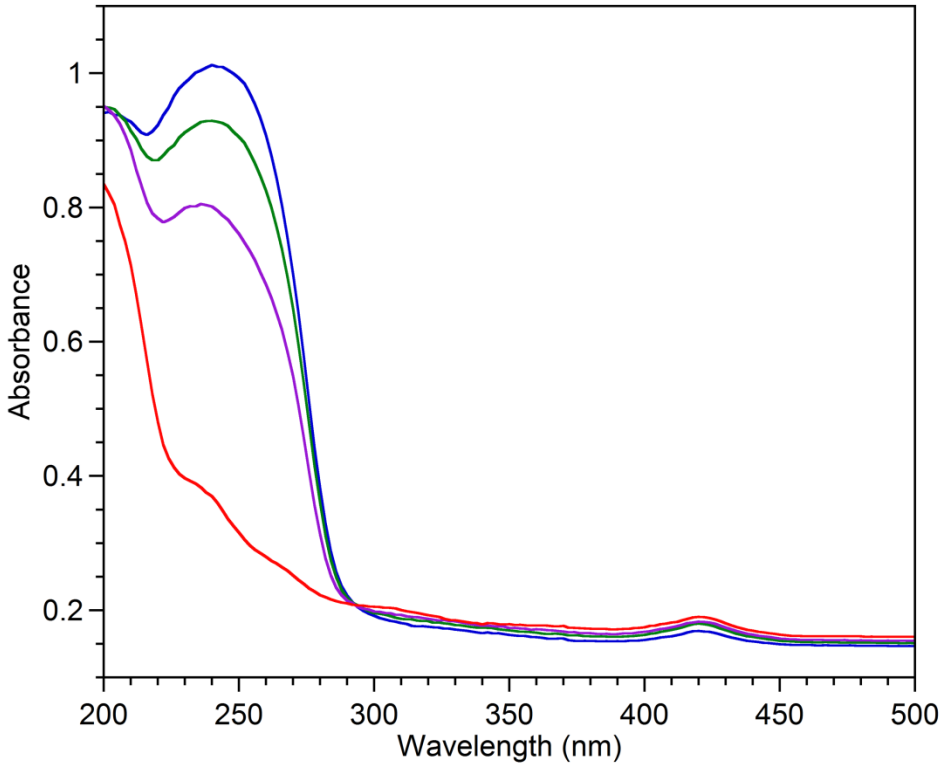

Figure 2.6. Diffuse reflectance UV-Vis spectrum of $(Me_4N)_3[(Cl_3Ga)_3N]$ (5): (blue) initial spectrum; (green) 1 min air exposure; (violet) 2 min air exposure; (red) 8 min air exposure.

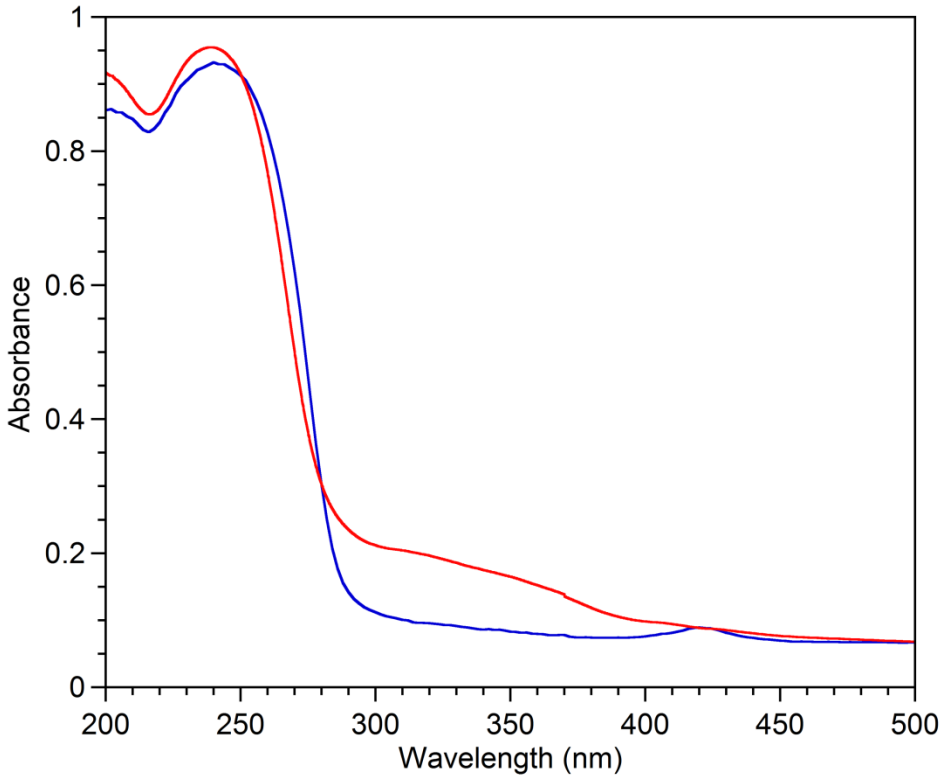

Figure 2.7. Diffuse reflectance UV-Vis spectrum of $(Me_4N)_3[(Cl_3Ga)_3N]$ (5) (blue) versus the amorphous intermediate (red).

Structure of (5)

The salt **5** crystallizes in the rhombohedral space group *R*3. The Flack *x* parameter of -0.004(12) indicates no racemic twinning. Additionally, structure refinement with merohedral twin laws did not result in significant improvement of the data. The C_3 symmetric anion in **5** consists of three $GaCl_3$ moieties bound to a μ_3-N atom (Figure 2.8). The Ga_3N core is bent slightly out of plane and the entire anion is disordered over two positions with the two μ_3-N atoms being related by reflection through the Ga–Ga–Ga plane (Figure 2.9b). The disordered $GaCl_3$ moieties are related to each other by a 40° rotation of the molecule about the C_3 rotational axis and a 180° rotation of the Ga–N bond (Figure 2.9a). Both orientations of the anion were refined without constraints.

The anion adopts a slightly pyramidal geometry similar to that of **1** and **2** with the sum of the Ga–N–Ga angles being 346° and the N atoms being on average 0.41 Å out of the Ga–Ga–Ga plane. As discussed in the previous section this bent conformation is unusual for μ_3-N compounds of the heavier p-block elements. The mean Ga–N bond length in **5** is 1.872(1) Å, slightly elongated in comparison to **1** and **2** (1.844(5) Å and 1.853(3) Å respectively). The mean Ga–Cl distance of 2.22(6) is identical to that of **1**.

The family of μ_3–nitrides with one or more group 13 metal bound to the nitrogen is small. The Ti– Ga–N dicubane, $[(Ga(\mu_3\text{-}N)_2(\mu_3\text{-}NH)Ti_3(\eta^5\text{-}C_5Me_5)_3(\mu_3\text{-}N))_2]$ contains a Ti_2NGa fragment. A Cp* ligated "broken cube" structure reported in the same article contains an Al_2NTi fragment.[24] There is also a previously

characterized zirconium carborane complex with a Zr_2NAl fragment.[25] The previously discussed structure, $[Cp^*_2((Me_3Si)_2N)Al_2N]_2$, has an Al–$NAl_2N$–Al planar core and is the only characterized group 13 metal nitride molecule. The tetrahydrazide thermolysis product, $[(GaMe)_4(GaMe_2)_4(N_2)(NH\text{-}NMe)_4]$, contains a Ga_3N–NGa_3 fragment.[26] However, **5** is the first molecule to contain a μ_3-N ligated solely gallium atoms and is thus the first reported gallium nitride molecule.

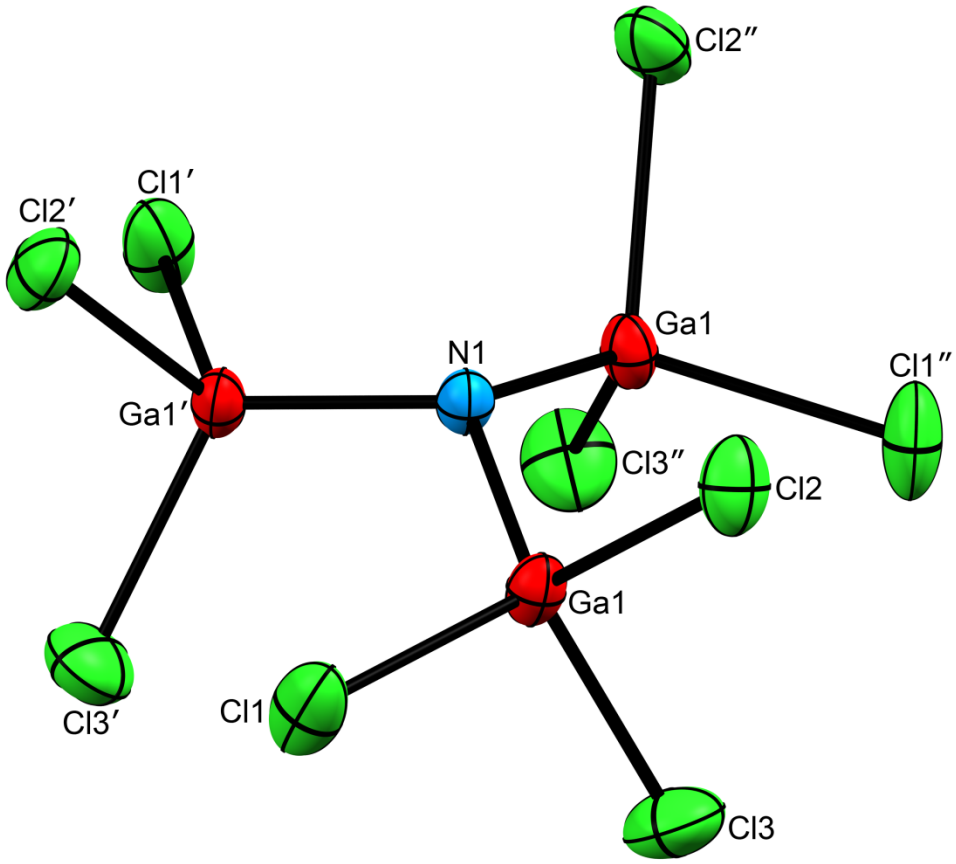

Figure 2.8. The Structure one of the disordered anions of $(Me_4N)_3[(Cl_3Ga)_3N]$ (5) with thermal ellipsoids drawn at 50% probability. The cations have been omitted for clarity. See Figure 2.9 for a diagram of the disorder in (5).

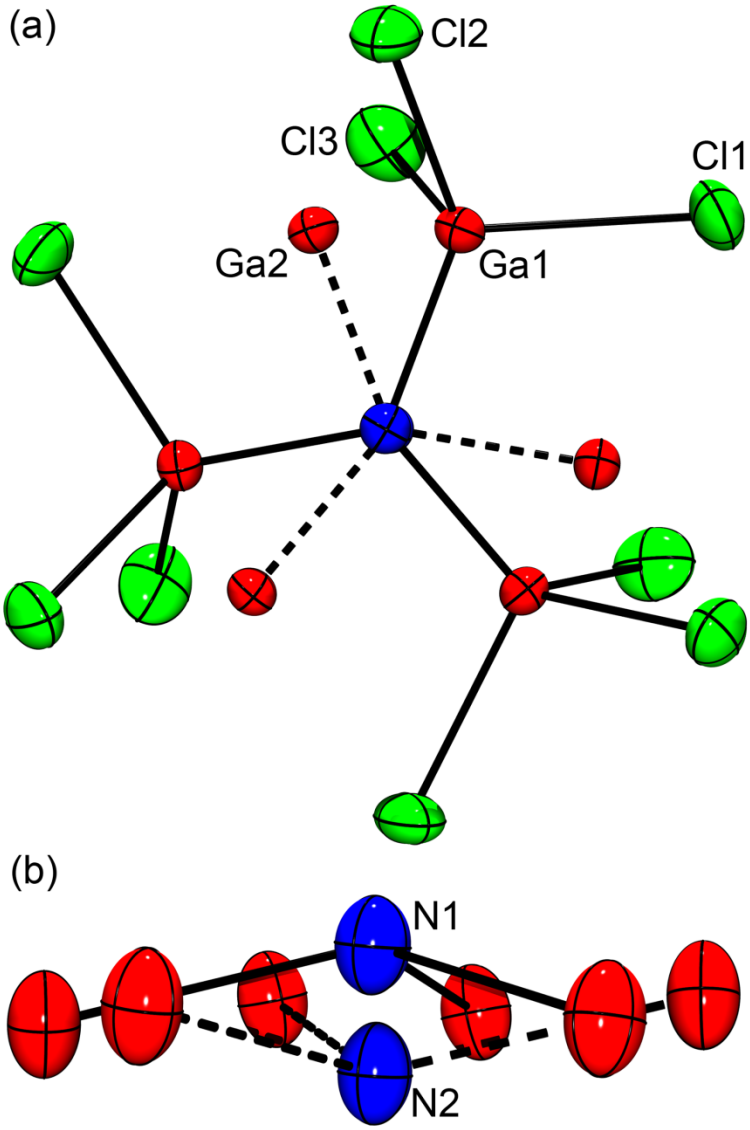

Figure 2.9. The Structure of the anion of $(Me_4N)_3[(Cl_3Ga)_3N]$ (5) showing the disorder (a) about the 3-fold rotational axis and (b) though the Ga–Ga–Ga plain. Thermal ellipsoids are drawn at 50% probability. The cations and some Cl atoms have been omitted for clarity.

Table 2.5. Selected bond lengths (Å) and angles (°) for $(Me_4N)_3[(Cl_3Ga)_3N]$, (5)

Ga1–N1	1.873(2)	Ga1–Cl1	2.215(3)
Ga1–N2	1.871(2)	Ga1–Cl2	2.275(2)
Ga–N (mean)	1.872(1)	Ga1–Cl3	2.159(2)
		Ga–Cl (mean)	2.22(6)
Ga1–N1–Ga1′	115.2(2)	Cl1–Ga1–Cl2	104.38(11)
Ga2–N2–Ga2′	115.5(2)	Cl1–Ga1–Cl3	104.52(10)
Ga–N–Ga (mean)	115.4(2)	Cl2–Ga1–Cl3	103.72(9)
N1–Ga1–Cl1	113.97(7)	Cl–Ga–Cl (mean)	104.2(4)
N1–Ga1–Cl2	111.1(3)		
N1–Ga1–Cl3	117.8(3)		
N–Ga–Cl (mean)	114(3)		

Conclusion

It has been demonstrated that, when reacted with $[GaX_4]^-$, $(Me_3Sn)_3N$ and $Cl_3Ga{\cdot}N(SnMe_3)_3$ can function as effective N sources to novel Ga–(μ_3-N) anionic compounds. These compounds are unique for two reasons. First, molecules that contain μ_3-N bonded to only main group metals of the *p*-block are rare. There are only six such example in the literature. The three unique anions reported in the current work expand this number to nine. Second, the anions in **1**-**5** do not oligomerize by intermolecular N–Ga association. Most monomeric compounds of this type have bulky mesityl or terphenyl ligands. This research identifies new synthetic routes to access activated Ga–N compounds. Compounds containing only Ga–N and other M–N bonds are potential precursors in the low temperature formation of GaN materials. The observation that Me_3SnCl is eliminated from **1** at relatively low temperatures lends credence to this idea.

Acknowledgements

Jason R. Jones and Savannah C. DeLorenzo first crystallized **2** and **4**; their work is included for completeness. Dr. Milan Gembicky provided helpful discussions on the structure of **5**.

This chapter contains material that has been published. Wilson, Robert J.; Jones, Jason R.; Bennett, Miriam V. "Unprecedented gallium-nitrogen anions: synthesis and characterization of $[(Cl_3Ga)_3N]^{3-}$ and $[(Cl_3Ga)_2NSnMe_3]^{2-}$" *Chem. Commun.* **2013**, *49*, 5049-5051.

References

(1) Schulz, S.; Häming, L.; Herbst-Irmer, R.; Roesky, H. W.; Sheldrick, G. M. *Angewandte Chemie International Edition in English* **1994**, *33*, 969.

(2) Plenio, H.; Roesky, H. W.; Noltemeyer, M.; Sheldrick, G. M. *Angewandte Chemie International Edition in English* **1988**, *27*, 1330.

(3) Bennett, M. V.; Stoian, S.; Bominaar, E. L.; Muenck, E.; Holm, R. H. *J. Am. Chem. Soc.* **2005**, *127*, 12378.

(4) Cheng, Q. M.; Stark, O.; Merz, K.; Winter, M.; Fischer, R. A. *J. Chem. Soc., Dalton Trans.* **2002**, 2933.

(5) Shishido, K.; Kojima, S. *J. Org. Chem.* **1964**, *29*, 907.

(6) Dolomanov, O. V.; Bourhis, L. J.; Gildea, R. J.; Howard, J. A. K.; Puschmann, H. *J. Appl. Crystallogr.* **2009**, *42*, 339.

(7) Sheldrick, G. *Acta Cryst.* **2008**, *A64*, 112.

(8) Macrae, C. F.; Bruno, I. J.; Chisholm, J. A.; Edgington, P. R.; McCabe, P.; Pidcock, E.; Rodriguez-Monge, L.; Taylor, R.; van de Streek, J.; Wood, P. A. *J. Appl. Crystallogr.* **2008**, *41*, 466.

(9) Hillwig, R.; Harms, K.; Dehnicke, K. *Z. Naturforsch., B Chem. Sci.* **1997**, *52*, 145.

(10) Hering, C.; Lehmann, M.; Schulz, A.; Villinger, A. *Inorg. Chem.* **2012**, *51*, 8212.

(11) Ristic, M.; Popovic, S.; Music, S. *Mater. Lett.* **2005**, *59*, 1227.

(12) Cheng, Q. M.; Stark, O.; Stowasser, F.; Wohlfart, A.; Fischer, R. A. *J. Mater. Chem.* **2002**, *12*, 2470.

(13) Appel, A.; Kober, C.; Neumann, C.; Noeth, H.; Schmidt, M.; Storch, W. *Chem. Ber.* **1996**, *129*, 175.

(14) Jockisch, A.; Schmidbaur, H. *Z. Naturforsch., B: Chem. Sci.* **1999**, *54*, 1529.

(15) Jockisch, A.; Schmidbaur, H. *Z. Naturforsch., B: Chem. Sci.* **1998**, *53*, 1386.

(16) Antcliff, K. L.; Baker, R. J.; Jones, C.; Murphy, D. M.; Rose, R. P. *Inorg. Chem.* **2005**, *44*, 2098.

(17) Luo, B.; Young, V. G.; Gladfelter, W. L. *J. Organomet. Chem.* **2002**, *649*, 268.

(18) Waggoner, K. M.; Ruhlandt-Senge, K.; Wehmschulte, R. J.; He, X.; Olmstead, M. M.; Power, P. P. *Inorg. Chem.* **1993**, *32*, 2557.

(19) Brothers, P. J.; Wehmschulte, R. J.; Olmstead, M. M.; Ruhlandt-Senge, K.; Parkin, S. R.; Power, P. P. *Organometallics* **1994**, *13*, 2792.

(20) Rudawska, K.; Ptasiewicz-Bak, H. *J. Coord. Chem.* **2003**, *56*, 1567.

(21) Kober, C.; Kroner, J.; Storch, W. *Angew. Chem. Int. Ed., Engl.* **1993**, *32*, 1608.

(22) Kober, C.; Noth, H.; Storch, W. *Chem. Ber./Recl.* **1997**, *130*, 765.

(23) Allen, F. *Acta Crystallographica Section B* **2002**, *58*, 380.

(24) Garcia-Castro, M.; Martin, A.; Mena, M.; Yelamos, C. *Chem.--Eur. J.* **2009**, *15*, 7180.

(25) Wang, Y.; Wang, H.; Wang, H.; Chan, H.-S.; Xie, Z. *J. Organomet. Chem.* **2003**, *683*, 39.

(26) Uhl, W.; Rezaeirad, B.; Layh, M.; Hagemeier, E.; Wuerthwein, E.-U.; Ghavtadze, N.; Kuzu, I. *Chem.--Eur. J.* **2010**, *16*, 12195.

Chapter 3: Metal–Nitrogen Cage Compounds of Indium and Tin: The Synthesis and Structure of $(Et_4N)[(ClIn)_6(NSnMe_3)_5(\mu\text{–}Cl)_3]$

Introduction

Compared to their aluminum (Al) and gallium (Ga) congeners oligomeric indium–nitrogen (In–N) compounds are less prevalent and display significantly less structural variety. The most common architectures are dimeric In amides with In_2N_2 rhomboid cores (Figure 3.1a) and tetrameric indium imides with In_4N_4 cubane cores (Figure 3.1b). Singular examples of deviations from these common architectures include: a diamidophenylene tetramer in which eight μ_2-NR bridging groups stabilize an In_4 tetrahedron (Figure 3.1c);[1] a mixed amide-imide "broken cube" with an In_3N_4 core (Figure 3.1d);[2] an oligimeric In hydrazide with an In_4N_4 core containing a bridging N–N group (Figure 3.1e);[3] and an eight member In_4N_4 ring stabilized by silylamide groups (Figure 3.1f).[4] Conspicuously absent among the characterized In–N compounds are higher oligomers, such as hexamers, heptamers, or octamers, which have been reported for imides of aluminum and gallium.[5] A search of the Cambridge Structural Database[6] (version 5.34) reveals 10 examples of In–N compounds containing four In atoms and no examples with more than four In atoms.

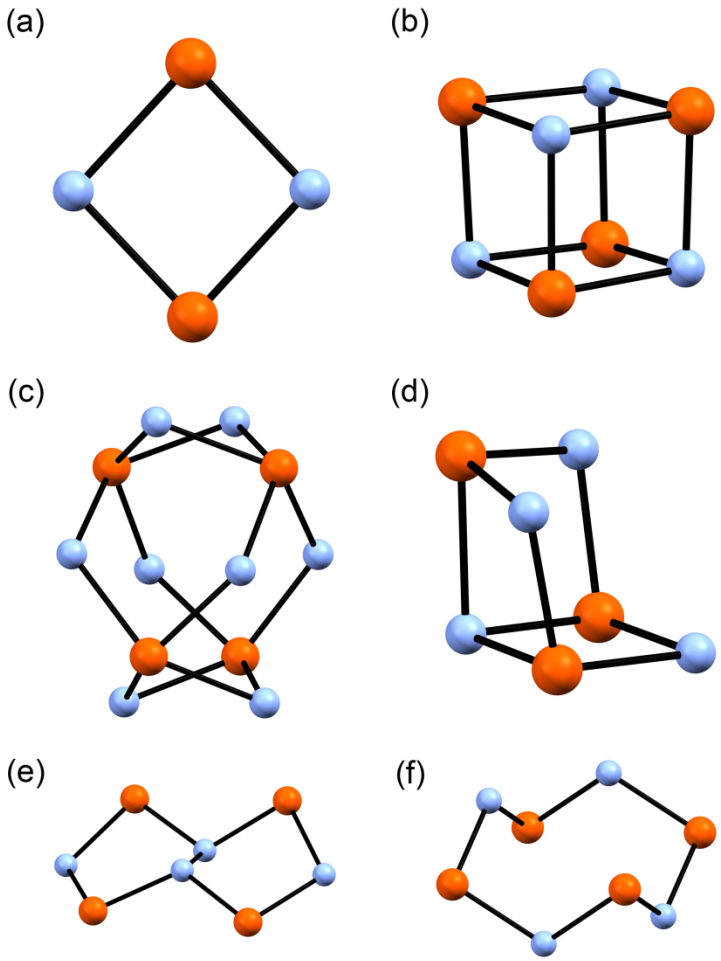

Figure 3.1. Core geometries of oligomeric indium nitrogen compounds: (a) common In_2N_2 rhomboid; (b) common In_4N_4 cubane; (c) In_4 tetrahedron stabilized by eight μ-N linker atoms; (d) In_3N_4 "broken cube"; (e) In_4N_4 with hydrazide bridge; (f) In_4N_4 eight member ring. Orange = In, Blue = N.

The Lewis adduct, $Cl_3In{\cdot}N(SnMe_3)_3$, decomposes in solution to form Me_3SnCl along with other unidentified products; it was proposed that dimerization to form $[Cl_2InN(SnMe_3)_2]_2$ was occurring, though this was not confirmed.[7] Introduction of anionic In halides into this system is a potential strategy for isolating such higher nuclearity compounds as anions. Anionic In–N clusters would be of interest given the successful employment of anionic compounds in the synthesis of colloidal quantum dots.[8-12]

Thus we explored the reaction of $Cl_3In{\cdot}N(SnMe_3)_3$ with $(Et_4N)_2[InCl_5]$ in THF. From this system we have isolated a salt of an unprecedented In–N anionic cluster, $(Et_4N)[(ClIn)_6(NSnMe_3)_5(\mu\text{-}Cl)_3]$, (Et_4N)(**1**). The anion **1** contains an In_6N_5 core and thus is the highest nuclearity In–N cage compound yet isolated. The synthesis, structure, and solution and solid state properties of (Et_4N)**1** are reported here.

Experimental Section

Preparation of Compounds

All manipulations were carried out under a pure dinitrogen atmosphere using standard Schlenk and glove-box techniques. Anhydrous tetrahydrofuran (THF), purchased from EMD, diethylether (Et_2O), purchased from EMD, and acetonitrile (MeCN), purchased from Burdick and Jackson were stored over activated 4 Å molecular sieves under a pure dinitrogen atmosphere. The compound $Cl_3In{\cdot}N(SnMe_3)_3$ was prepared according to the literature procedure.[7] Preparation of the salt $(Et_4N)_2[InCl_5]$ is described in appendix B. Elemental analysis was performed at the Mikroanalytisches Laboratorium Kolbe, Mülheim an der Ruhr, Germany.

$(Et_4N)[(ClIn)_6(NSnMe_3)_5(\mu\text{-}Cl)_3]$ (Et_4N)(1). A suspension of $(Et_4N)_2[InCl_5]$ (0.15 g, 0.27 mmol) and $Cl_3In{\cdot}N(SnMe_3)_3$ (0.56 g, 0.77 mmol) in 3.3 mL of anhydrous THF was stirred for 24 h. Solids were removed by filtration through celite and the filtrate was then concentrated by diffusion into toluene in a sealed vial. Faint yellow crystals formed over the course of a week. After an additional 12 days the crystals were collected on a fritted glass filter and washed with MeCN (4 × 1 mL) and Et_2O (4 × 1 mL) and dried *in vacuo* to afford 116 mg (0.057 mmol, 37%) of (Et_4N)**1**. Anal. Calcd for $C_{23}H_{65}Cl_9In_6N_6Sn_5$: C, 13.63; H, 3.23; In, 33.98; N, 4.15; Sn, 29.28. Found: C, 13.99; H, 3.29; In, 33.74; N, 4.12; Sn, 29.12.

$(Et_4N)[(ClIn)_6(NSnMe_3)_5(\mu\text{-}Cl)_3]$ (Et_4N)(1) (Synthesis 2). A suspension of $(Et_4N)_2[InCl_5]$ (0.26 g, 0.47 mmol) and $Cl_3In{\cdot}N(SnMe_3)_3$ (0.82 g, 1.1 mmol) in 5.7 mL of anhydrous THF was stirred for 48 h. The remaining solids were removed by filtration through celite and the filtrate was concentrated by diffusion into toluene in a sealed vial. Faint yellow crystals formed within 6 days and were collected on a fritted glass filter and washed with MeCN (4 × 1 mL) then Et_2O (4 × 1 mL) and dried *in vacuo* to afford 146 mg (0.072 mmol, 32%) of (Et_4N)**1**. ^{1}H NMR (CD_3CN): 0.42 ppm, s, $J_{^1H\text{-}^{119}Sn}$ = 56 Hz; 0.43 ppm, s, $J_{^1H\text{-}^{119}Sn}$ = 55 Hz; 0.60 ppm, s, $J_{^1H\text{-}^{119}Sn}$ = 59 Hz; 0.62 ppm, s, $J_{^1H\text{-}^{119}Sn}$ = 57 Hz; 0.64 ppm, s, $J_{^1H\text{-}^{119}Sn}$ = 58 Hz; 0.65 ppm, s, $J_{^1H\text{-}^{119}Sn}$ = 60 Hz. ^{1}H NMR (THF-d_8): 0.43 ppm, s, $J_{^1H\text{-}^{119}Sn}$ = 55 Hz; 0.44 ppm, s, $J_{^1H\text{-}^{119}Sn}$ = 55 Hz; 0.63 ppm, s, $J_{^1H\text{-}^{119}Sn}$ = 59 Hz; 0.65 ppm, s, $J_{^1H\text{-}^{119}Sn}$ = 58 Hz; 0.67 ppm, s, $J_{^1H\text{-}^{119}Sn}$ = 58 Hz; 0.68 ppm, s, $J_{^1H\text{-}^{119}Sn}$ = 59 Hz. ES$^-$-MS (MeCN): *m/z* 1897 ($[In_6(NSnMe_3)_5Cl_9]^-$). Diffuse reflectance spectrum: λ_{max} (nm) 263, 291 (sh), 323. Anal. Calcd for $C_{23}H_{65}Cl_9In_6N_6Sn_5$: C 13.63, H 3.23, N 4.15. Found: C 13.89, H 3.37, N 4.04.

X-ray Structure Determination

Crystals were coated in Paratone oil and mounted by mean of a glass capillary fiber on a Bruker APEX-II CCD area detector instrument operated by the APEX

software package. Data reduction was performed by SAINT, absorption correction was applied using SADABS, and the space group was assigned using XPREP. The structure of (Et_4N)**1** was solved by direct methods and refined against all data by full-matrix least squares on F_2. Hydrogen atoms were attached at idealized positions on carbon atoms and were refined as riding atoms with uniform isotropic thermal parameters. Structure solution, refinement, graphics and report generation were performed using SHELXTL[13] and Mercury.[14]

Other Physical Measurements

The solid state electronic reflectance spectra were recorded on a JASCO V-670 UV-Vis spectrophotometer fitted with and integrating sphere. NMR spectra were collected on a Varian Inova 400 MHz instrument at 30°C with chemical shifts referenced to the signal of residual protons in the deuterated solvent. Infrared spectroscopy was performed on a Perkin-Elmer RX I spectrometer equipped with an attenuated total reflectance accessory. Mass spectrometry was performed on a Thermo Finnigan LCQ Duo ion trap spectrometer with an ESI ion source and the data was examined using mMass software.[15]

Table 3.1. Crystallographic data for $(Et_4N)[(ClIn)_6(NSnMe_3)_5(\mu\text{-}Cl)_3]$, (Et_4N)1.

	(Et_4N)**1**
formula	$C_{23}H_{65}Cl_9In_6N_6Sn_5$
formula weight, g/mol	2027.23
T, K	100
crystal system	Orthorhombic
space group	*Ama*2
a, Å	19.7198(10)
b, Å	25.7427(14)
c, Å	11.3287(6)
α, deg	90
β, deg	90
γ, deg	90
V, Å^3	5750.9(5)
Z	4
ρ_{calc}, g/cm^3	2.341
2θ range, deg	2.22 to 32.03
GOF (F^2)	1.04
R_1/wR_2, %	3.87/7.63

Results and Discussion

Synthesis of (Et_4N)**1**

Initial reactions were carried out in MeCN, in which $(Et_4N)_2[InCl_5]$ is soluble; however no products were isolated from this system. Experiments in THF had more positive results, despite the sparing solubility of $(Et_4N)_2[InCl_5]$ in this solvent. It was found that a simple one-pot synthesis, in which $(Et_4N)_2[InCl_5]$ and $Cl_3In{\cdot}N(SnMe_3)_3$ are combined in a single flask in an approximate 2:5 ratio and stirred for 24 h, was the most successful. The ^1H NMR spectrum (CD_3CN) of the solid remaining after 24 h shows the presence of $[Me_3SnCl_2]^-$ and additional Et_4N^+ that may be from unreacted $(Et_4N)_2[InCl_5]$. Removal of solids by filtration through celite followed by slow concentration of the solution for 3-5 days results in the precipitation of faint yellow crystals of $(Et_4N)[(ClIn)_6(NSnMe_3)_5(\mu\text{-}Cl)_3]$, (Et_4N)**1**. These are then rinsed with MeCN to remove the $(Et_4N)[Me_3SnCl_2]$ byproduct. This procedure consistently produces the desired product in a 32-37% yield. Several samples have been examined by X-ray diffraction and no other products besides (Et_4N)**1** and $(Et_4N)[Me_3SnCl_2]$ have been identified. We therefore attribute the low yield to incomplete dissolution of $(Et_4N)_2[InCl_5]$. In light of the extremely low solubility of $(Et_4N)_2[InCl_5]$ in THF it is somewhat impressive that any appreciable quantity of (Et_4N)**1** is isolated from this system. This may be explained by the reaction stoichiometry which requires only a $1/5^{th}$ equivalent $(Et_4N)_2[InCl_5]$ (Scheme 3.1).

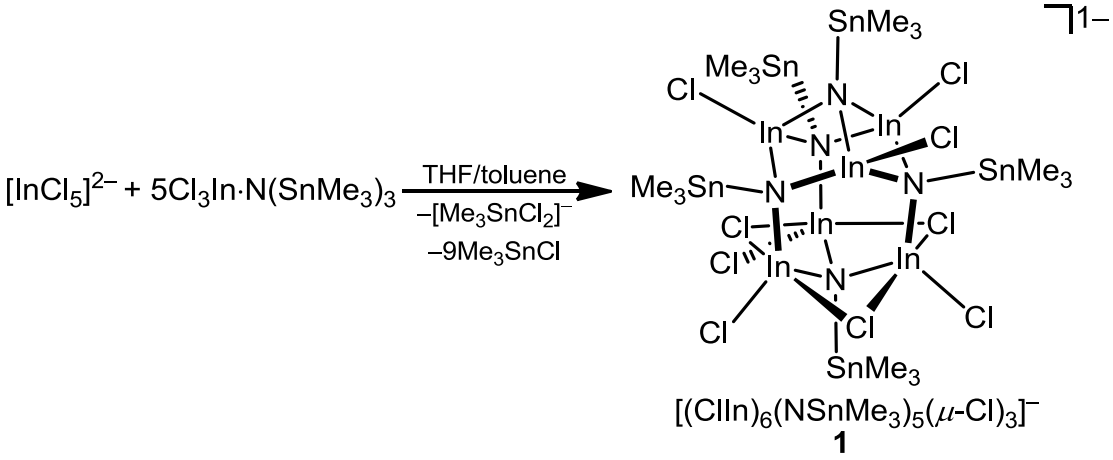

Scheme 3.1. Formation $[(ClIn)_6(NSnMe_3)_5(\mu\text{-}Cl)_3]^-$ (1) from the reaction of $[InCl_5]^{2-}$ with $Cl_3In{\cdot}N(SnMe_3)_3$ in THF.

Properties of (1)

The electronic spectrum of (Et_4N)**1** reveals broad absorptions at 263 nm and 323 nm with a shoulder between at 291 nm. These peaks decay upon exposure of the sample to air for 48 h (Figure 3.2). The infrared spectra of the air exposed sample shows a broad band at 3400 cm^{-1}, indicative of O–H stretching of adsorbed water molecules, and a band and shoulder at 3325 cm^{-1} and 3220 cm^{-1} respectively that are likely due to O–H stretching of hydroxyl groups bound to a metal (Figure 3.3).[16] The salt (Et_4N)**1** is soluble in THF and MeCN and is insoluble in CH_2Cl_2. In theory, **1** should have three chemically distinct resonances in the ^1H NMR spectrum consisting of the three "equatorial" $SnMe_3$ groups bound to N2, N3, and N3′, one "axial" group bound to N1, and a second axial group bound to N4 which is adjacent to the μ_2-Cl atoms (See Figure 3.8 for structure of **1**). However, a significantly more complex

spectrum is observed in both THF-d_8 and CD_3CN (Figure 3.4), suggesting the possibility of restricted rotation of the Sn–N bond, conformational equilibrium, or perhaps an interaction with the coordinating solvent. There are three clusters of peaks in the spectra in both solvents. In THF-d_8 the most downfield of these clusters occur at 0.43, 0.44, and 0.45 ppm. These peaks are tentatively assigned to the protons of the $SnMe_3$ group bound to N1. Two large peaks at 0.63 and 0.65 ppm are tentatively assigned to the "equatorial" $SnMe_3$ protons. Lastly, two peaks at 0.67 and 0.68 ppm are assigned to the protons of the $SnMe_3$ group bound to N4. Similar assignments can made for the ^1H NMR spectrum in CD_3CN. Peaks at 0.42, 0.43, and 0.44 ppm are tentatively assigned to the protons of the $SnMe_3$ group bound to N1. The peaks at 0.60 and 0.62 ppm are tentatively assigned to the "equatorial" $SnMe_3$ protons. The peaks at 0.64 and 0.65 ppm are then assigned to the protons of the $SnMe_3$ group bound to N4.

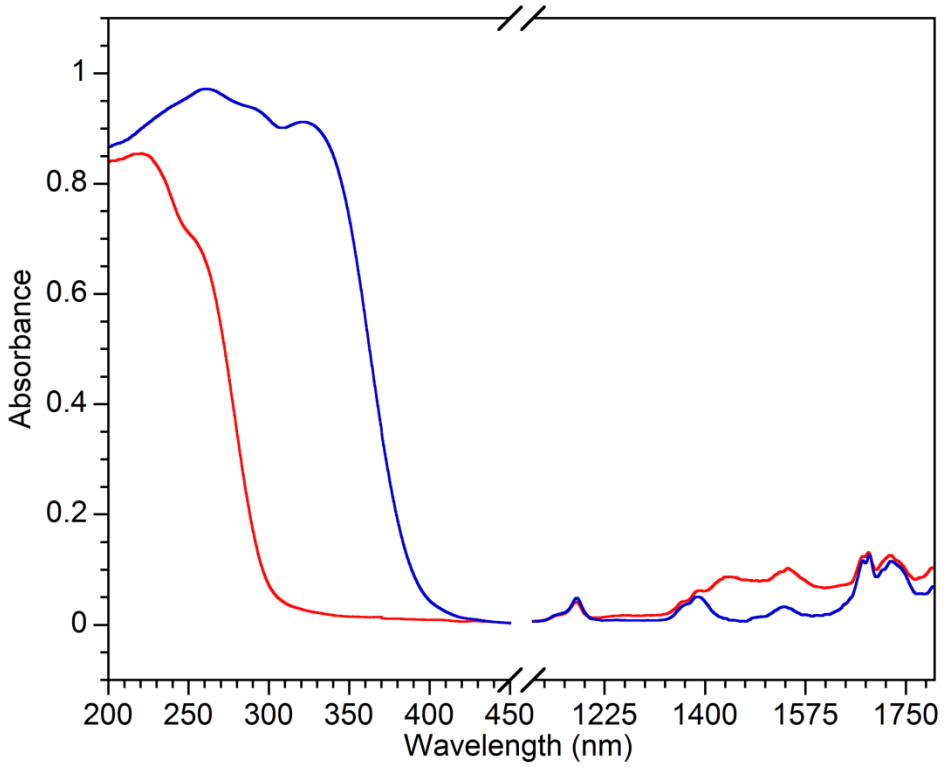

Figure 3.2. The diffuse reflectance UV-Vis spectrum of $(Et_4N)[(ClIn)_6(NSnMe_3)_5(\mu\text{-}Cl)_3]$, (Et_4N)1, before (blue) and after (red) exposure to air for 48 h.

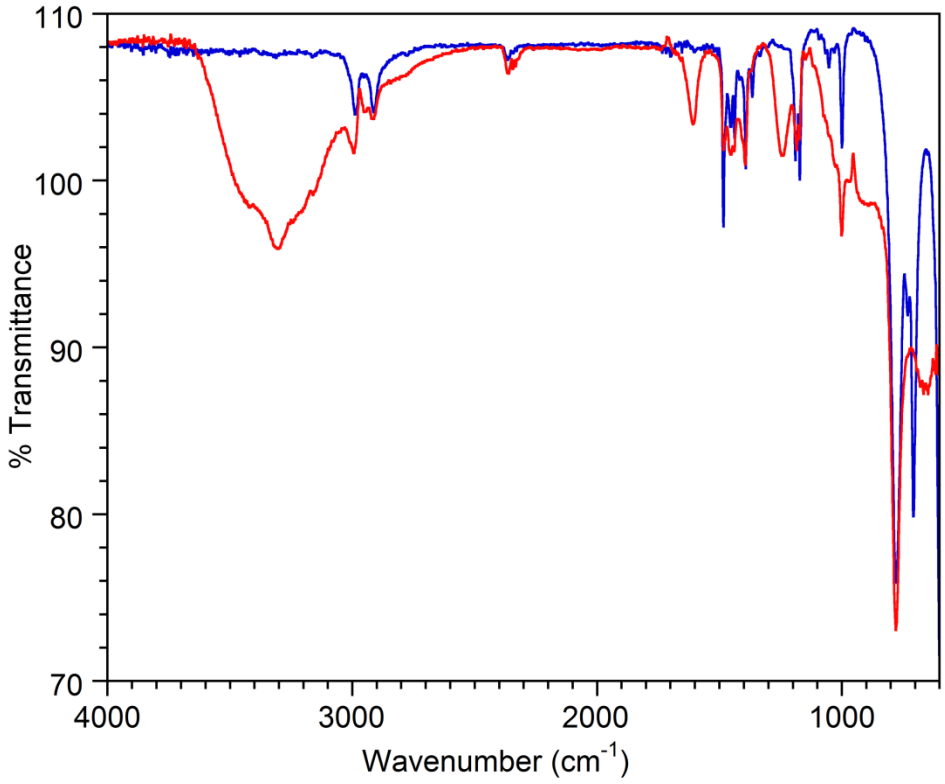

Figure 3.3. The IR spectrum of $(Et_4N)[(ClIn)_6(NSnMe_3)_5(\mu\text{-}Cl)_3]$, (Et_4N)1, before (blue) and after (red) exposure to air for 48 h.

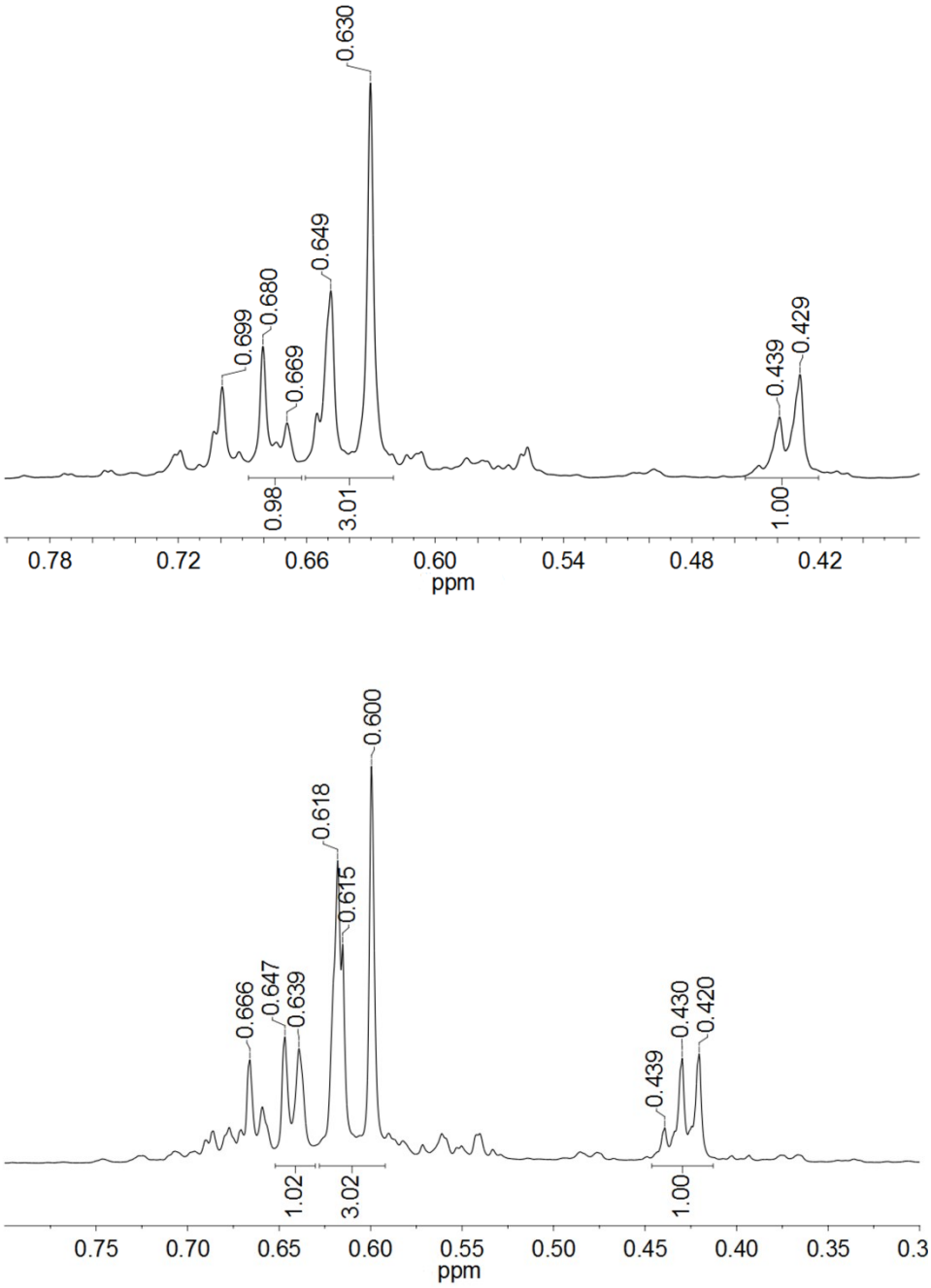

Figure 3.4. The ^{1}H NMR spectrum of $[(ClIn)_6(NSnMe_3)_5(\mu\text{-}Cl)_3]^-$ (1) in THF-d_8 (top) and CD_3CN (bottom).

The anion **1** exhibits stability to mild heat in THF as inferred from the lack of change in the ^{1}H NMR spectrum when heated as high as 75 °C. When heated to 85 °C for several days some degradation of the compound occurs as indicated by the appearance of a resonance at 0.06 ppm, assigned as Me_4Sn, as well as the appearance of peaks at 0.56, 0.58, 0.59, and 0.61 ppm (Figure 3.5a). These resonances have not been assigned, though the peak at 0.59 ppm corresponds with the chemical shift previously observed in our work for Me_3SnCl.

In contrast, **1** is much less stable in MeCN. A sample heated to 65 °C over the course of one week in CD_3CN decomposes to $Me_3SnCl/[Me_3SnCl_2]^-$ (0.62 ppm), Me_4Sn (0.06 ppm), and an unknown compound (0.29 ppm) with integration ratios of 4:1:2 respectively (Figure 3.6b).

Electrospray ionization mass spectrometry (ESI-MS) was used to analyze **1** in MeCN. In the negative ion mode the parent peak of $[In_6(NSnMe_3)_5Cl_9]^{1-}$ at 1897 *m*/*z* was clearly observed and the calculated isotope pattern was in excellent agreement with the observed pattern (Figure 3.6). No fragments of interest were observed in positive ion mode.

Tandem mass spectrometry (MS/MS) is a technique in which ions of a specific *m*/*z* in a spectrum may be selectively fragmented to produce a new spectrum. This technique was used to study the decomposition of **1** by successively targeting the most abundant mass peaks for fragmentation. Fragmentation of the parent ion at 1897 *m*/*z* produced a new spectrum with an intense peak at 1697 *m*/*z*. The loss of 200 amu corresponds to the isotopic mass of Me_3SnCl. Fragmentation of 1697 *m*/*z* resulted in a

spectrum with the most intense peak located at 1517 *m*/*z*. The loss of $SnMe_4$ is consistent with the difference of 180 amu and has also been observed in solution. Further fragmentation of 1517 *m*/*z* again results in a difference of 180 amu to the most abundant peak at 1337. Thus **1** fragments in the order 1897 → 1697 → 1517 → 1337 *m*/*z* corresponding to a loss of Me_3SnCl, followed by the successive loss of two units of Me_4Sn (Figure 3.7).

(a)

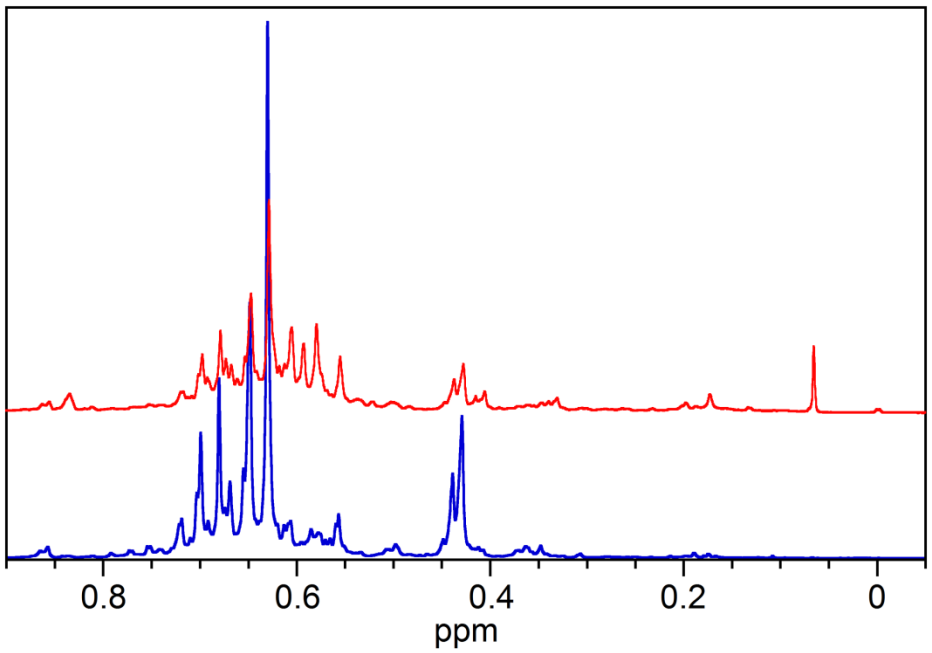

(b)

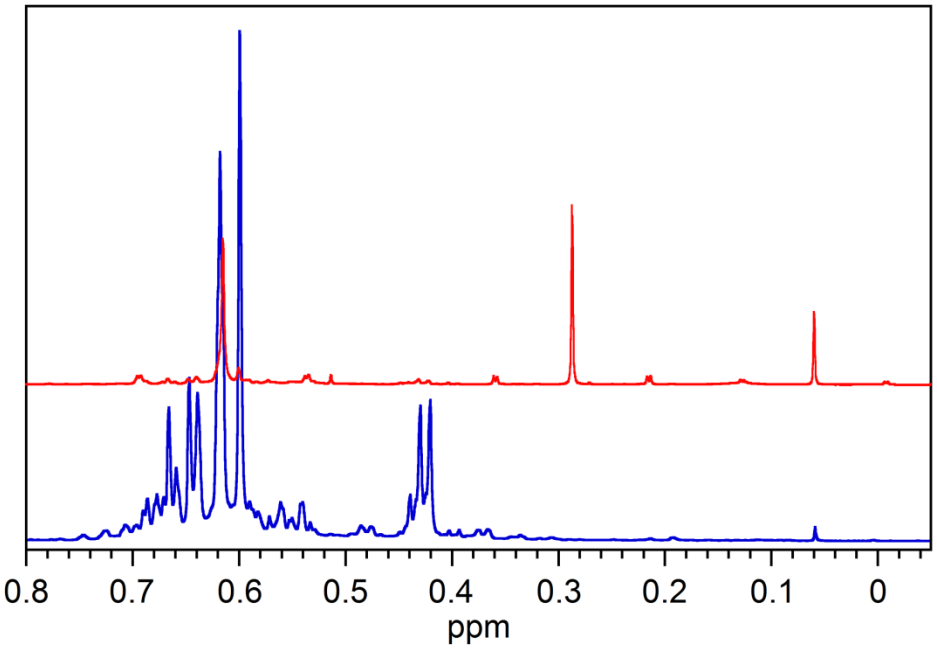

Figure 3.5. ^{1}H NMR of $[(ClIn)_6(NSnMe_3)_5(\mu\text{-}Cl)_3]^-$ (1) before (blue) and after (red) heating to (a) 85 °C in THF-d_8 and (b) 65 °C in CD_3CN.

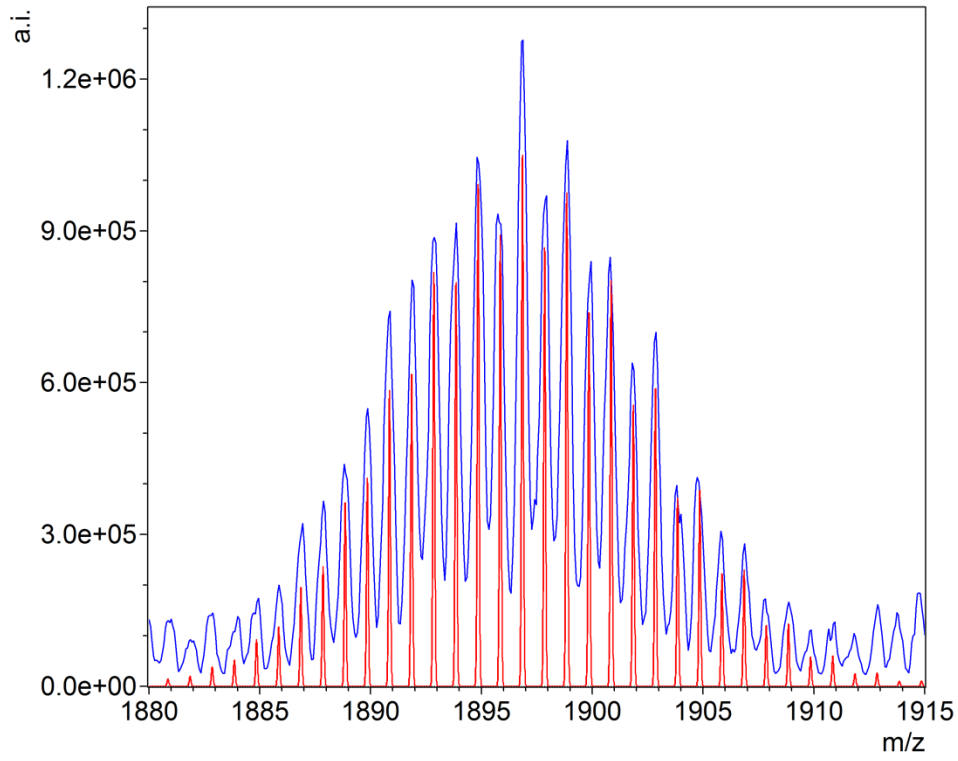

Figure 3.6. The recorded (blue) and an calculated (red) ESI mass spectrum in negative ion mode for $[(ClIn)_6(NSnMe_3)_5(\mu\text{-}Cl)_3]^-$ (1).

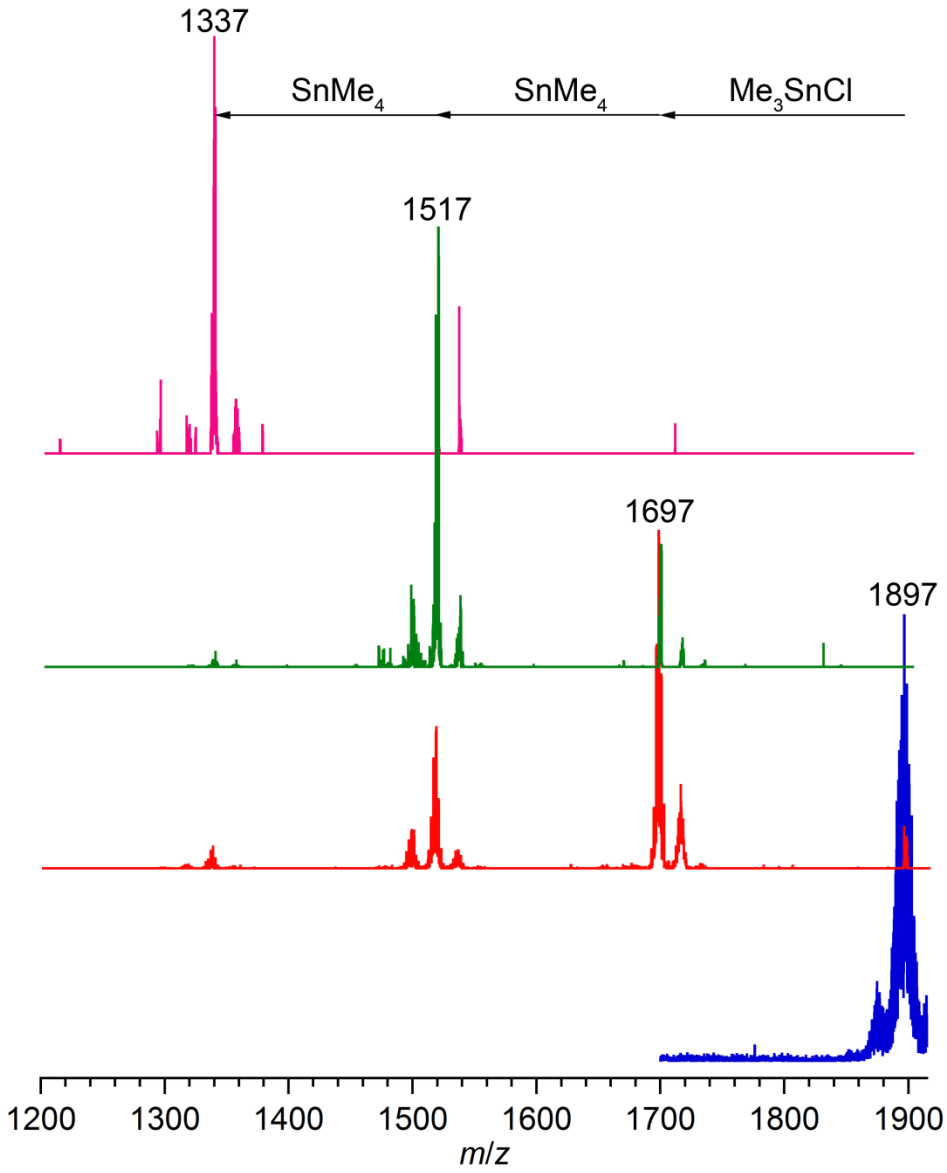

Figure 3.7. Tandem mass spectrometry of $[(ClIn)_6(NSnMe_3)_5(\mu\text{-}Cl)_3]^-$ (1): (Blue) initial spectrum; (red) 1897; (green) 1897→1697; (pink) 1897→1697→1517

Structure of (1).

The salt (Et_4N)**1** crystalizes in the non-centrosymmetric space group *Ama*2 with a Flack *x* parameter of -0.006(34) indicating no racemic twinning. As we are cognizant of the similarity in the size of tin and indium, the structure was refined with the metal sites switched, resulting in R_1/wR_2 (%) values of 3.94/8.78 versus 3.87/8.27 for the correctly assigned metal sites. A crystallographic mirror plane bisects the anion and passes through the metals Sn1, Sn2, Sn4, In2, and In3.

The structure of **1** consists of a cage of six indium atoms arranged in a trigonal antiprism with μ_3-N atoms capping five of the eight possible In_3 faces (Figure 3.8). There is a 3-fold rotational axis (non-crystallographic) passing through the Sn1–N1 and N4–Sn4 bonds giving **1** apparent C_{3v} symmetry (Figure 3.9a). There is an asymmetry of the In–In distances, with the average inter-metal In1–In1′/In1–In2 distance being 3.13(2) Å while that for In4–In4′/In4–In5 is 3.400(4) Å. This asymmetry arises from three μ_2-Cl atoms that form bridges between In4, In4′, and In5 leading to an expansion of the In–In distance and these atoms adopting a distorted trigonal bipyramidal geometry. The In1, In1′, and In2 atoms adopt a T_d geometry with the distance between these atoms approaching the sum of their crystal radii (3.10 Å) as calculated by Slater.[17]

The In–N bond distances must be split into two groups, $N–In_{tetrahedral}$ and $N–In_{trigonal\ bipyramidal}$. The average distance between the tetrahedral coordinated In atoms (In1 and In2) and their adjacent N atoms (N1, N2, and N3) is 2.19(2) Å with the

individual distances ranging from 2.164(5) Å to 2.215(6) Å. This value is within error of In–N distances in the In imide tetrameric cubanes, $[ClIn–NBu^t]_4$ (2.181(6) Å),[2] $[MeIn–NBu^t]_4$ (2.193(2) Å),[18] and $[MeIn–N(C_6F_5)]_4$ (2.21(2) Å).[19] The Lewis adduct $Cl_3In{\cdot}N(SnMe_3)_3$ has a somewhat shorter In–N bond length of 2.148(6) Å.[7] The N atoms (N2, N3, and N4) in **1** bound to the trigonal bipyramidal coordinated In atoms (In3 and In4) occupy equatorial positions (the μ_2-Cl occupy the axial positions) and thus the bonds have greater "s" character. This leads to a somewhat shorter average In–N distance of 2.12(2) Å with the values ranging from 2.097(5) Å to 2.130(4) Å. The imido cubane, $[MeIn(THF)N(C_6H_4F)]_4$,[20] contains THF ligated to each of the In atoms which adopt a distorted trigonal biyramidal geometry with the THF molecules occupying one of the axial positions. In this structure there are then two In–N equatorial bonds, the shortest of which is 2.136(5) Å; a value that is within error of $N–In_{trig.\ bipyr.}$ in **1**.

The Sn–N bond lengths in **1** range from 2.046(6) Å to 2.112(6) Å with a mean value of 2.10(3) Å. However, the Sn1–N1 bond is significantly shorter than the other three. Since N1 caps the contracted In1–In2–In2′ (*vide supra*) face, this alters the electronic environment of the N atom and may explain the slight difference in bond length. Other In/Sn–N compounds such as the adduct, $Cl_3In{\cdot}N(SnMe_3)_3$,[7] and the stannylamide dimers, $[Cl(Me)InN(SnMe_3)_2]_2$ and $[Cl(Et)InN(SnMe_3)_2]_2$,[21] have mean Sn–N bond lengths of 2.166(2) Å, 2.126(9) Å, and 2.12(1) Å respectively.

The terminal In–Cl bonds in **1** have an average length of 2.32(2) Å with no significant difference observed in the $In_{tetrahedral}$–Cl bonds (Cl1 and Cl2) versus the

$In_{trig.\ bipyr.}$–$Cl_{equatorial}$ (Cl3 and Cl4). The observed In–Cl bond length is slightly shorter than the value of 3.365(1) Å in the adduct $Cl_3In{\cdot}N(SnMe_3)_3$,[7] but within error of the value of 2.321(3) Å in the imido cubane $[ClInNBu^t]_4$.[2] The terminal In–Cl bonds in **1** are also shorter than those in tetrahedral $[InCl_4]^-$ (2.350(5) Å in $[Bu^n{}_4N][InCl_4]$ and 2.34(1) Å in $[(Ph_3P)_2CH_2][InCl_4]_2$)[22,23] and in the equatorial positions of trigonal bipyramidal $[InCl_5]^{2-}$ (2.415(6) Å in $[Ph_2Cl_2P]_2[InCl_5]$ and 2.413(4) Å in $[Ph_4P]_2[InCl_5]$)[24,25]. The In–(μ_2-Cl) bonds have an average length of 2.71(2) Å, which is quite long for In–Cl, but is comparable to other In–Cl bonds where the Cl forms a μ_2-bridge and occupies the axial position on a trigonal bipyramidal In atom. For example the coordination polymer $[(Me_3SiCH_2)InCl_2]_\infty$ has bridging chlorides bound to indium in both axial and equatorial positions.[26] Those in the equatorial position have an average bond distance of 2.435(3) Å while the In–Cl distance to the axial chlorides is 2.72(2) Å, within error of the value in **1**.[26]

A search of the Cambridge Structural Database reveals that no In amide, imide, hydrazide, or azide containing more than four In atoms has been characterized. Only a peripherally related hexameric In amine macrocycle adduct could be found which does not contain any In–N–In fragments.[27] The highest nuclearity cage or cluster indium nitrogen compounds contain only four In atoms and include: Tetrameric imido In compounds with a cubane like geometry,[2,18,19,20] two In amide cage compounds,[1,4] and an In hydrazide.[3] The anion **1** is comprised of an In_6N_5 core (Figure 3.9b). Thus to the best of our knowledge **1** is the highest nuclearity In–N cage compound yet characterized.

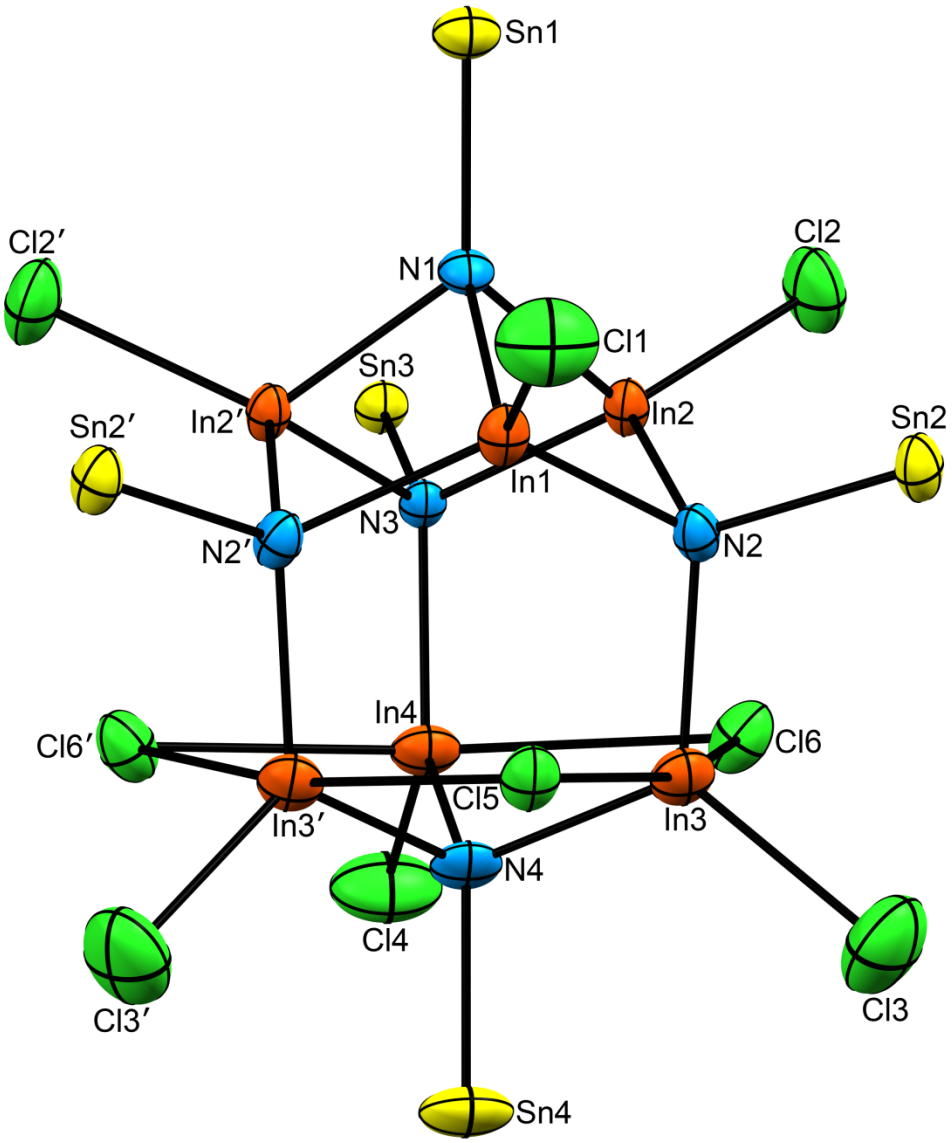

Figure 3.8. The structure of $(Et_4N)[(ClIn)_6(NSnMe_3)_5(\mu\text{-}Cl)_3]$, (Et_4N)1, with ellipsoids set at 50% probability. The cation and methyl groups of the $SnMe_3$ moieties have been omitted for clarity.

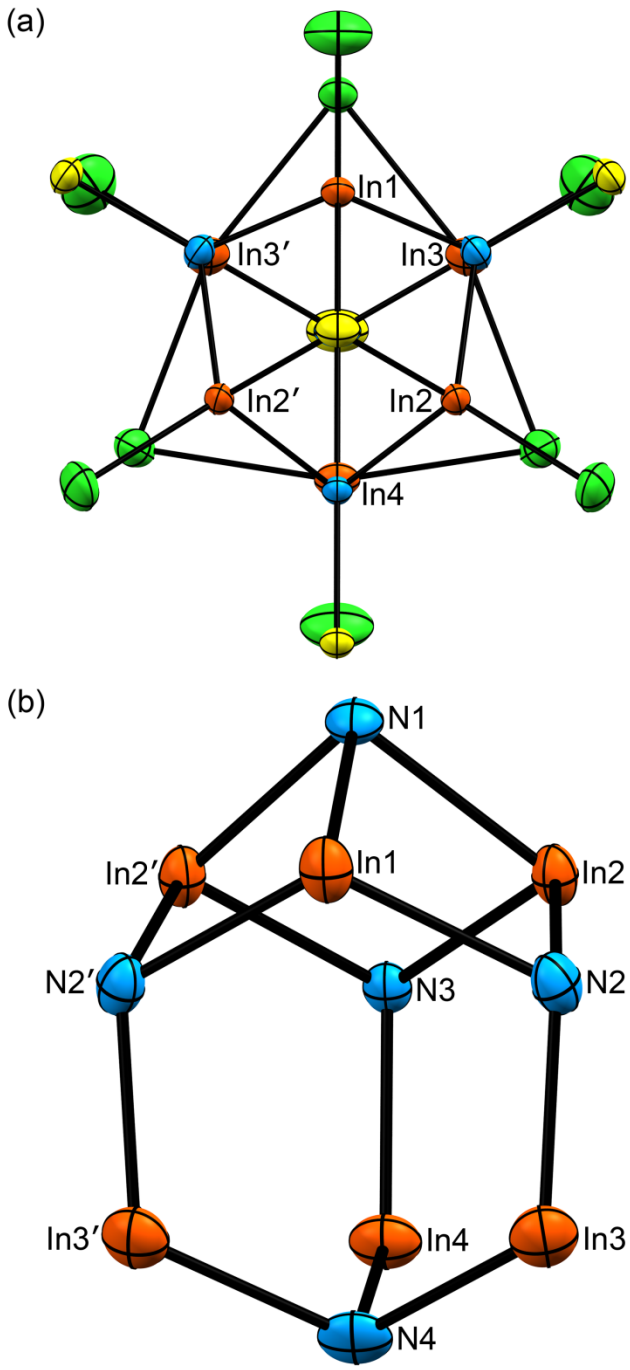

Figure 3.9. (a) The structure of $[(ClIn)_6(NSnMe_3)_5(\mu\text{-}Cl)_3]^-$ (1) viewed down the 3-fold rotational axis (not crystallographic) with methyl groups omitted for clarity. (b) The In_6N_5 core of (1). Thermal ellipsoids set at 50% probability.

Table 3.2. Selected and mean interatomic distances (Å) and angles for $[(ClIn)_6(NSnMe_3)_5(\mu\text{-}Cl)_3]^-$ (1).

N1–Sn1	2.046(6)	In1–Cl1	2.308(3)
		In2–Cl2	2.343(2)
N2–Sn2	2.109(4)	In3–Cl3	2.305(2)
N3–Sn3	2.113(6)	In3–Cl3	2.338(3)
N4–Sn4	2.114(7)	mean	2.32(2)
mean	2.112(3)		
		In3–Cl5	2.730(2)
Sn-C, mean	2.14(1)	In3–Cl6	2.706(2)
		In4–Cl6	2.703(2)
N1–In1	2.214(6)	mean	2.71(2)
N1–In2	2.196(4)		
mean	2.205(9)	In1–In2	3.1375(6)
		In1–In2′	3.1122(7)
N2–In1	2.190(5)	mean	3.13(1)
N2–In2	2.164(5)		
N3–In2	2.165(4)	C–Sn1–C	109.2(7)
mean	2.173(3)	C–Sn(2-4)–C	114(1)
		N1–Sn1–C(1-2)	109.9(9)
N2–In3	2.097(5)		
N3–In4	2.106(6)	N–In–N1	87.5(6)
mean	2.102(5)	N–In–N(2-4)	115(2)
		N–In–Cl(1-4)	121(2)
N4–In3	2.128(4)	N–In–Cl(5-6)	85(3)
N4–In4	2.128(6)	Cl–In–Cl	77.6(4)
mean	2.128(0)		
		Sn–N1–In	124.6(8)
		Sn–N(2-4)–In	113(1)

Solid State Reactivity of (1)

The solid state reactivity of **1** was explored. When a ground sample of (Et_4N)**1** was sealed in an evacuated glass tube and heated to 150 °C the solid changed from a very faint yellow to a dark yellow color. A colorless condensate formed at the cooler end of the tube. ^{1}H NMR identified this as Me_3SnCl and (to a slight extent) $SnMe_4$. The remaining solid was insoluble in MeCN. The electronic spectrum of the pyrolysed solid displays a broad absorption with a maximum at 330 nm and a shoulder extending to 800 nm (Figure 3.10). After exposure of this solid to air for 48 h the intensity of the absorption was reduced significantly, but still spanned the same range of wavelengths. This shows that the material is still somewhat susceptible to hydrolysis. Upon heating of (Et_4N)**1** to 250 °C in a sealed tube the material turned black. Powder X-ray diffraction of this sample showed significant contamination with Sn metal. These observations are consistent with those observed for the pyrolysis of $Cl_3In{\cdot}N(SnMe_3)_3$.[28] In that study a color change from white to yellow to brown to black was observed as the sample was heated to 650 °C and Me_3SnCl was eliminated between 100-200 °C. Crystalline InN was obtained after heating to 650 °C with some oxide impurities.

The elimination of Me_3SnCl from **1** was studied by heating a solid sample of (Et_4N)**1** under dynamic vacuum. The sample was first heated to 150 °C with the vacuum running through a liquid N_2 cooled trap. After four hours of heating a white film had formed in the trap and was identified as Me_3SnCl and $SnMe_4$ by ^{1}H NMR. The sample turned brown after heating up to 250 °C overnight. The mass of the

remaining solid was found to have reduced by ~50%. Loss of 5 equivalents of Me_3SnCl from (Et_4N)**1** would result in a 49% mass reduction. This result is promising for the possibility of tin-free InN growth from **1**.

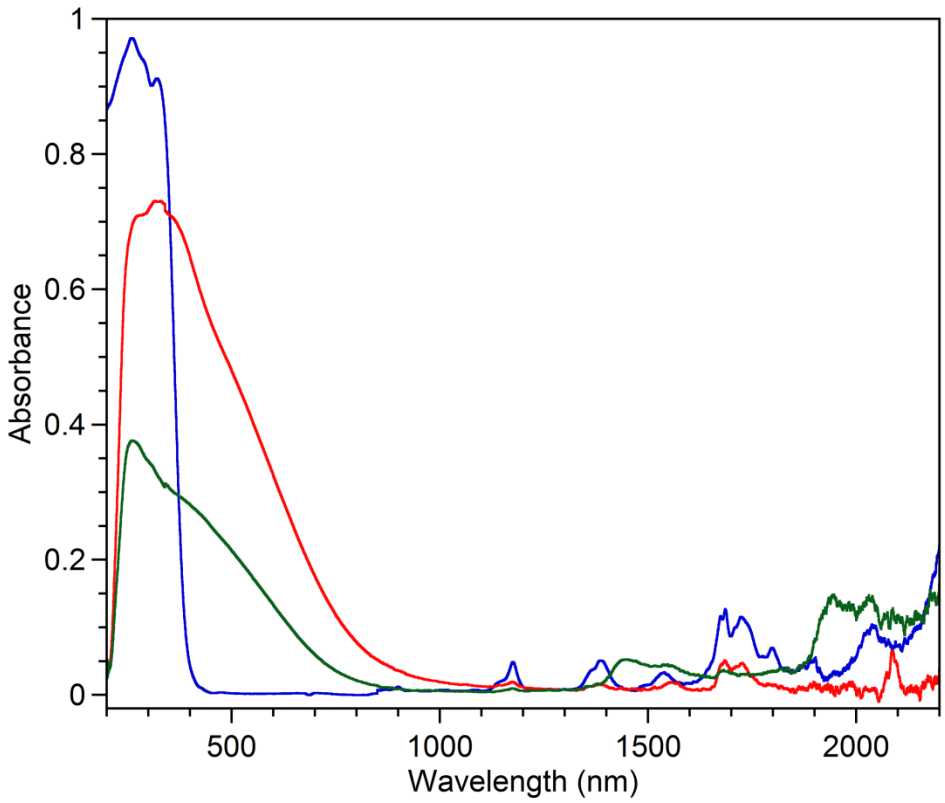

Figure 3.10. Diffuse reflectance UV-Vis spectra of $(Et_4N)[(ClIn)_6(NSnMe_3)_5(\mu\text{–}Cl)_3]$, (Et_4N)1, after being heated at 150 °C for 48 h (red); the spectrum of the same sample after 48 h of air exposure (green); the spectrum of a pure sample of (Et_4N)1 (blue).

Conclusion

Reported in this chapter is the facile synthesis of the novel Indium–Nitrogen compound, $[(ClIn)_6(NSnMe_3)_5(\mu\text{-}Cl)_3]^-$ (**1**), as the Et_4N^+ salt by reaction of $(Et_4N)_2[InCl_5]$ with $Cl_3In{\cdot}N(SnMe_3)_3$ in THF. The formulation of (Et_4N)**1** is confirmed by X-ray crystallography, elemental analysis, and mass spectrometry. The anion **1** was shown to be susceptible to hydrolysis by diffuse reflectance UV-Vis and infrared spectroscopy. The (Et_4N)**1** salt is soluble in THF, in which it is stable, and MeCN, in which it decomposes upon mild heating. When subjected to temperatures 150 °C or greater in the solid state, **1** decomposes with the release of Me_3SnCl. A search of the Cambridge Structural Database (version 5.34) reveals that no In–N clusters containing more than four In atoms (of which there are only 10 examples) have been characterized. Thus the anion **1** is the highest nuclearity In–N cage or cluster compound yet characterized. The ability to access such compounds is important as they may lead to low temperature precursors for the growth of InN semiconducting materials. In particular they are of interest in colloidal systems where large clusters could potentially serve as nucleation sites for nanoparticle synthesis. Research into the precursor chemistry of **1** is ongoing.

Acknowledgements

We thank Dr. Dale Chatfield for assistance with mass spectrometry measurements.

This chapter contains material which is being prepared for submission. Wilson, R. J.; Bennett, M. V. "The Highest Nuclearity Indium-Nitrogen Compound: $[In_6(NSnMe_3)_5Cl_9]^{1-}$" *Manuscript in preparation.*

References

(1) Rahbarnoohi, H.; Wells, R. L.; Rheingold, A. L. *Chemical Communications* **1996**, *0*, 2661.

(2) Grabowy, T.; Merzweiler, K. *Z. Anorg. Allg. Chem.* **2000**, *626*, 736.

(3) Uhl, W.; Abel, T.; Hepp, A.; Grimme, S.; Steinmetz, M. *Eur. J. Inorg. Chem.* **2008**, 543.

(4) Rennekamp, C.; Müller, P.; Prust, J.; Wessel, H.; Roesky, Herbert W.; Usón, I. *Eur. J. Inorg. Chem.* **2000**, *2000*, 1861.

(5) Timoshkin, A. Y. *Coord. Chem. Rev.* **2005**, *249*, 2094.

(6) Allen, F. *Acta Crystallographica Section B* **2002**, *58*, 380.

(7) Cheng, Q. M.; Stark, O.; Merz, K.; Winter, M.; Fischer, R. A. *J. Chem. Soc., Dalton Trans.* **2002**, 2933.

(8) Cumberland, S. L.; Hanif, K. M.; Javier, A.; Khitrov, G. A.; Strouse, G. F.; Woessner, S. M.; Yun, C. S. *Chem. Mater.* **2002**, *14*, 1576.

(9) Archer, P. I.; Santangelo, S. A.; Gamelin, D. R. *J. Am. Chem. Soc.* **2007**, *129*, 9808.

(10) Lovingood, D. D.; Oyler, R. E.; Strouse, G. F. *J. Am. Chem. Soc.* **2008**, *130*, 17004.

(11) Radha, B.; Kiruthika, S.; Kulkarni, G. U. *J. Am. Chem. Soc.* **2011**, *133*, 12706.

(12) Jiang, C.; Lee, J.-S.; Talapin, D. V. *J. Am. Chem. Soc.* **2012**, *134*, 5010.

(13) Sheldrick, G. *Acta Cryst.* **2008**, *A64*, 112.

(14) Macrae, C. F.; Bruno, I. J.; Chisholm, J. A.; Edgington, P. R.; McCabe, P.; Pidcock, E.; Rodriguez-Monge, L.; Taylor, R.; van de Streek, J.; Wood, P. A. *J. Appl. Crystallogr.* **2008**, *41*, 466.

(15) Strohalm, M.; Kavan, D.; Novak, P.; Volny, M.; Havlicek, V. *Anal. Chem.* **2010**, *82*, 4648.

(16) Ristic, M.; Popovic, S.; Music, S. *Mater. Lett.* **2005**, *59*, 1227.

(17) Slater, J. C. *J. Chem. Phys.* **1964**, *41*, 3199.

(18) Schmid, K.; Kuhner, S.; Hausen, H. D.; Weidlein, J. *Z. Anorg. Allg. Chem.* **1997**, *623*, 1499.

(19) Belgardt, T.; Roesky, H. W.; Noltemeyer, M.; Schmidt, H. G. *Angew. Chem.* **1993**, *105*, 1101.

(20) Schnitter, C.; Waezsada, S. D.; Roesky, H. W.; Teichert, M.; Uson, I.; Parisini, E. *Organometallics* **1997**, *16*, 1197.

(21) Hillwig, R.; Harms, K.; Dehnicke, K. *J. Organomet. Chem.* **1995**, *501*, 327.

(22) Khan, M.; Tuck, D. G. *Acta Crystallogr., Sect. B* **1982**, *B38*, 803.

(23) Petz, W.; Fahlbusch, M.; Gromm, E.; Neumueller, B. *Z. Anorg. Allg. Chem.* **2008**, *634*, 682.

(24) Taraba, J.; Zak, Z. *Inorg. Chem.* **2003**, *42*, 3591.

(25) Bubenheim, W.; Frenzen, G.; Mueller, U. *Acta Crystallogr., Sect. C: Cryst. Struct. Commun.* **1995**, *C51*, 1120.

(26) Self, M. F.; McPhail, A. T.; Jones, L. J., III; Wells, R. L.; Huffman, J. C. *Polyhedron* **1994**, *13*, 199.

(27) Coward, K. M.; Jones, A. C.; Steiner, A.; Bickley, J. F.; Smith, L. M.; Pemble, M. E. *J. Chem. Soc., Dalton Trans.* **2001**, 41.

(28) Cheng, Q. M.; Stark, O.; Stowasser, F.; Wohlfart, A.; Fischer, R. A. *J. Mater. Chem.* **2002**, *12*, 2470.

Chapter 4: Synthesis and Structure of Gallium–Tin and Indium–Tin μ_4–Nitrogen Compounds

Introduction

Molecular nitrides containing an M_4N fragment (M = a *p*-block metal) are currently limited to only 16 examples. These consist of monomeric[1,2] and oligomeric[3-5] tin nitrogen (Sn–N) compounds, Lewis adducts of $(Me_3Sn)_3N$, and group 13 metal alkyls and halides,[6,7] and indium/tin–nitrogen (In/Sn–N) dimers.[6] As discussed in chapter 2, we have successfully synthesized gallium (Ga) and gallium-tin (Ga–Sn) μ_3-N molecules by the dehalostannylation of $(Me_3Sn)_3N$ and $Cl_3Ga{\cdot}N(SnMe_3)_3$ in the presence of $[GaX_4]^-$ (X = Cl, Br). Anions have been used successfully as precursors to colloidal quantum dots and thus we were motivated to explore the synthesis of high nuclearity anionic Ga–N compounds for their potential as single source precursors to gallium nitride nanomaterials.

We chose to further explore the reactivity of $Cl_3Ga{\cdot}N(SnMe_3)_3$ and $(Me_3Sn)_3N$ with $[GaX_4]^-$ (X = Cl, Br). Our previous work with this system led to the synthesis of the μ_3–N compounds, $[(X_3Ga)_2NSnMe_3]^{2-}$ (X = Cl (**1**), Br (**2**)) and $[(Cl_3Ga)_3N]^{3-}$ (**3**) (See Chapter 2 and our recently published report).[8] This reaction system could also potentially lead to new 4-coordinate Ga–N compounds (Scheme 4.1).

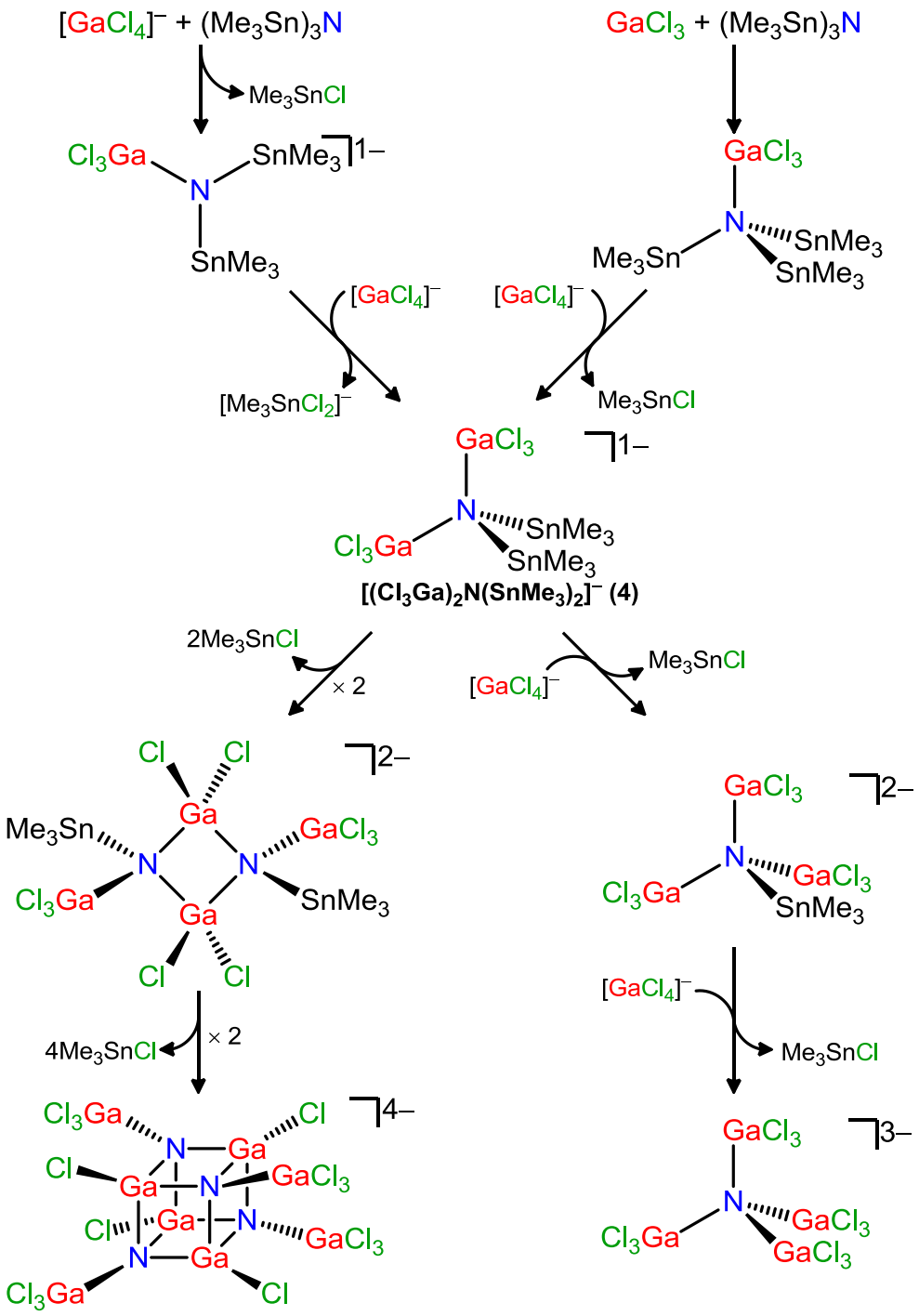

Scheme 4.1. Possible reaction pathways to μ_4–N gallium compounds.

It was found that in the high concentration regime in THF the reaction of both $(Me_3Sn)_3N$ and $Cl_3Ga{\cdot}N(SnMe_3)_3$ with $[GaCl_4]^-$ could produce the unassociated (monomeric) Ga/Sn–(μ_4-N) anion, $[(Cl_3Ga)_2N(SnMe_3)_2]^-$ (**4**) (Scheme 4.1). This is the first compound to contain a Ga_2NSn_2 fragment. It was found that an analogous reaction of $[InCl_4]^-$ with $Cl_3In{\cdot}N(SnMe_3)_3$ afforded the indium analogue, $[(Cl_3In)_2N(SnMe_3)_2]^-$, (**5**). In pursuit of high nuclearity Ga–N anions, we explore concentrated 1:1 reactions of $[GaX_4]^-$ (X = Cl, Br) and $(Me_3Sn)_3N$ in which $[Me_3SnX_2]^-$ was eliminated. This led to the structural characterization of the unprecedented Ga–N trimers, $[(Cl_2GaNSnMe_3)_3(\mu\text{-}SnMe_2Cl)]^{2-}$ (**6**) and $[Ga_3(NSnMe_3)_3(SnMe_2)MeBr_5]^-$ (**7**) as the Et_4N^+ salts. The structures of **6** and **7** provide evidence of either direct formation of a trimeric species in solution or a stepwise formation through a dimeric intermediate (Scheme 4.2). The Ga–N trimer is then ostensibly "trapped" by further reaction with Me_3SnX, forming a μ–$SnMe_2$ bridging moiety and eliminating $[Me_3SnX_2]^-$. The formation of the μ–$SnMe_2$ moiety implies that room temperature methyl–halogen exchange is occuring in this reaction system. The formation of **6** and **7** shows that reactions of $(Me_3Sn)_3N$ and $[GaX_4]^-$ are capable of yielding oligomeric compounds under appropriate conditions.

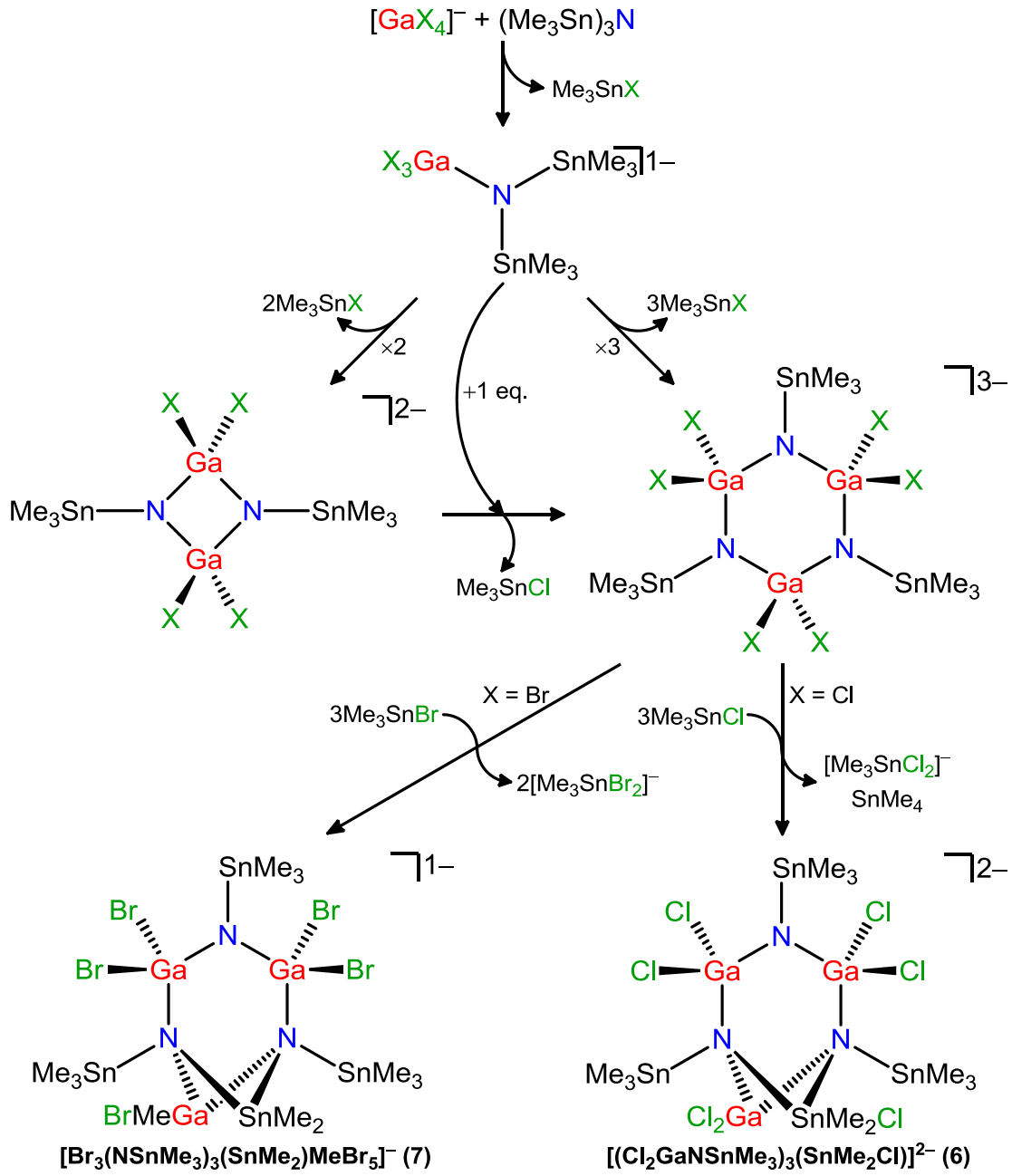

Scheme 4.2. Possible reaction pathways in the formation of $[(Cl_2GaNSnMe_3)_3(\mu\text{-}SnMe_2Cl)]^{2-}$ (6) and $[Ga_3(NSnMe_3)_3(SnMe_2)MeBr_5]^-$ (7).

Experimental Section

Preparation of Compounds

All manipulations were carried out under a pure dinitrogen atmosphere using standard Schlenk and glove-box techniques. Anhydrous tetrahydrofuran (THF), purchased from EMD, diethylether (Et_2O), purchased from EMD, and acetonitrile (MeCN), purchased from Burdick and Jackson were stored over activated 4 Å molecular sieves under a pure dinitrogen atmosphere. The compounds $(Me_3Sn)_3N$[9] and $Cl_3Ga{\cdot}N(SnMe_3)_3$[7] were prepared according to the literature procedures. Syntheses of salts of $[MX_4]^{1-}$ (M = Ga, In; X = Cl, Br) are outlined in appendix B. Elemental analysis was performed at the Mikroanalytisches Laboratorium Kolbe, Mülheim an der Ruhr, Germany.

$(Et_4N)[(Cl_3Ga)_2N(SnMe_3)_2]$, (Et_4N)4. A solution of $(Et_4N)[GaCl_4]$ (0.21 g, 0.63 mmol) and $Cl_3Ga{\cdot}N(SnMe_3)_3$ (0.42 g, 0.62 mmol) in 2.5 mL of THF was stirred for 30 min. The colorless solution was then slowly concentrated via diffusion of the solvent into toluene in a sealed vial for 4 days at which time colorless, block shaped, crystals of (Et_4N)**4** were observed. The crystals were collected on a fritted glass filter and washed with successive aliquots of THF (3 × 1 mL) and Et_2O (3 × 1 mL) to afford 0.33 g (0.40 mmol, 65%) of (Et_4N)**4**. Diffuse reflectance spectrum: λ_{max} (nm) 260 (sh). ^{1}H NMR (CD_2Cl_2): δ = 0.74 ppm ($J_{^1H\text{-}^{117}Sn}$ = 54.5 Hz, $J_{^1H\text{-}^{119}Sn}$ = 56.7 Hz). ^{1}H NMR (THF-d_8): δ = 0.71 ppm ($J_{^1H\text{-}^{117/119}Sn}$ = 57.3 Hz; in THF **4** is in equilibrium with a

minor species at δ = 0.29 ppm ($J_{^1H\text{-}^{117}Sn}$ = 55 Hz, $J_{^1H\text{-}^{119}Sn}$ = 57 Hz), which is unidentified but likely results from the elimination of Me_3SnCl, observed at δ = 0.58 ppm. Anal. Calcd for $C_{14}H_{38}Cl_6Ga_2N_2Sn_2$: C, 20.41; H, 4.65; Cl, 25.81; Ga, 16.92; N, 3.40; Sn, 28.81. Found: C, 20.55; H, 4.69; Cl, 25.63; Ga, 16.93; N, 3.42; Sn, 28.71.

(Pr^n_4N)[$(Cl_3Ga)_2N(SnMe_3)_2$], (Pr^n_4N)4. A solution of (Pr^n_4N)[$GaCl_4$] (0.40 g, 1.0 mmol) and $Cl_3Ga{\cdot}N(SnMe_3)_3$ (0.68 g, 0.99 mmol) in 7.2 mL of THF was stirred for 24 hours. Vapor diffusion of Et_2O into this colorless solution afforded colorless, block shaped, crystals. These were collected on a fritted glass filter and washed with successive aliquots of THF (4 × 5 mL) and Et_2O (3 × 5 mL) and dried *in vacuo* to yield 0.65 g (0.74 mmol, 74%) of (Pr^n_4N)**4**. Diffuse reflectance spectrum: λ_{max} (nm) 263 (sh). ^1H NMR (CD_2Cl_2): δ = 0.73 ppm ($J_{^1H\text{-}^{117/119}Sn}$ = 54.6 Hz). ^1H NMR (CD_3CN): δ = 0.69 ppm ($J_{^1H\text{-}^{117/119}Sn}$ = 58.0 Hz. Anal. Calcd for $C_{18}H_{46}Cl_6Ga_2N_2Sn_2$: C, 24.56; H, 5.27; Cl, 24.17; Ga, 15.84; N, 3.18; Sn, 26.97. Found: C, 24.68; H, 5.18; Cl, 24.10; Ga, 15.69; N, 3.17; Sn, 26.70.

(Et_4N)[$(Cl_3In)_2N(SnMe_3)_2$], (Et_4N)5. A mixture of (Et_4N)[$InCl_4$] (0.09 g, 0.23 mmol) and $Cl_3In{\cdot}N(SnMe_3)_3$ (0.16 g, 0.22 mmol) in 1.1 mL of THF was stirred for 24 h forming a colorless solution. Diffusion with Et_2O afforded colorless crystals of (Et_4N)**5** (unit cell isomorphic with (Et_4N)**4**). ^1H NMR (CD_2Cl_2): δ = 0.74 ppm (s,

$J_{^1H\text{-}^{117}Sn}$ = 54 Hz, $J_{^1H\text{-}^{119}Sn}$ = 56 Hz), δ = 0.75 ppm (s, $J_{^1H\text{-}^{117}Sn}$ = 54 Hz, $J_{^1H\text{-}^{119}Sn}$ = 56 Hz), δ = 0.77 ppm (s, $J_{^1H\text{-}^{117}Sn}$ = 54 Hz, $J_{^1H\text{-}^{119}Sn}$ = 56 Hz).

$(Et_4N)_2[(Cl_2GaNSnMe_3)_3(SnMe_2Cl)]$, $(Et_4N)_2$6. Solid $(Me_3Sn)_3N$ (0.29 g, 0.58 mmol) was added to a solution of $(Et_4N)[GaCl_4]$ (0.20 g, 0.58 mmol) in 5.7 mL of THF. The solution was allowed to stand while slowly concentrating by diffusion of the solvent into toluene in a sealed container. After three days colorless rectangular block crystals of $(Et_4N)[Me_3SnCl_2]$ (confirmed by unit cell) formed. The mother liquor was decanted off of the crystals and further concentrated to afford colorless wedge shaped crystals of $(Et_4N)_2$**6** as well as $(Et_4N)[Me_3SnCl_2]$. Diffuse reflectance spectrum: λ_{max} (nm) 267.

$(Et_4N)[Br_3(NSnMe_3)_3(SnMe_2)Br_5]$, (Et_4N)7. Solid $(Me_3Sn)_3N$ (0.09 g, 0.2 mmol) was added to a solution of $(Et_4N)[GaBr_4]$ (0.09 g, 0.2 mmol) in 1.5 mL of THF. Slow concentration of this colorless solution by diffusion of the solvent into toluene in a sealed container produced colorless blocky crystals of $(Et_4N)[Me_3SnBr_2]$ (confirmed by unit cell). The mother liquor was decanted and further concentrated to afford colorless wedge shaped crystals of (Et_4N)**7** as well as $(Et_4N)[Me_3SnBr_2]$.

X-ray Structure Determination

Crystals were coated in Paratone oil and mounted by mean of a glass capillary fiber on a Bruker APEX-II CCD area detector instrument operated by the APEX

software package. Data reduction was performed by SAINT, absorption correction was applied using SADABS, and the space group was assigned using XPREP. All structures were solved by direct methods and refined against all data by full-matrix least squares on F_2. OLEX2[10] was used to calculate a solvent accessible void of 275 $Å^3$ in (Et_4N)**7** containing 37 electrons which were masked for further refinement. Hydrogen atoms were attached at idealized positions on carbon atoms and were refined as riding atoms with uniform isotropic thermal parameters. Structure solution, refinement, graphics and report generation were performed using SHELXTL[11] and Mercury.[12]

Other Physical Measurements

The solid state electronic reflectance spectra were recorded on a JASCO V-670 UV-Vis spectrophotometer fitted with an integrating sphere. NMR spectra were collected on a Varian Inova 400 MHz instrument at 30°C with chemical shifts referenced to the signal of residual protons in the deuterated solvent. Infrared spectroscopy was performed on a Perkin-Elmer RX I spectrometer equipped with an attenuated total reflectance accessory.

Table 4.1 X-ray crystallographic data for salts of $[(Cl_3Ga)_2N(SnMe_3)_2]^-$ (4).

	(Et_4N)**4**	$(Pr^n{}_4N)$**4**
formula	$C_{14}H_{38}Cl_6Ga_2N_2Sn_2$	$C_{18}H_{46}Cl_6Ga_2N_2Sn_2$
form. weight	823.98	880.09
T, K	100	100
cryst. syst.	Monoclinic	Orthorhombic
space group	$P2_1/c$	$P2_12_12_1$
a, Å	17.231(5)	11.5362(11)
b, Å	24.438(7)	12.3411(11)
c, Å	13.310(4)	23.265(2)
α, deg	90	90
β, deg	90.180(13)	90
γ, deg	90	90
V, Å^3	5605(3)	3312.2(5)
Z	8	4
ρ_{calc}, g/cm^3	1.953	1.765
2θ range, deg	1.45 to 30.07	1.87 to 25.02
GOF (F^2)	0.989	1.188
R_1/wR_2, %	3.58/4.87	2.15/5.19
largest peak/ hole (e$^-$/Å^3)	0.831/-0.825	0.626/-0.484
Flack x parameter		0.182(13)

Table 4.2 X-ray crystallographic data for salts of $[(Cl_2GaNSnMe_3)_3(SnMe_2Cl)]^{2-}$ (6) and $[Br_3(NSnMe_3)_3(SnMe_2)Br_5]^-$ (7).

	$(Et_4N)_2$**6**	(Et_4N)**7**
formula	$C_{34}H_{81}Cl_7Ga_3N_5Sn_4$	$C_{20}H_{56}N_4Ga_3Br_5Sn_4$
form. weight	1492.11	1436.16
T, K	100	100
cryst. syst.	Monoclinic	Triclinic
space group	$P2_1/c$	$P\bar{1}$
a, Å	21.338(4)	11.9612(6)
b, Å	13.314(3)	12.6936(6)
c, Å	19.376(4)	16.4263(9)
α, deg	90	83.047(3)
β, deg	94.341(9)	85.168(3)
γ, deg	90	65.277(2)
V, Å^3	5488.9(19)	2247.2(2)
Z	4	2
ρ_{calc}, g/cm^3	1.806	2.122
2θ range, deg	1.80 to 31.00	3.54 to 55.76
GOF (F^2)	1.028	1.054
R_1/wR_2, %	4.11/10.25	4.54/12.64
largest peak/ hole (e$^-$/Å^3)	4.065/-2.444	1.29/-0.55

Results and Discussion

Synthesis of (4)

In an attempt to access higher nuclearity compounds from the reaction of $[GaCl_4]^-$ and $(Me_3Sn)_3N$ we explored the effects of cation size. Combining THF solutions of $(Me_4N)[GaCl_4]$ and $(Me_3Sn)_3N$ in a 2:1 ratio results in the almost immediate precipitation of $(Me_4N)_2[(Cl_3Ga)_2NSnMe_3]$, $(Me_4N)_2$**1**, in good yield (Chapter 2).[8] The analogous reaction of $(Pr^n_4N)[GaCl_4]$ and $(Me_3Sn)_3N$ in a 2:1 ratio does not readily produce any insoluble products and vapor diffusion of Et_2O into this solution affords only $(Pr^n_4N)[GaCl_4]$. However, at high concentrations this reaction precipitates a mixture of the byproduct salt, $(Pr^n_4N)[Me_3SnCl_2]$, and the $Pr^n_4N^+$ salt of the μ_4-N compound, $[(Cl_3Ga)_2N(SnMe_3)_2]^{1-}$ (**4**) (Scheme 4.3).

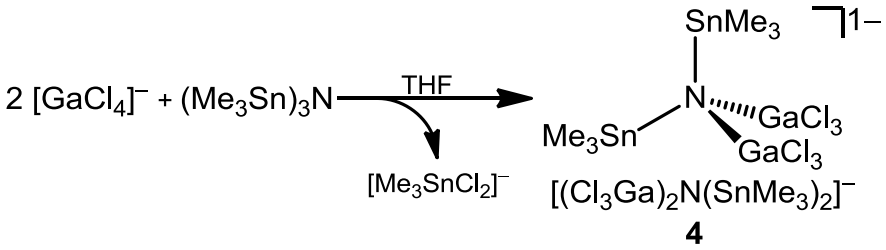

Scheme 4.3. The isolation of $[(Cl_3Ga)_2N(SnMe_3)_2]^-$ (4) from the reaction of $[GaCl_4]^-$ and $(Me_3Sn)_3N$ at high concentrations.

Presumably this product was formed via a metathesis reaction of one equivalent of $[GaCl_4]^-$ and $(Me_3Sn)_3N$ to form the monosubstituted intermediate,

$[Cl_3GaN(SnMe_3)_2]^{1-}$ (**8**). Chloride transfer from $[GaCl_4]^{1-}$ to Me_3SnCl would give $GaCl_3$ and $[Me_3SnCl_2]^{1-}$ and allow for the subsequent reaction of **8** with $GaCl_3$ to afford **4**.

The above synthetic route to **4** is undesirable as the separation of $[Me_3SnCl_2]^-$ salts is difficult and inefficient. It was recognized that the previously reported Lewis adduct, $Cl_3Ga{\cdot}N(SnMe_3)_3$,[7] could be an ideal reactant for the direct synthesis of **4** via metathesis with $[GaCl_4]^-$. The byproduct Me_3SnCl is easily separable from most ionic products. Indeed direct reaction of $[GaCl_4]^-$ with $Cl_3Ga{\cdot}N(SnMe_3)_3$ lead to the isolation of the salts, (Et_4N)**4** and $(Pr^n{}_4N)$**4**, in yields of 65% and 74% respectively (Scheme 4.4).

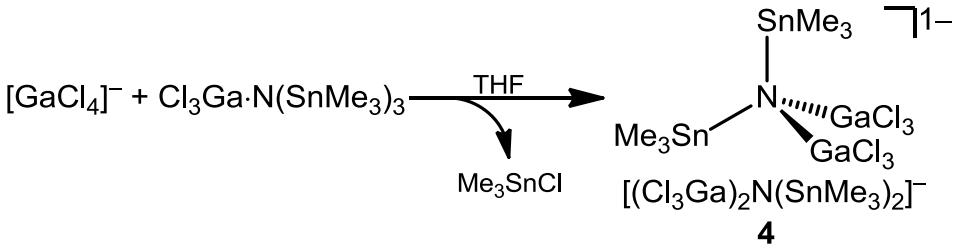

Scheme 4.4. The direct synthesis of $[(Cl_3Ga)_2N(SnMe_3)_2]^-$ (4) from the reaction of $[GaCl_4]^-$ and $Cl_3Ga{\cdot}N(SnMe_3)_3$.

Properties of (4)

The solid state electronic spectrum of **4** exhibits a slight shoulder at 260 nm which decays in intensity upon exposure to air (Figure 4.1). Both (Et_4N)**4** and (Pr^n_4N)**4** are soluble in CH_2Cl_2, THF, and MeCN and were characterized in the deuterated forms of those solvents by their ^1H NMR spectra. Both salts may be recrystallized quantitatively from CH_2Cl_2, and THF (as confirmed by unit cell) after 24 h by vapor diffusion with Et_2O. The ^1H NMR spectrum of **4** in CD_2Cl_2 consists of a single sharp peak between 0.73 and 0.74 ppm ($J_{^{119}Sn-\ ^1H} = 57$ Hz) which may be assigned to the methyl protons of the $SnMe_3$ moieties. In CD_2Cl_2 **4** displays stability to mild heat (50 °C), and additional $[GaCl_4]^-$, even after several days (Figure 4.2). When dissolved in THF-d_8 there is an equilibrium between the product and an unknown species, characterized by a $SnMe_3$ resonance at 0.29 ppm, and Me_3SnCl. This equilibrium is slight and **4** is still stable enough in THF to be recrystallized after 24 hours in solution. Addition of one equivalent of $[GaCl_4]^-$ to a THF-d_8 solution of **4** does not result in additional Sn–N bond cleavage at room temperature after 24 h. Heating results in the elimination of one equivalent of Me_3SnCl and the formation of several unidentified byproducts (Figure 4.3). The potential monosubstituted product, $[(Cl_3Ga)_3NSnMe_3]^{2-}$ (**9**), would have a $SnMe_3$ resonance downfield of **4**, but is not observed. The addition of $[GaCl_4]^-$ to a CD_3CN solution of **4** does not immediately result in a reaction. However, when left to stand at room temperature, the components react (or decompose) to give Me_3SnCl as well as an unidentified by product characterized by a ^1H NMR resonance at 0.29 ppm (Figure 3.4). Presumably an anion(s) that contains no Me_3Sn (inferred from the relative integrations of the cation and the Me_3Sn groups) is

present as well. Attempts to crystallize byproducts from reactions in THF and MeCN have so far been unsuccessful. From the ^{1}H NMR spectra we can infer that **4** is reactive in polar aprotic solvents (THF, MeCN) and is stable in CD_2Cl_2. Attempts to recrystallize decomposition products of **4** are underway.

Synthesis and properties of (5)

The ease of synthesis of salts of **4** prompted us to investigate the analogous reaction of $[InCl_4]^-$ and $Cl_3In{\cdot}N(SnMe_3)_3$. The radii of In(III) and Ga(III) are 0.76 Å and 0.61 Å respectively.[13] Because of its larger radius, In(III) has a tendency to form 5-coordinate complexes, e.g. $[InCl_5]^{2-}$. Consequently the reactivity of $[InCl_4]^-$ and resulting μ_4-In complexes show marked differences compared to $[GaCl_4]^-$. When stirred in THF, a suspension of $[InCl_4]^-$ and $Cl_3In{\cdot}N(SnMe_3)_3$ formed a solution in 24 h; which was significantly longer than was observed in the gallium system. Diffusion of Et_2O into these solutions afforded crystals of $[(Cl_3In)_2N(SnMe_3)_2]^-$ (**5**) as the Et_4N^+ and $Pr^n{}_4N^+$ salts in low yield. The structures of (Et_4N)**5** and $(Pr^n{}_4N)$**5** were not solved due to excessive disorder, but were identified by their unit cells which were isomorphic with the analogous salts of **4**. The salt (Et_4N)**5** was only partially soluble in CD_2Cl_2. The ^{1}H NMR spectra of (Et_4N)**5** in CD_2Cl_2 showed three resonances at 0.74, 0.75, and 0.77 ppm which all had ^{117}Sn/^{119}Sn–^{1}H J values of 54/56 Hz (Figure 4.5). The combined integration of these three peaks gives a value of 18 protons per equivalent of Et_4N^+, supporting the formulation of **5**. Decomposition of **5** in CD_2Cl_2 occurs quickly when heated to 50 °C. The ^{1}H NMR spectrum shows complete

decomposition of **5** and the non-quantitative formation of Me_3SnCl. Attempts to crystallize the decomposition products of **5** are underway. The evidence suggests that isolation of an In analog of **4** is possible, however yields are low. The product **5** also exhibits far less stability in solution. Efforts to optimize this synthesis are ongoing.

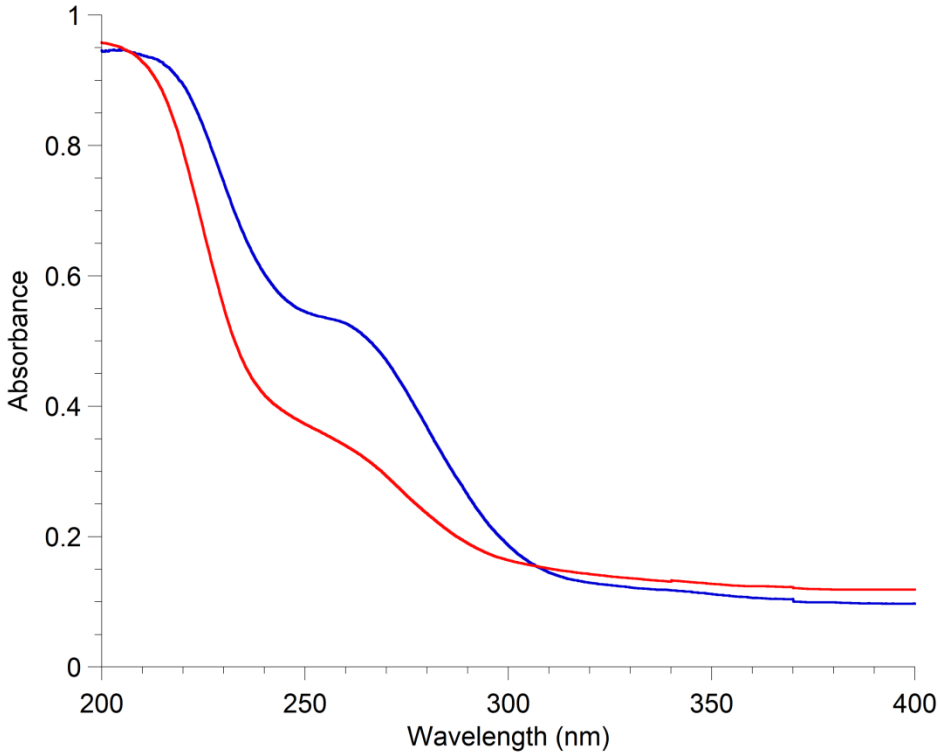

Figure 4.1. Diffuse reflectance UV-Vis spectrum of $(Et_4N)4$ before (blue) and after (red) exposure to air overnight.

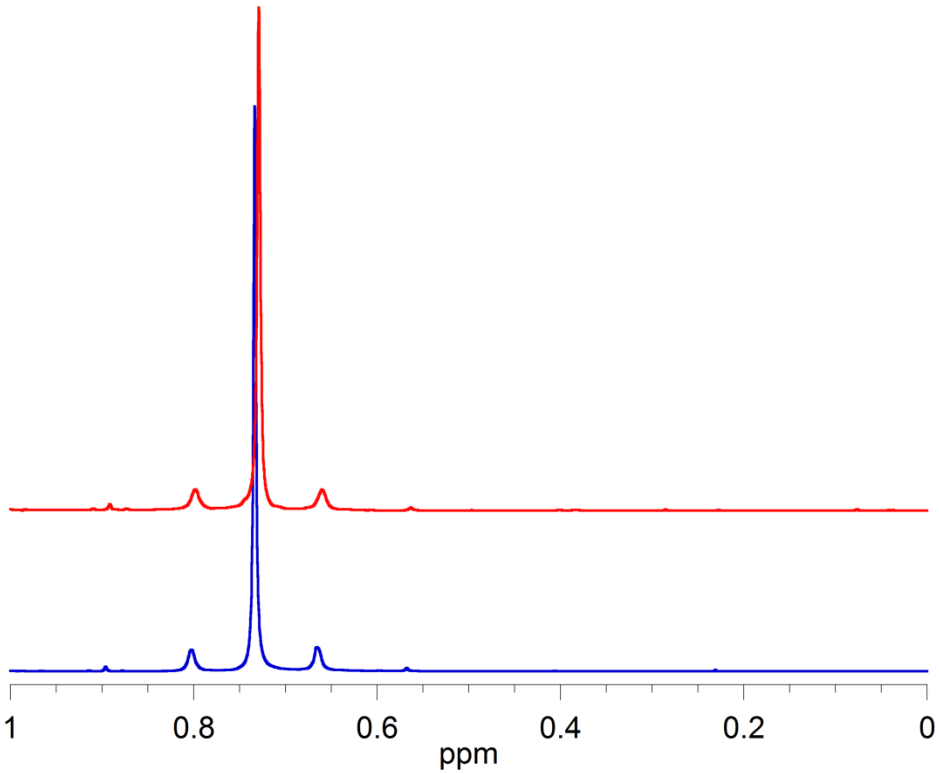

Figure 4.2. The ^{1}H NMR spectrum of ($Pr^{n}_{4}N$)4 in CD_2Cl_2; the initial spectrum (blue); and the spectrum after standing for 2 weeks in the presence of additional $[GaCl_4]^-$.

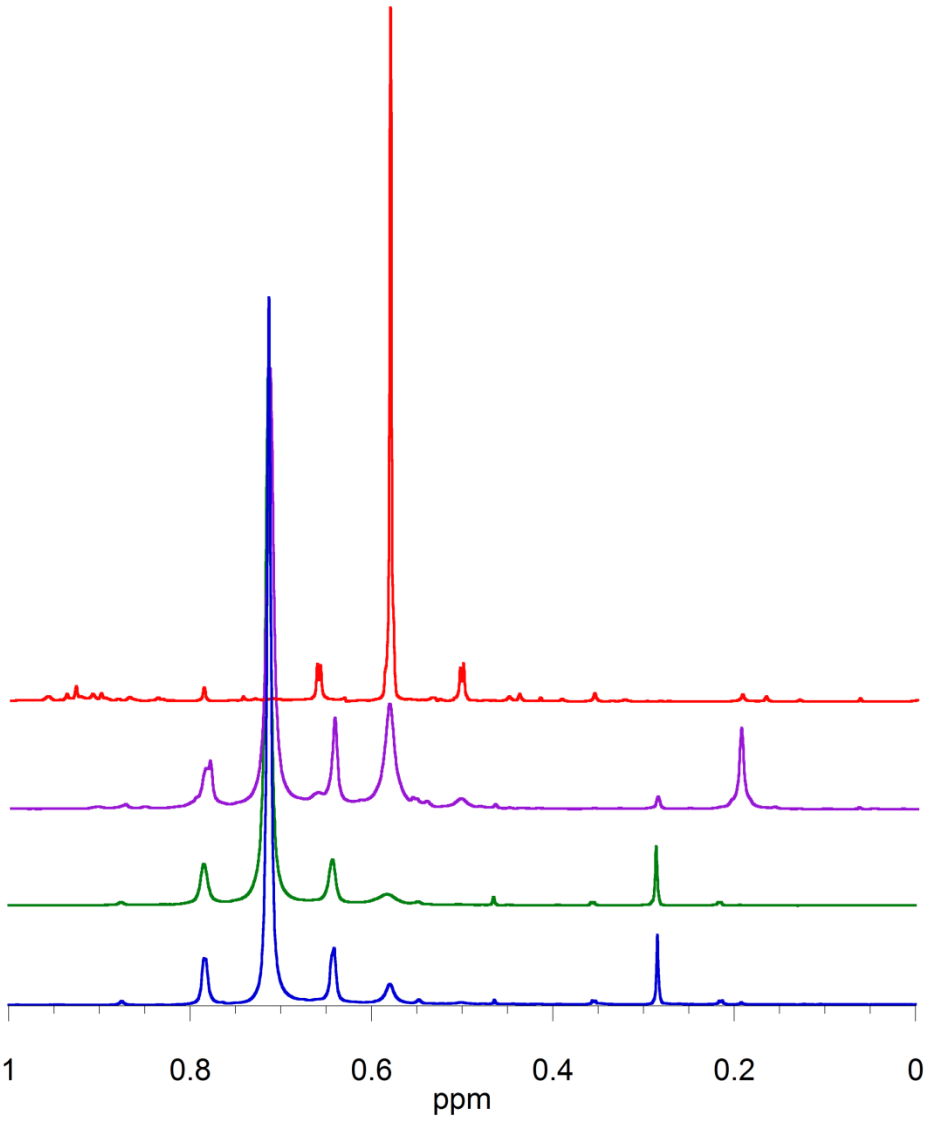

Figure 4.3. The ^{1}H NMR spectrum of $(Et_4N)4$ in THF-d_8; the initial spectrum (blue); in the presence of additional $[GaCl_4]^-$ for 24 h (green); after heating for 1 h at 65 °C (violet); after heating for 24 h at 65 °C (red).

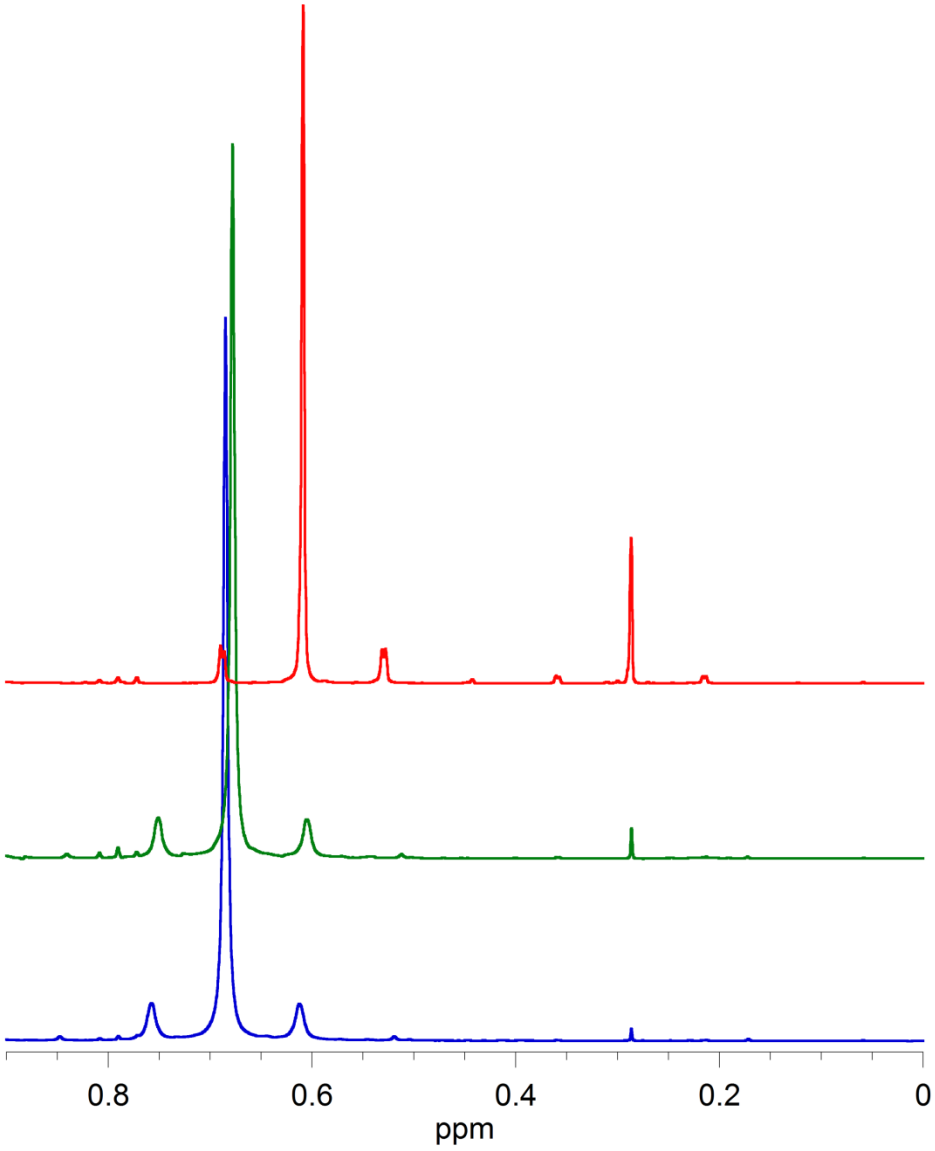

Figure 4.4. ^{1}H NMR spectrum of ($Pr^{n}_{4}N$)4 in CD_3CN; the initial spectrum (blue); immediately after addition of $[GaCl_4]^-$ (green); after standing for 24 h at RT (red).

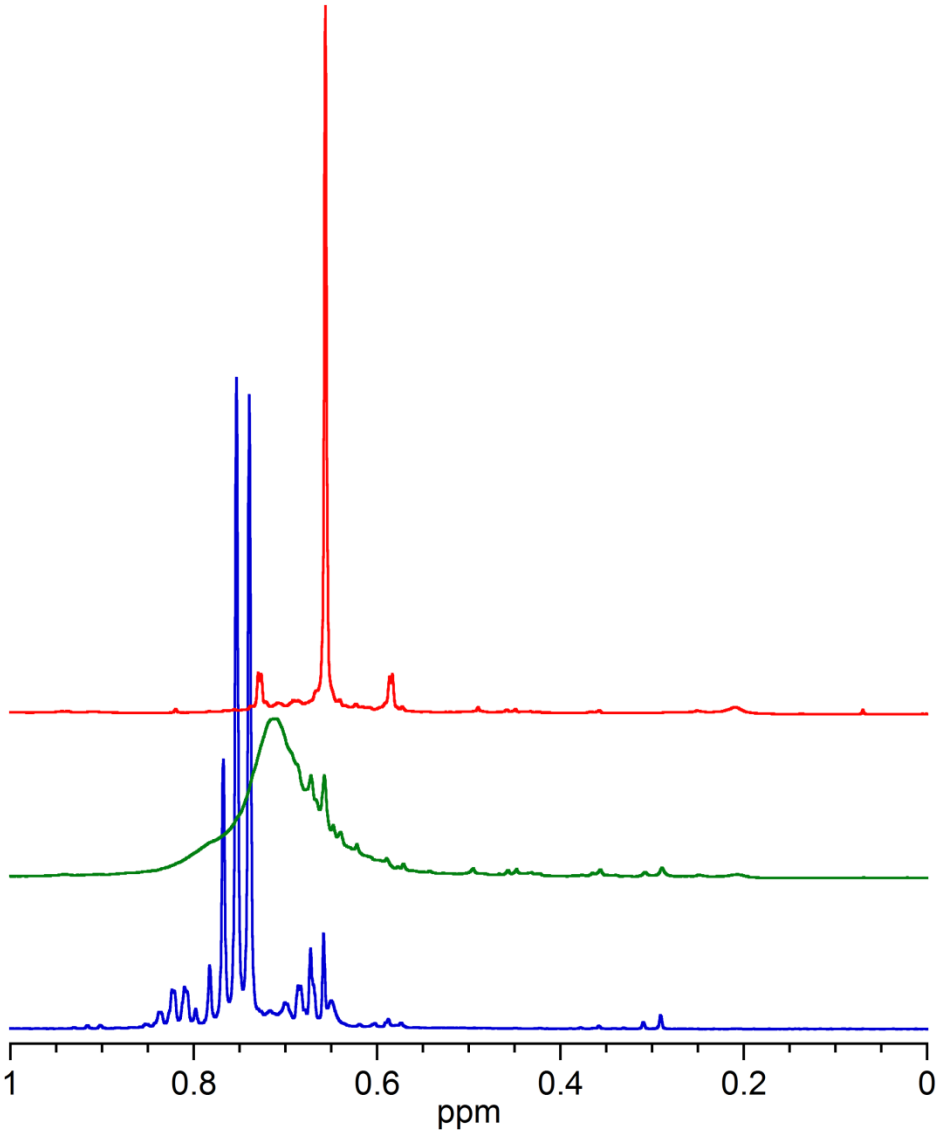

Figure 4.5. The ^{1}H NMR spectrum of $(Et_4N)5$ in CD_2Cl_2; the initial spectrum (blue); after heating at 50 °C for 30 min (green); after heating at 50 °C for 24 h (red).

Structure of (4)

Characterization of Et_4N^+ and $Pr^n{}_4N^+$ salts of **4** by X-ray diffraction revealed a tetrahedrally coordinated μ_4-N atom bound to two $SnMe_3$ and two $GaCl_3$ moieties (Figure 4.6). The salt ($Pr^n{}_4N$)**4** crystallizes in the chiral orthorhombic space group $P2_12_12_1$. The Flack *x* parameter of 0.182(13) deviated significantly from zero and thus the structure was refined as a racemic twin with the BASF value of 0.18. The anion of ($Pr^n{}_4N$)**4** is disordered via a rotation about the N1–Sn1 bond with the minor component having an approximate occupancy of 8.5%. This disorder is characterized by the ligands on the gallium and tin atoms of both the major and minor components essentially occupying the same space (Figure 4.7). (Et_4N)**4** crystallizes as a pseudomerohedral twin with an apparent orthorhombic space group ($\beta \approx 90°$). The structure was solved in the monoclinic space group $P2_1/c$ with a twofold rotation about the *c*-axis as the twin law and a BASF value of 0.35. There are two formula units in the asymmetric unit with excellent agreement between their bond parameters. The mean bond distances and angles of (Et_4N)**4** and ($Pr^n{}_4N$)**4** agree with each other within error. Since the structure refinement of ($Pr^n{}_4N$)**4** required considerable restraints, the values for (Et_4N)**4** will be used for discussions of **4**.

The Ga–N distances in (Et_4N)**4** range from 1.920(3) Å to 1.936(3) Å with an average of 1.929(7) Å. This is only slightly shorter than the Ga–N length of 1.950(7) Å in the parent compound $Cl_3Ga{\cdot}N(SnMe_3)_3$.[7] The structurally similar ethyl and silyl amides, $[(Cl_3Ga)_2NEt_2]^-$,[14] and $[(Cl_3Ga)_2N(SiMe_3)_2]^-$,[15] have mean Ga–N bond lengths of 1.986(9) Å and 1.984(5) Å respectively, longer than that observed for

(Et_4N)**4**. The Sn–N bond lengths in (Et_4N)**4** range from 2.168(3) Å to 2.188(3) Å with an average of 2.180(9) Å. This agrees within error of the average Sn–N distance of 2.164(9) Å in parent compound, $Cl_3Ga{\cdot}N(SnMe_3)_3$.[7] The compound $(Me_3Sn)_3N$ has a significantly shorter mean Sn–N bond length of 2.04(3) Å as expected. The Ga–Cl bond distances in (Et_4N)**4** range from 2.164(1) Å to 2.199(1) Å with a mean value of 2.18(1) Å. This is equivalent within error of the mean values of 2.184(6) Å and 2.169(6) Å in $Cl_3Ga{\cdot}N(SnMe_3)_3$ and $(Bu^n{}_4N)[GaX_4]$[16] respectively, and just slightly shorter than the value of 2.22(1) Å observed for **1**.[8]

The isolation of the monovalent anion, **4**, was serendipitous, as it was noted that there are only 8 examples of structures containing a μ_4-N atom with a M_2NE_2 (M = Ga, In; E = Element of 3rd period or greater) coordination sphere. These examples consist of two Ga silylamide dimers[17,18] a Ga silylimide tetramer,[19] dimeric In silyl[20] and germyl[21] amides, and an In stannylnitride dimer.[6] Recently the Si analogue of **4**, $[(Cl_3Ga)_2N(SiMe_3)_2]^-$, was isolated as the counter ion to a highly reactive aminostibenium cation, $[ClSbN(SiMe_3)_2]^{1+}$, from the low temperature reaction of $Cl_2SbN(SiMe_3)_2$ and $GaCl_3$ in methylene chloride.[15] There are 16 examples of μ_4-nitrides of the form M_4N (M = Al, Ga, In, Tl, Sn, Pb, Bi), two of which contain two group 13 metals,[6] and 7 of which contain one metal of that group.[6,7] Thus **4** joins a relatively small structural family.

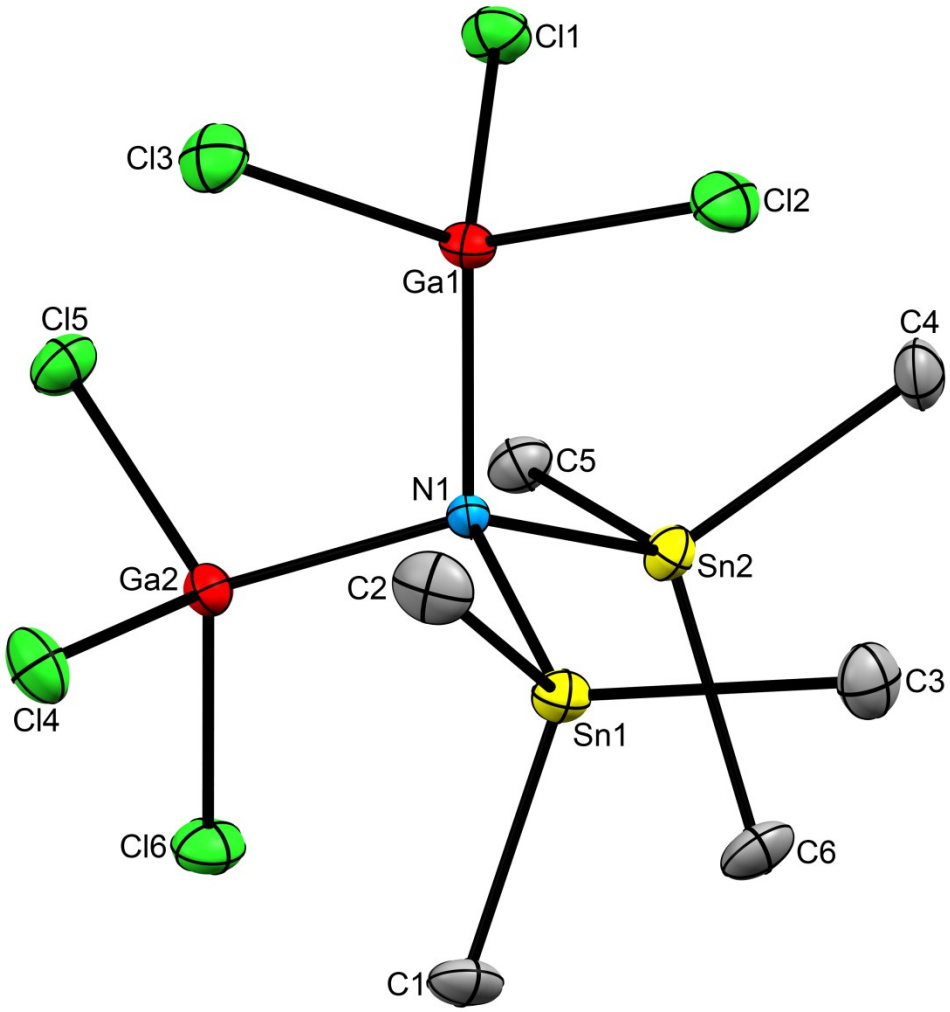

Figure 4.6. The structure of the anion of $(Et_4N)[(Cl_3Ga)_2N(SnMe_3)_2]$, (Et_4N)4, with thermal ellipsoids drawn at 50% probability. Only one of the two formula units present in the asymmetric unit is shown. The cation and hydrogen atoms have been omitted for clarity.

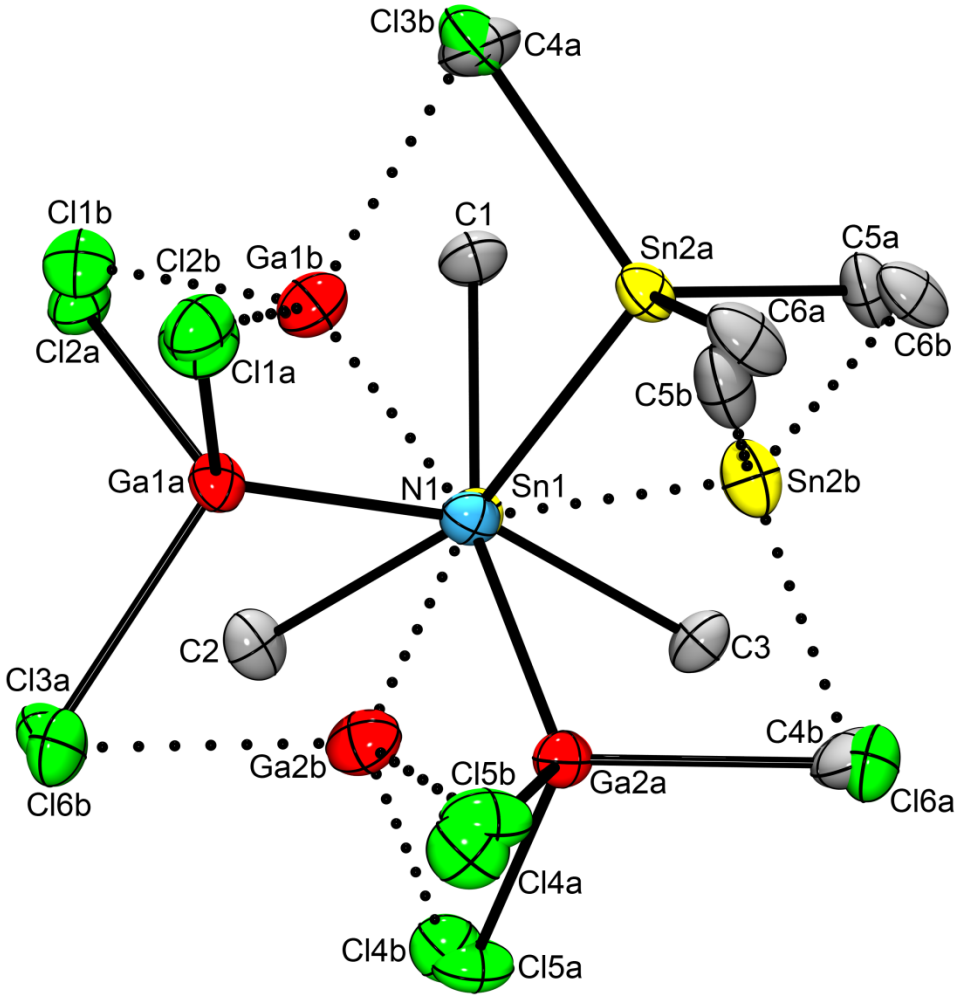

Figure 4.7. The structure of $(Pr^{n}_{4}N)[(Cl_3Ga)_2N(SnMe_3)_2]$, $(Pr^{n}_{4}N)$4, viewed down the N1–Sn1 bond with thermal ellipsoids drawn at 50% probability. Dotted lines indicate bonds in the minor component of disorder. The cation and hydrogen atoms have been omitted for clarity.

Table 4.3. Selected mean bond lengths (Å) and angles (°) for salts of $[(Cl_3Ga)_2N(SnMe_3)_2]^-$ (4).

	(Et_4N)**4**	$(Pr^n{}_4N)$**4**
Sn–N	2.180(9)	2.174(11)
Ga–N	1.929(7)	1.950(52)
Sn–C	2.124(8)	2.140(4)
Ga–Cl	2.183(10)	2.197(13)
Sn–N–Sn	109.2(7)	109.2(1)
Ga–N–Ga	109.4(5)	108.8(3)
Ga–N–Sn	109.6(7)	110(1)
C–Sn–C	112(2)	112(1)
N–Sn–C	107(1)	107(5)
Cl–Ga–Cl	107(2)	107(1)
N–Ga–Cl	112(2)	112(2)

Synthesis of (6) and (7)

It was noted during the course of our work that highly concentrated solutions of $(Me_3Sn)_3N$ and $[GaX_4]^-$ (X = Cl, Br) often precipitated salts of $[Me_3SnX_2]^-$ (See appendix A). It was recognized that the formation of these salts could be exploited to drive the formation of larger anionic clusters, especially in light of our isolation of the In–N cluster, $[(ClIn)_6(NSnMe_3)_5(\mu\text{-}Cl)_3]^-$ (**11**), from a reaction that eliminates $[Me_3SnCl_2]^-$. The reaction of $(Et_4N)[GaCl_4]$ and $(Me_3Sn)_3N$ in a 1:1 ratio in THF yields colorless crystals of $(Et_4N)[Me_3SnCl_2]$ upon slow concentration. Separation of the mother liquor from these crystals and continued concentration of the solution afforded a mixture of $(Et_4N)[Me_3SnCl_2]$ and colorless crystals of $(Et_4N)_2[(Cl_2GaNSnMe_3)_3(SnMe_2Cl)]$, $(Et_4N)_2$**6**, as identified by X-ray crystallography (Figure 4.9). Isolation of the product in a purity sufficient for elemental analysis has not been achieved as of yet. However, the solid state electronic spectrum of a sample of $(Et_4N)_2$**6** with some $(Et_4N)[Me_3SnCl_2]$ contamination showed an intense absorption at 267 nm (Figure 4.11). This absorption is not present in the spectrum of Et_4NCl or $(Et_4N)[Me_3SnCl_2]$. Additionally, **6** contains a Ga_2NSnMe_3 fragment that is similar in structure to $[(Cl_3Ga)_2NSnMe_3]^{2-}$ (**1**), which has a characteristic absorption at 248 nm.[8] Repeating the same reaction procedure with $(Et_4N)[GaBr_4]$ and $(Me_3Sn)_3N$ results in the isolation of a structurally similar $(Et_4N)[Ga_3(NSnMe_3)_3(SnMe_2)MeBr_5]$, (Et_4N)**7** (Figure 4.10). Most interestingly, **6** and **7** provide structural evidence of methyl–halogen exchange in the $(Me_3Sn)_3N/[GaX_4]^-$ system.

Structure of (6) and (7)

$(Et_4N)_2$**6** crystallizes in the monoclinic space group $P2_1/c$ with a single formula unit and one toluene molecule in the asymmetric unit. (Et_4N)**7** crystallizes in triclinic space group $P\bar{1}$. The asymmetric unit also appeared to contain a toluene that was disordered over a crystallographic inversion center. A solvent mask was employed due to excessive disorder which prevented modeling.

The anion **6** can be view as consisting of the trimeric anion $[Cl_2GaNSnMe_3]^{3-}$ with two of the N atoms bridged by a $SnMe_2Cl^+$ cation (Figure 4.10). Similarly **7** can be viewed as $[Ga_3(NSnMe_3)_3MeBr_5]^{3-}$ with two N atoms bridged by a $SnMe_2^{2+}$ group (Figure 4.11). The core structures of **6** and **7** bear resemblance to the organic molecule bicyclo[3.1.1]heptane (Figure 4.9d). A previously characterized Sn–N compound, $[(Me_2Sn)_4(NSnMe_2Cl)_3Cl_2]$, also contains a bicyclo[3.1.1]heptane core (Figure 4.9c). This compound was synthesized by a base catalyzed rearrangement of $(ClMe_2Sn)_3N$.[4] Eight examples of Ga_3N_3 six membered rings have been previously characterized. These consist of trimeric gallium amides[22,23,24,25,26,27] and azides.[28,29] There are also larger cage structures[30-35] containing a six membered Ga_3N_3 ring. Like the previously describe anions, $[(X_3Ga)_2NSnMe_3]^{2-}$ (X = Cl (**1**), Br (**2**)), **6** and **7** contain a μ_3-N atom with a Ga_2NSn coordination sphere. The geometry around N1 in **6** is only slightly deviated from planar with the sum of the M–N–M bonds equaling 355° and N1 being 0.24 Å out of the Ga1–Ga2–Sn1 plane. Similarly the sum of the M–N–M bonds in **7** equal 359° and N1 is 0.12 Å out of the Ga1–Ga2–Sn1 plane. The other two nitrogen atoms along with Ga3 and Sn4 form a strained four member ring where the

N2–Ga3–N3 angles are 92.6(1)° and 88.9(2)°, the N2–Sn4–N3 angles are 76.9(1)° and 83.2(2)°, for **6** and **7** respectively.

There is significant asymmetry in the Sn4–N bond distances in **6**. This arises from the nature of the $SnMe_2Cl^+$ bridge in which Sn4 is at the center of a distorted trigonal bipyramid with N3 and N2 occupying the axial and equatorial positions respectively. The equatorial Sn4–N3 bond has a bond length of 2.359(3) Å while the equatorial Sn4–N2 bond is 2.130(3) Å. In **7** Sn4 adopts a more tetrahedral geometry with the bond distances of Sn4–N3 and Sn4–N2 being 2.109(6) Å and 2.123(6) Å respectively. The mean Ga–(μ_3-N) bond lengths in **6** and **7** are 1.841(4) Å and 1.843(8) Å respectively, within error of each other and of the values in **1** and **2**. The mean Ga–(μ_4-N) bond distances in **6** and **7** are 1.94(2) Å and 1.98(3) Å, also within error of each other and of the values in $Cl_3Ga{\cdot}N(SnMe_3)_3$ (1.950(7) Å) and $Br_3Ga{\cdot}N(SnMe_3)_3$ (1.954(1) Å).[7] The Sn1–N1 bond distances are 2.037(3) Å and 2.052(6) Å for **6** and **7** respectively. These values are identical within error of those in the parent compound $(Me_3Sn)_3N$ (2.04(3) Å),[36] and are just slightly shorter than the values of 2.060(2) Å and 2.076(2) Å in $(Me_4N)_2$**1** and $(Me_4N)_2$**2**. The mean Ga–Cl distance in **6** is 2.22(3) Å and the mean Ga–Br distance in **7** is 2.384(9). These values are within error of those recorded for $(Me_4N)_2$**1** (2.22(1) Å) and (Me_4N)**2** (2.38(2) Å) and just slightly elongated compared to $Cl_3Ga{\cdot}N(SnMe_3)_3$ (2.184(6) Å) and $Br_3Ga{\cdot}N(SnMe_3)_3$ (2.34(1) Å).

The structures of **6** and **7** provide evidence for the occurrence of methyl–halogen exchange in reactions of $(Me_3Sn)_3N$ and $[GaX_4]^-$ (X = Cl, Br) in THF. Both structures contain a μ–$SnMe_2$ moiety indicating loss of a methyl group from Me_3SnX. In the case of **6**, the reaction stoichiometry suggests the formation of $SnMe_4$. Spectroscopic evidence for the formation $SnMe_4$ has been observed during the decomposition of $[(ClIn)_6(NSnMe_3)_5(\mu\text{-}Cl)_3]^-$ (See Chapter 3, Figures 3.6 and 3.8). For compound **7**, Sn → Ga methyl migration occurs as seen from the Ga–Me bond (Ga3–C12, Figure 4.11). The thermal ellipsoid of C12 is small which reflects a slightly higher than expected electron density. The assignment of a methyl group is supported by charge (the group at that position must have a 1– charge) and bond distance (Ga3–C12 = 1.963(6) Å, mean Ga–CH_3 distance from the CSD = 1.97(4) Å). Ga–NH_2 and Ga–OH distances would be significantly shorter.

Methyl–halogen exchange in the presence of $GaCl_3$ has been observed for silyl amino-arsanes[37] and stibanes[15] (Scheme 4.3a-b). The proposed mechanism for this reaction involved abstraction of Cl^- by $GaCl_3$, followed by addition of Cl^- to Si and an intramolecular methyl migration from Si to As/Sb. A similar mechanism could explain the methyl–halogen exchange in **6** and **7**. In this system both $GaX_3/[GaX_4]^-$ and $Me_3SnX/[Me_3SnX_2]^-$ could potentially act as halogen acceptors/donors. The precipitation of $[Me_3SnX_2]^-$ salts suggests that the $Me_3SnX/[Me_3SnX_2]^-$ acceptor/donor pair play a role in this exchange process.

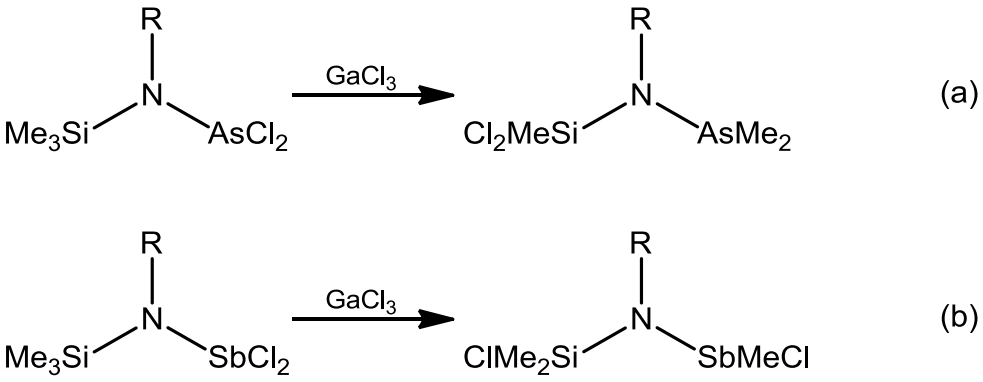

Scheme 4.5. Methyl–chlorine exchange previously observed in amino (a) arsanes[37] and (b) stibanes.[15] R = terphenyl group.

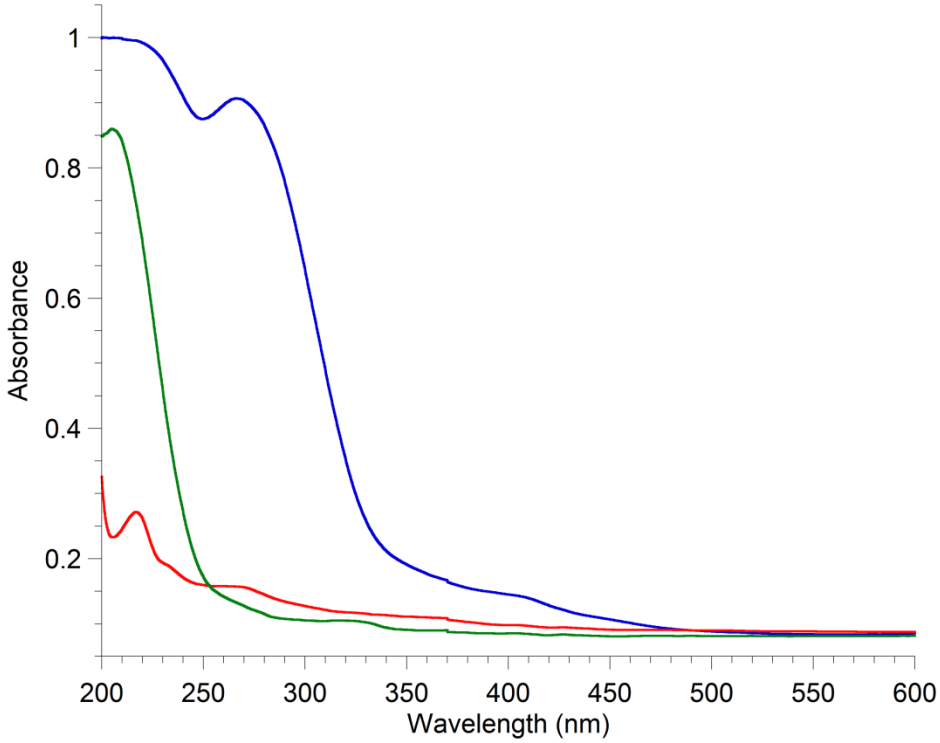

Figure 4.8. The diffuse reflectance UV-Vis spectrum of $(Et_4N)_26/[Me_3SnCl_2]^-$ (blue). The spectra of $(Et_4N)[Me_3SnCl_2]$ (green) and (Et4N)Cl (red) are shown

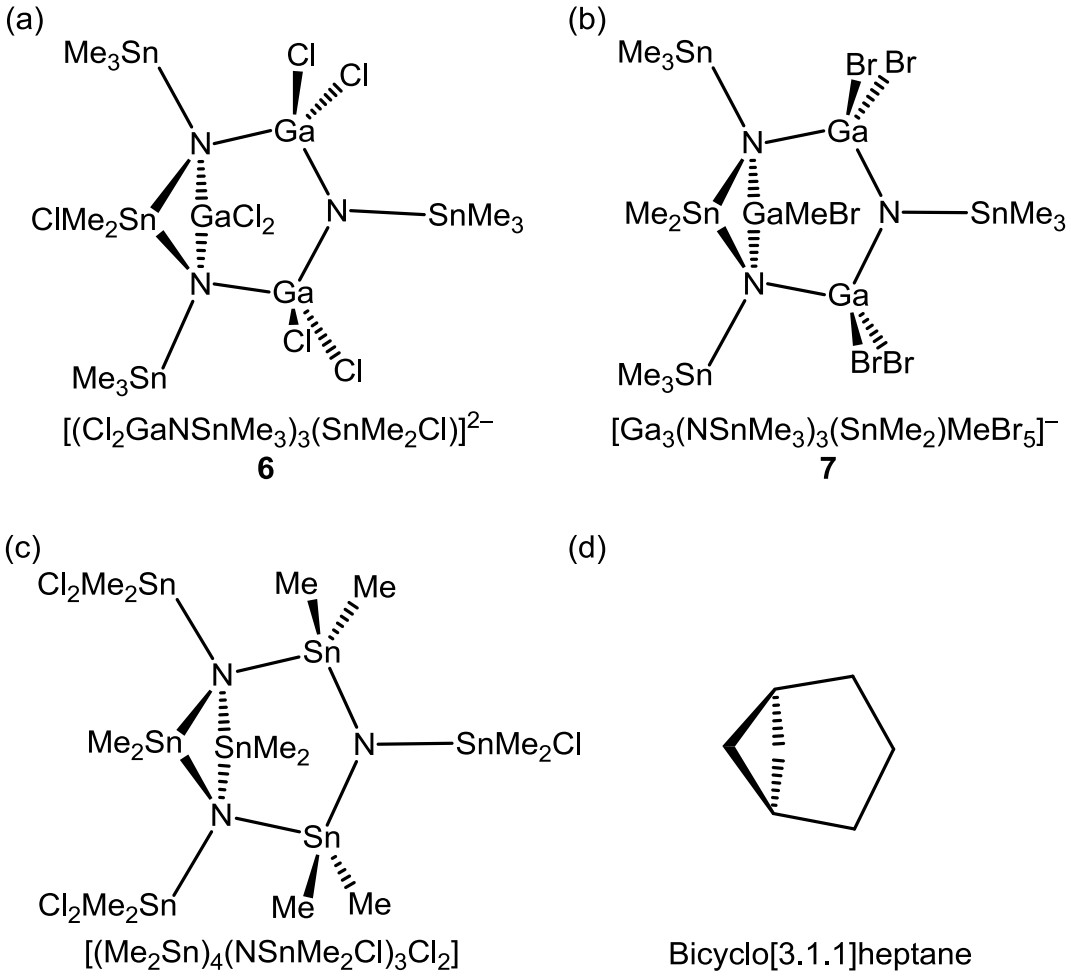

Figure 4.9. Comparison of the structures of (a) 6 and (b) 7 with (c) $[(Me_2Sn)_4(NSnMe_2Cl)_3Cl_2]$ and (d) bicycle[3.1.1]heptane.

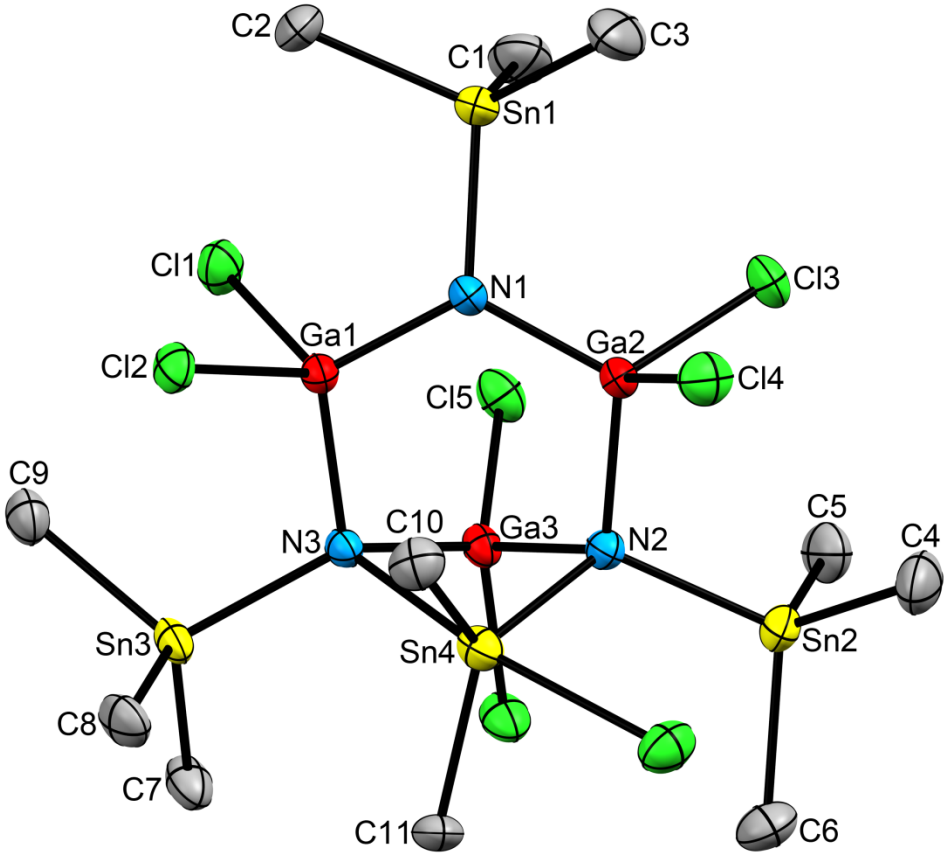

Figure 4.10. Molecular structure of $[(Cl_2GaNSnMe_3)_3(SnMe_2Cl)]^{2-}$ (6) with thermal ellipsoids drawn at 50% probability. The cations, hydrogen atoms, and toluene have been omitted for clarity.

Table 4.4. Selected bond lengths for $(Et_4N)_2$6.

Sn1–N1	2.037(3)	Sn–C1-9 (mean)	2.137(10)
Sn2–N2	2.108(3)	Sn4–C10	2.107(4)
Sn3–N3	2.092(3)	Sn4–C11	2.107(4)
Sn4–N2	2.130(3)		
Sn4–N3	2.359(3)	Sn4–Cl7	2.5875(12)
Ga1–N1	1.845(3)	Ga1–Cl1	2.2514(12)
Ga1–N3	1.939(3)	Ga1–Cl2	2.2471(11)
Ga2–N1	1.837(3)	Ga2–Cl3	2.2307(12)
Ga2–N2	1.963(3)	Ga2–Cl4	2.2336(12)
Ga3–N2	1.958(3)	Ga3–Cl5	2.1683(12)
Ga3–N3	1.911(3)	Ga3–Cl6	2.2075(11)

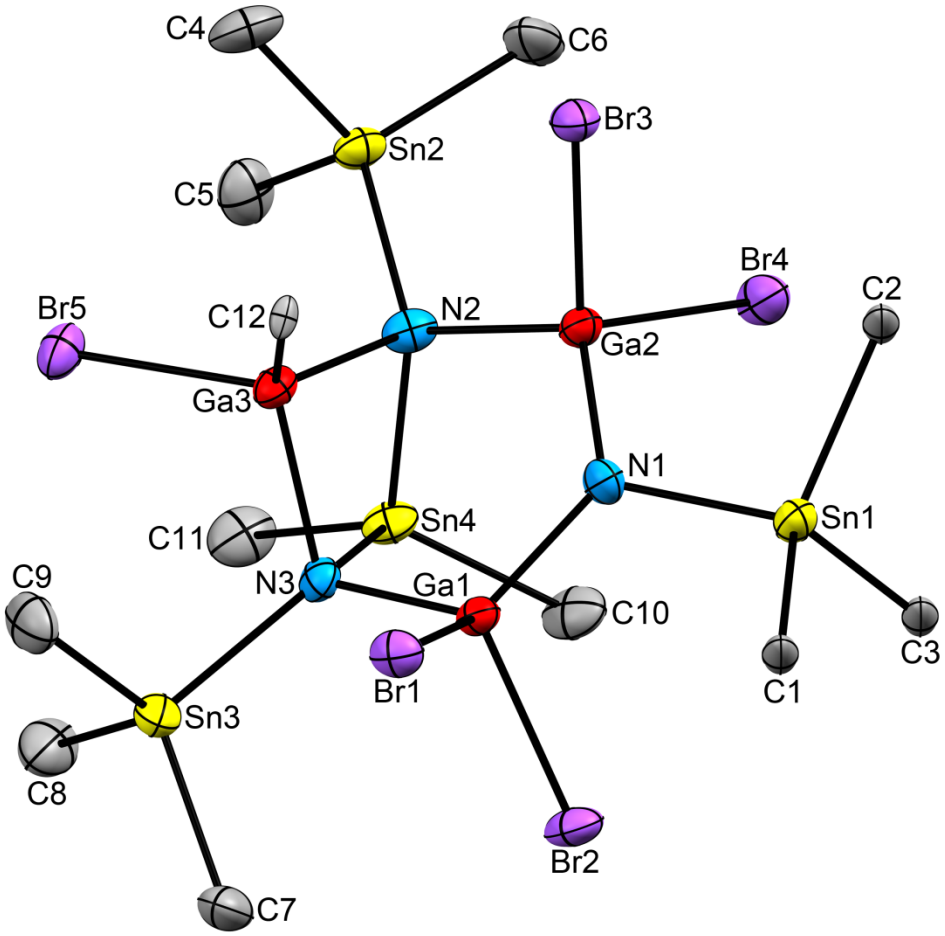

Figure 4.11. Molecular structure of $[Ga_3(NSnMe_3)_3(SnMe_2)MeBr_5]^-$ (7) with thermal ellipsoids drawn at 50% probability. The cation and hydrogen atoms have been omitted for clarity.

Table 4.5. Selected bond lengths for $(Et_4N)7$.

Sn1–N1	2.052(6)	Sn1–C1	2.202(7)
Sn2–N2	2.127(6)	Sn1–C2	2.225(7)
Sn3–N3	2.130(6)	Sn1–C3	2.186(7)
Sn4–N2	2.123(6)	Sn2–C4	2.143(9)
Sn4–N3	2.109(6)	Sn2–C5	2.128(8)
Ga1–N1	1.835(6)	Sn2–C6	2.131(8)
Ga1–N3	1.961(6)	Sn3–C7	2.152(8)
Ga2–N1	1.850(6)	Sn3–C8	2.130(8)
Ga2–N2	1.944(6)	Sn3–C9	2.128(8)
Ga3–N2	2.006(6)	Sn4–C10	2.132(8)
Ga3–N3	2.005(6)	Sn4–C11	2.117(8)
Ga1–Br1	2.3787(10)	Ga3–C12	1.963(6)
Ga1–Br2	2.3830(10)		
Ga2–Br3	2.3980(10)		
Ga2–Br4	2.3742(11)		
Ga3–Br5	2.3841(10)		

Conclusion

We report here the synthesis of the novel Ga–N and In–N compounds $[(Cl_3M)_2N(SnMe_3)_2]^-$ (M = Ga (**4**), In (**5**)) from highly concentrated reactions of $(Et_4N)[MCl_4]$ with $Cl_3M{\cdot}N(SnMe_3)_3$. The formulation of **4** was confirmed by elemental analysis, X-ray crystallography, and NMR. In CH_2Cl_2 and THF **4** exhibits room temperature stability, but decomposes when heated in THF and at room temperature in MeCN. Addition of $[GaCl_4]^-$ to solutions of **4** did not readily result in metathesis. The formation of **5** is supported by X-ray crystallography and NMR. The anion **5** decomposes quickly in CH_2Cl_2 with mild heating. Highly concentrated reactions of $(Et_4N)[GaX_4]$ (X = Cl, Br) with $(Me_3Sn)_3N$ resulted in the elimination of $[Me_3SnCl_2]^-$. This was exploited to drive the formation of the Ga–N clusters, $[(Cl_2GaNSnMe_3)_3(SnMe_2Cl)]^{2-}$ (**6**) and $[Ga_3(NSnMe_3)_3(SnMe_2)MeBr_5]^-$ (**7**) which have been structurally characterized. Compounds **6** and **7** provide evidence of Lewis acid assisted methyl–halogen exchange. Taken together, the formation of **4**-**7** support the use of the $(Me_3Sn)_3N$ and $X_3M{\cdot}N(SnMe_3)_3$ (M = Ga, In; X = Cl, Br) to produce both small and high nuclearity M–N molecules when reacted with salts of $[MX_4]^-$.

Acknowledgements

Michelle R. Beoris crystallized and characterized of **4** and **6**. Jason R. Jones first crystallized **7**. Their work is included for completeness. Dr. Curtis Moore provided assistance in modeling the disordered solvent molecule of **6**.

This chapter contains material which is being prepared for submission. Wilson, Robert J.; Beoris, Michelle R.; Bennett, Miriam V. "Unique Gallium-Tin Nitrogen Compounds Via Dehalostannylation: Pathways to Small Molecules and Oligomers" *Manuscript in preparation.*

References

(1) Pi, C.; Elguero, J.; Wan, L.; Alkorta, I.; Zheng, W.; Weng, L.; Chen, Z.; Wu, L. *Chem.--Eur. J.* **2009**, *15*, 6581.

(2) Driess, M.; Monse, C.; Merz, K.; van Wullen, C. *Angew. Chem., Int. Ed.* **2000**, *39*, 3684.

(3) Eichler, J. F.; Just, O.; Rees, W. S., Jr. *Inorg. Chem.* **2006**, *45*, 6706.

(4) Kober, C.; Noth, H.; Storch, W. *Chem. Ber./Recl.* **1997**, *130*, 765.

(5) Bettenhausen, R.; Milius, W.; Schnick, W. *Chem.--Eur. J.* **1997**, *3*, 1337.

(6) Hillwig, R.; Harms, K.; Dehnicke, K. *J. Organomet. Chem.* **1995**, *501*, 327.

(7) Cheng, Q. M.; Stark, O.; Merz, K.; Winter, M.; Fischer, R. A. *J. Chem. Soc., Dalton Trans.* **2002**, 2933.

(8) Wilson, R. J.; Jones, J. R.; Bennett, M. V. *Chem. Commun. (Cambridge, U. K.)* **2013**, *49*, 5049.

(9) Shishido, K.; Kojima, S. *J. Org. Chem.* **1964**, *29*, 907.

(10) Dolomanov, O. V.; Bourhis, L. J.; Gildea, R. J.; Howard, J. A. K.; Puschmann, H. *J. Appl. Crystallogr.* **2009**, *42*, 339.

(11) Sheldrick, G. *Acta Cryst.* **2008**, *A64*, 112.

(12) Macrae, C. F.; Bruno, I. J.; Chisholm, J. A.; Edgington, P. R.; McCabe, P.; Pidcock, E.; Rodriguez-Monge, L.; Taylor, R.; van de Streek, J.; Wood, P. A. *J. Appl. Crystallogr.* **2008**, *41*, 466.

(13) Shannon, R. D. *Acta Crystallogr., Sect. A* **1976**, *A32*, 751.

(14) Nutt, W. R.; Blanton, J. S.; Boccanfuso, A. M.; Silks, L. A., III; Garber, A. R.; Odom, J. D. *Inorg. Chem.* **1991**, *30*, 4136.

(15) Hering, C.; Lehmann, M.; Schulz, A.; Villinger, A. *Inorg. Chem.* **2012**, *51*, 8212.

(16) Rudawska, K.; Ptasiewicz-Bak, H. *J. Coord. Chem.* **2003**, *56*, 1567.

(17) Hill, J. B.; Talley, T. A.; Pennington, W. T.; Robinson, G. H. *J. Chem. Crystallogr.* **1994**, *24*, 61.

(18) von, H. C.; Stahl, S. *Z. Anorg. Allg. Chem.* **2008**, *634*, 701.

(19) Kuehner, S.; Kuhnle, R.; Hausen, H. D.; Weidlein, J. *Z. Anorg. Allg. Chem.* **1997**, *623*, 25.

(20) Aitchison, K. A.; Backer-Dirks, J. D. J.; Bradley, D. C.; Faktor, M. M.; Frigo, D. M.; Hursthouse, M. B.; Hussain, B.; Short, R. L. *J. Organomet. Chem.* **1989**, *366*, 11.

(21) Trapp, M.; Hausen, H. D.; Weckler, G.; Weidlein, J. *J. Organomet. Chem.* **1993**, *450*, 53.

(22) Harrison, W.; Storr, A.; Trotter, J. *J. Chem. Soc., Dalton Trans.* **1972**, 1554.

(23) Almond, M. J.; Drew, M. G. B.; Jenkins, C. E.; Rice, D. A. *J. Chem. Soc., Dalton Trans.* **1992**, 5.

(24) Atwood, D. A.; Cowley, A. H.; Harris, P. R.; Jones, R. A.; Koschmieder, S. U.; Nunn, C. M.; Atwood, J. L.; Bott, S. G. *Organometallics* **1993**, *12*, 24.

(25) Wells, R. L.; Rahbarnoohi, H.; Glaser, P. B.; Liable-Sands, L. M.; Rheingold, A. L. *Organometallics* **1996**, *15*, 3204.

(26) Tang, C. Y.; Coxall, R. A.; Downs, A. J.; Greene, T. M.; Parsons, S. *J. Chem. Soc., Dalton Trans.* **2001**, 2141.

(27) Marchant, S.; Tang, C. Y.; Downs, A. J.; Greene, T. M.; Himmel, H.-J.; Parsons, S. *Dalton Trans.* **2005**, 3281.

(28) Kouvetakis, J.; McMurran, J.; Steffek, C.; Groy, T. L.; Hubbard, J. L. *Inorg. Chem.* **2000**, *39*, 3805.

(29) Dingman, S. D.; Rath, N. P.; Buhro, W. E. *Dalton Trans.* **2003**, 3675.

(30) Rettig, S. J.; Storr, A.; Trotter, J. *Can. J. Chem.* **1975**, *53*, 753.

(31) Amirkhalili, S.; Hitchcock, P. B.; Smith, J. D. *J. Chem. Soc., Dalton Trans.* **1979**, 1206.

(32) Schnitter, C.; Waezsada, S. D.; Roesky, H. W.; Teichert, M.; Uson, I.; Parisini, E. *Organometallics* **1997**, *16*, 1197.

(33) Schmid, K.; Niemeyer, M.; Weidlein, J. *Z. Anorg. Allg. Chem.* **1999**, *625*, 186.

(34) Luo, B.; Gladfelter, W. L. *J. Cluster Sci.* **2002**, *13*, 461.

(35) Luo, B.; Gladfelter, W. L. *Inorg. Chem.* **2002**, *41*, 6249.

(36) Appel, A.; Kober, C.; Neumann, C.; Noeth, H.; Schmidt, M.; Storch, W. *Chem. Ber.* **1996**, *129*, 175.

(37) Michalik, D.; Schulz, A.; Villinger, A. *Inorg. Chem.* **2008**, *47*, 11798.

Chapter 5: Synthesis and Structure of Bismuth-Tin Nitride Cage Compounds

Introduction

While imido phosphorous compounds are prolific in the literature (numbering in the thousands), imides of the heavier pnictogens (As, Sb, Bi) are significantly less common. Reactivity studies of E–N compound show that Lewis acidity of pnictogens increase in the order E = As < Sb < Bi.[1-3] Given this increase in Lewis acidity for the heavier group 15 elements it would be logical to assume that Bi–N compounds would be stabilized by oligomerization as with their group 13 metal counterparts. There are 14 examples of such oligomers. These include: the mixed amide–imide clusters, $[(Dipp(H)N)BiNDipp]_2$,[4] $[Bi_3(\mu\text{-}NR)_4(N(H)R)]$ (R = 2,6-$Me_2C_6H_3$),[5] and $[(Me_3Si)_2NBiNSiMe_3]_2$;[6] A chlorobismuth terphenylimide dimer of the form $[ClBiNAr]_2$ (Ar = 2,6-$MesC_6H_3$; Mes = 2,4,6-$Me_3C_6H_2$);[7] a bimetallic lithium-bismuth imide cubane, $[Bi_2Li_2(NBu^t)_4(thf)]$;[8] and a tetrameric oxypyridine bismuth imide cubane, $[pyOBiNCy]_4$ (Cy = cyclohexyl, py = 2-pyridyl).[9] The strategies employed in the synthesis of these compounds were alkali halide salt elimination,[4-6] base catalyzed rearangement,[7,8] and amine elimination.[9] Our previous work (*vide supra*) has shown that, when reacted with $[GaX_4]^-$ (X = Cl, Br), tris(trimethylstannyl)amine, $(Me_3Sn)_3N$, is an effective precursor to novel anionic Ga–N compounds. This fact, in addition to the lack of Bi–N compounds in which N is bonded solely to metals, led us to explore the reaction of anionic Bi halides with $(Me_3Sn)_3N$. We had synthesized various Bi halide salts in our lab. It was found that when $[Bi_2Cl_9]^{3-}$ is reacted with $(Me_3Sn)_3N$ in

a 1:2 ratio the novel Bi–N cubane cluster, $[Bi_4(NSnMe_3)_4(\mu\text{-}Cl_6)]^{2-}$ (**1**), is isolated as the $Pr^n{}_4N^+$ salt (Scheme 5.1). $(Pr^n{}_4N)_2$**1** has been characterized by elemental analysis, single crystal x-ray diffraction, nuclear magnetic resonance, and diffuse reflectance spectroscopy. Compound **1** is the first structurally characterized Bi–N molecule containing only metals bonded to N. Reaction of $(Me_3Sn)_3N$ with the neutral $BiCl_3$ produced an intractable orange precipitate in MeCN, THF, and Et_2O which was studied by proton NMR and diffuse reflectance spectroscopy. This bolsters the use of anionic metal halides as efficient precursors to novel M–N compounds.

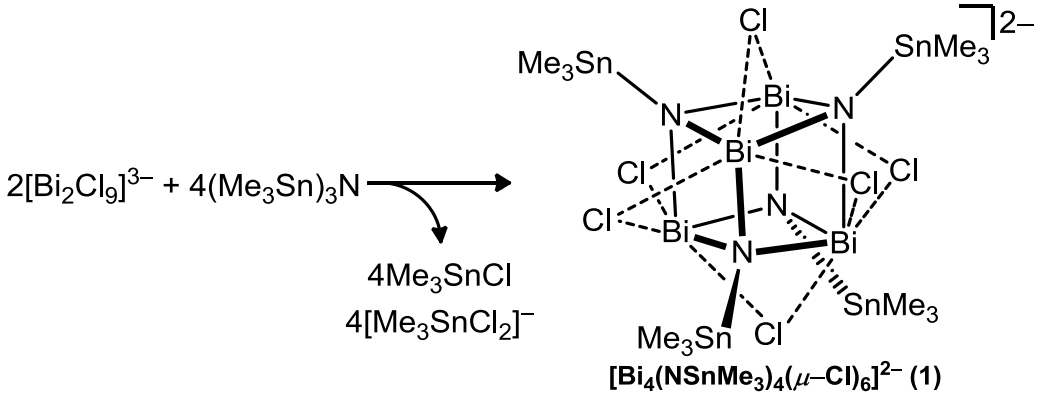

Scheme 5.1. The synthesis of $[Bi_4(NSnMe_3)_4(\mu\text{-}Cl_6)]^{2-}$ (1).

Experimental

Preparation of Compounds

All manipulations were carried out under a pure dinitrogen atmosphere using standard Schlenk and glove-box techniques. Anhydrous tetrahydrofuran (THF), purchased from EMD, diethylether (Et_2O), purchased from EMD, and acetonitrile (MeCN), purchased from Burdick and Jackson were stored over activated 4 Å molecular sieves under a pure dinitrogen atmosphere. The compound $(Me_3Sn)_3N$ was prepared according to the literature procedure.[10] Preparation of the salt $(Pr^n{}_4N)_3[Bi_2Cl_9]$ is described in appendix B. Elemental analysis was performed at Columbia Analytics Laboratory in Tucson, AZ.

$(Pr^n{}_4N)_2[Bi_4(NSnMe_3)_4(\mu\text{-}Cl)_6]$, $(Pr^n{}_4N)_2$1. A solution of $(Pr^n{}_4N)_3[Bi_2Cl_9]$ (0.67 g, 0.52 mmol) in 6.0 mL of MeCN was added to a solution of $(Me_3Sn)_3N$ (0.52 g, 1.0 mmol) in 6.0 mL of MeCN. The reaction mixture was stirred for 1 min then left undisturbed for 17 h resulting in the formation of a bright orange solution and a yellow precipitate. The yellow solid was removed by vacuum filtration through a nylon filter. Vapor diffusion of diethyl ether into the filtrate over 4 days afforded orange crystals along with yellow powder. The supernatant liquid was decanted and the solids were washed with successive aliquots of THF (3 × 10 mL) in order to effect removal of the powder by mechanically mixing and decanting. The remaining orange crystals were washed with Et_2O (3 x 10 mL) and ground with a mortar and pestle. These were

collected on a nylon filter and washed again with Et_2O (2 x 3 mL) and dried *in vacuo* to afford 0.109 g (0.0510 mmol, 20%) of $(Pr^n_4N)_2$**1**. ^{1}H NMR (CD_3CN): 0.35 ppm, s, $J(^{117}Sn, ^1H)$ 56 Hz $J(^{119}Sn, ^1H)$. 58 Hz. Diffuse reflectance spectrum: λ_{max} (nm) 314, 368, 468 (sh). UV-Vis (MeCN): λ_{max} (nm) 370 (sh). ES^--MS (MeCN): *m/z* 1724 ($[Bi_4(NSnMe_3)_4Cl_5]^-$). Anal. Calcd for $C_{36}H_{92}Bi_4Cl_6N_6Sn_4$: C, 20.27; H, 4.35; N, 3.94. Found: C, 19.90; H, 4.67; N, 3.86.

X-ray Structure Determination

Crystals were coated in Paratone oil and mounted by mean of a glass capillary fiber on a Bruker APEX-II CCD area detector instrument operated by the APEX software package. Data reduction was performed by SAINT, absorption correction was applied using SADABS, and the space group was assigned using XPREP. The structure of $(Pr^n_4N)_2$**1** was solved by direct methods and refined against all data by full-matrix least squares on F_2. Hydrogen atoms were attached at idealized positions on carbon atoms and were refined as riding atoms with uniform isotropic thermal parameters. Structure solution, refinement, graphics and report generation were performed using SHELXTL[11] and Mercury.[12]

Other Physical Measurements

The solid state electronic reflectance spectra were recorded on a JASCO V-670 UV-Vis spectrophotometer fitted with an integrating sphere. NMR spectra were

collected on a Varian Inova 400 MHz instrument at 30°C with chemical shifts referenced to the signal of residual protons in the deuterated solvent. Infrared spectroscopy was performed on a Perkin-Elmer RX I spectrometer equipped with an attenuated total reflectance accessory. Mass spectrometry was performed on a Thermo Finnigan LCQ Duo ion trap spectrometer with and ESI ion source and the data was examined using mMass software.[13]

Table 5.1. Crystallographic data for $(Pr^n_4N)_2$1.

	$(Pr^n_4N)_2$**1**
formula	$C_{36}H_{92}Bi_4Cl_6N_6Sn_4$
form. weight	2132.54
T, K	100
cryst. syst.	Monoclinic
space group	$P2_1/c$
a, Å	12.1068(9)
b, Å	23.8434(19)
c, Å	21.3314(16)
α, deg	90
β, deg	96.283(3)
γ, deg	90
V, Å^3	6120.7(8)
Z	4
ρ_{calc}, g/cm^3	2.314
2θ range, deg	2.10 to 27.48
GOF (F^2)	1.098
R_1/wR_2, %	6.00/11.31
largest peak/ hole (e^-/Å^3)	5.975/-4.681

Results and Discussion

Synthesis of (1)

Previous work in our lab has produced M–N clusters (M = Ga, In) from the reactions of $[GaX_4]^-$ and $[InCl_5]^{2-}$ with $(Me_3Sn)_3N$ and $Cl_3In{\cdot}N(SnMe_3)_3$ respectively. In our lab we had synthesized salts of $[Bi_2Cl_9]^{3-}$ thus wished to explore their potential as precursors to high nuclearity Bi–N clusters. We found that the addition of a MeCN solution of $(Pr^n{}_4N)_3[Bi_2Cl_9]$ to a MeCN solution of $(Me_3Sn)_3N$ in a 1:2 ratio results in an immediate color change from colorless to orange with the concomitant formation of a fine yellow precipitate. Filtration of the solution followed by vapor diffusion of Et_2O into the filtrate affords orange crystals of $(Pr^n{}_4N)_2[Bi_4(NSnMe_3)_4(\mu\text{-}Cl)_6]$, $(Pr^n{}_4N)_2$**1,** in a 20% yield.

Properties of (1)

The solid state electronic spectrum of $(Pr^n{}_4N)_2$**1** exhibits broad peaks at 314 nm and 368 nm with a shoulder at 467 nm and a tail extending to almost 600 nm, giving the product its orange color (Figure 5.1). Upon exposure of the sample to air for 24 h there is a reduction in the intensity of the peaks at 314 nm and 368 nm and the shoulder at 467 nm completely vanishes with the absorption tail extending only to 500 nm. $(Pr^n{}_4N)_2$**1** is soluble in MeCN and displays a single resonance (excluding the cation peaks) at 0.35 ppm in the deuterated solvent which is assigned to the $SnMe_3$ protons (Figure 5.2). Heating for 2 days results in some decay of the peak at 0.35 ppm

and formation of a product(s) characterized by a broad resonance at 0.39 ppm along with $[Me_3SnCl_2]^{1-}$ (0.64 ppm), a peak at 0.29 ppm (possibly $(Me_3Sn)_3CCN$), and a small amount of Me_4Sn (0.06 ppm). The electronic spectrum of $(Pr^n{}_4N)_2$**1** in acetonitrile has a shoulder at 370 nm which decays with air exposure over 24 h. Electrospray ionization mass spectrometry of $(Pr^n{}_4N)_2$**1** in MeCN shows a peak at 1724 *m*/*z* in negative ion mode with excellent correlation to the calculated isotopic splitting pattern for $[Bi_4(NSnMe_3)_4Cl_5]^{1-}$, which results from the loss of one chloride from **1** (Figure 5.3). The anion **1** appears to be less prone to hydrolysis than $[(ClIn)_6(NSnMe_3)_5(\mu\text{-}Cl)_3]^{1-}$ (**2**) and $[(Cl_3Ga)_2NSnMe_3]^{2-}$, (**3**) (See Chapters 2 and 3). After 24 h of air exposure the IR spectrum of $(Pr^n{}_4N)_2$**1** does not display the intense broad peak around 3400 cm^{1-} that would be indicative of O–H stretching.

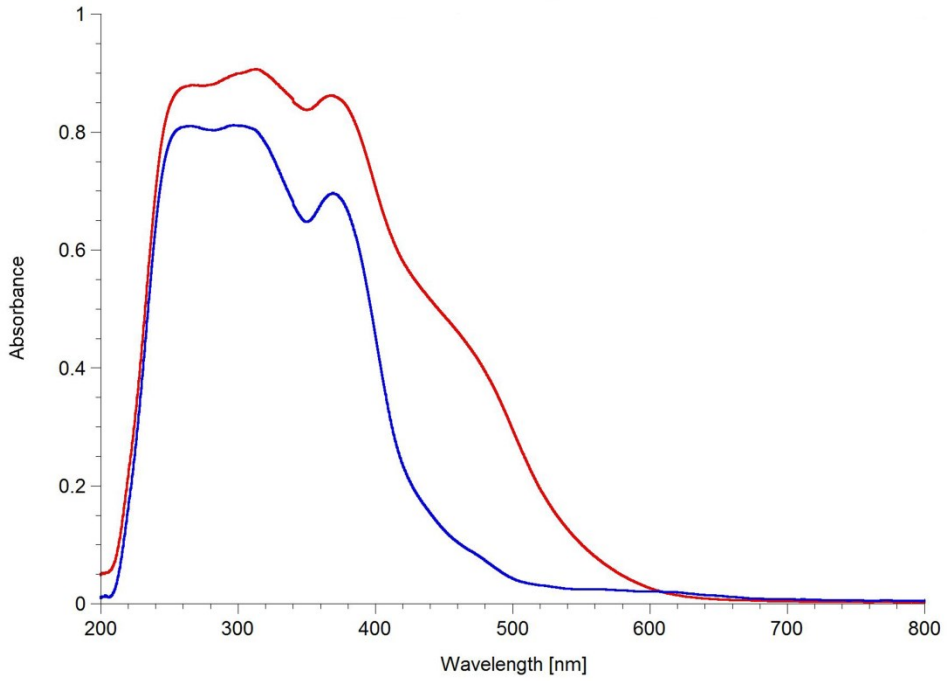

Figure 5.1. Diffuse reflectance UV-Vis spectrum of $(Pr^{n}_{4}N)_2$1 before (red) and after (blue) exposure to air for 24 h.

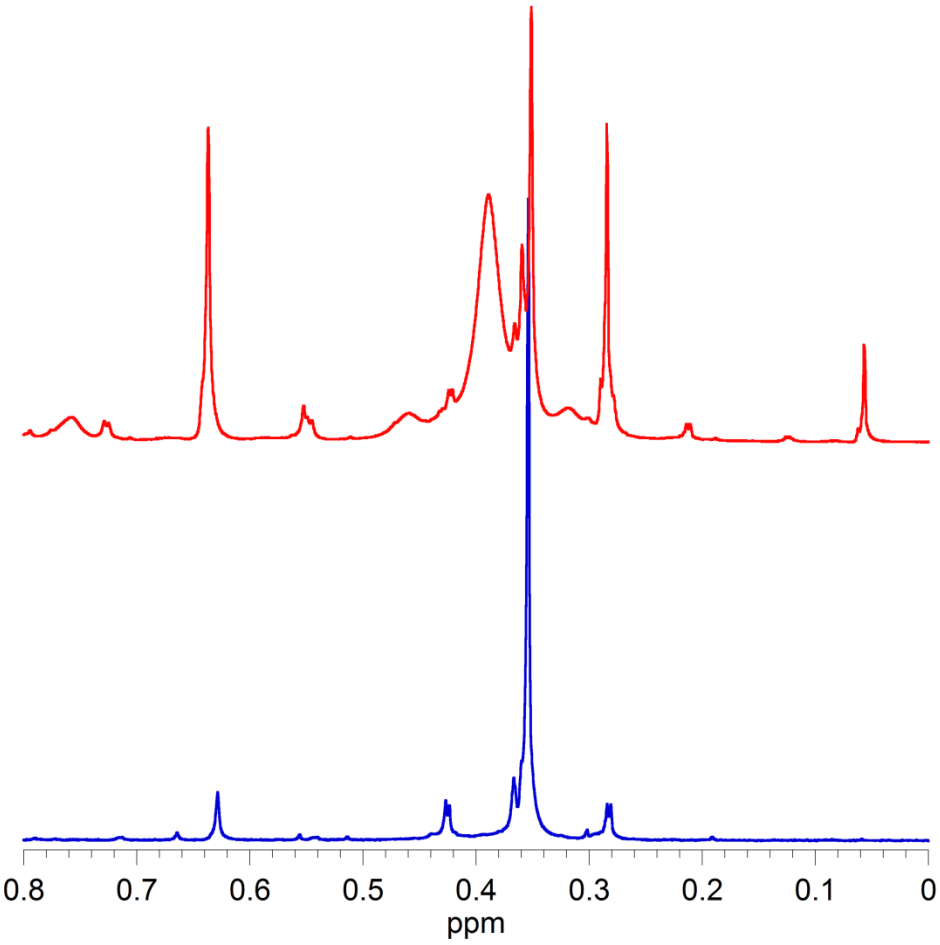

Figure 5.2. ^{1}H NMR of $(Pr^{n}_{4}N)_{2}$1 before (blue) and after (red) heating for 2 days at 60 °C.

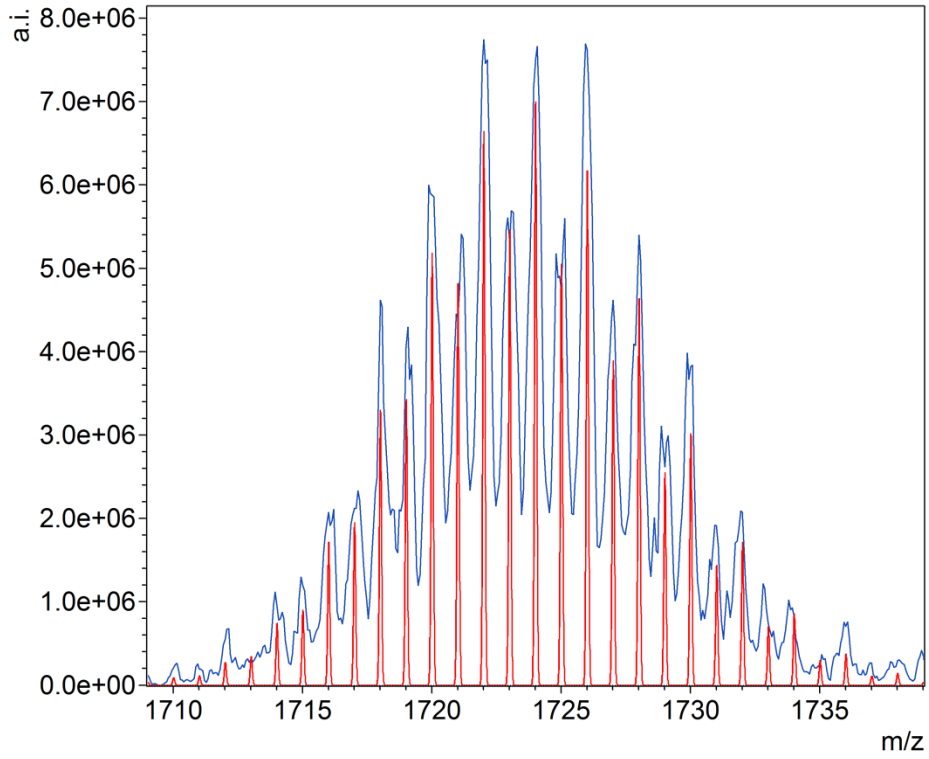

Figure 5.3. The calculated (red) and actual (blue) isotopic splitting pattern for $[Bi_4(NSnMe_3)_4Cl_5]^{1-}$ in the ESI mass spectrum of $(Pr^n{}_4N)_2$1 in negative ion mode.

Structure of (1)

The salt $(Pr^n_4N)_2$**1** crystallizes in the monoclinic space group $P2_1/c$ with one formula unit in the asymmetric unit. The anion **1** consists of a Bi_4N_4 core with a distorted cubane structure. A $SnMe_3$ moiety is bonded to each N atom and a μ_2-Cl bridge caps each face of the cube (Figure 5.4). The anion **1** can be thought of as being formed from a Bi_4 tetrahedron capped on each face with a μ_3-$NSnMe_3$ group. The Bi–Bi interatomic distances have a mean value of 3.41(2) Å which is longer than twice the atomic radius (3.20 Å)[14] and longer than the closest contact in crystalline Bi (3.071 Å);[15] therefore no direct Bi–Bi bonding can be inferred. One other Bi_4N_4 cubane structure has been characterized, the cyclohexylimide tetramer $[pyOBiNCy]_4$ (py = 2-pyridyl). This molecule has somewhat longer and more varied Bi–Bi interatomic distances with a mean value of 3.542(81) Å.[9] The transition metal Bi_4M_4 (M = Co, Fe) cubane structures, $[(CO)_3CoBi]_4$[16] and $[(CO)_3FeBi(Fe(CO)_4)]_4$[17], have short non-bonding Bi–Bi distances of 3.360 Å and 3.435(5) Å respectively. The cation, $[Bi–Pd(PMePh_2)]_4^{2+}$, has a Pd_4Bi_4 core that may be described as a true tetracapped tetrahedron with four bonding and two non-bonding Bi–Bi pairs with mean interatomic distances of 3.22(2) Å and 3.481(29) respectively.[18] Interatomic N–N distances in **8** average 2.87(2) Å, almost twice the N–N distance in hydrazine of 1.449(2) Å.[19]

The Bi–N bond lengths in **1** range from 2.21(1) Å to 2.26(1) Å with a mean value of 2.24(2) Å. The aforementioned Bi_4N_4 cubane, $[pyOBiNCy]_4$, has far more varied Bi–N bond lengths ranging from 2.201(6) Å to 2.481(6) Å with a mean value of

2.3(1) Å. This inconsistency arises from asymmetric bridging interactions across two of the Bi_2N_2 a faces by the 2-pyridyloxide ligands and of the Bi atoms being chelated by a pyO ligand. The bimetallic bismuth-lithium imide cubane, $[BiLi(thf)(NBu^t)_2]_2$, containing a $Bi_2Li_2N_4$ core has Bi–N distances ranging from 2.101(7) Å to 2.237(7) Å with a mean value of 2.182(58) Å. For comparison the Bi–N distances for the sterically stabilized bismuth amide dimer, $[ClBiN(2,6\text{-}Mes_2C_6H_3)]_2$, and monomer, $[Cl_2BiN(H)(2,6\text{-}Mes_2C_6H_3)]$, are 2.160(9) Å (av.) and 2.123(3) Å respectively.[7] The Sn–N bonds are 2.099(10) Å on average, only a slight elongation from that observed for the parent compound $(Me_3Sn)_3N$ (2.04(3) Å).[20]

Each face of the Bi_4N_4 cubane core in **1** is bridged by an asymmetrically bonded μ-Cl. Each of these μ-Cl bridges consists of a "short" and "long" Bi–Cl interactions with mean interatomic distances of 3.05(4) Å and 3.23(9) Å respectively. The "short" Bi–Cl distances are slightly longer than those typically observed for bridging Bi–Cl–Bi bonds. For example, mean Bi–(μ-Cl) distance in $[Ph_4P]_3[Bi_2Cl_9]$ is 2.89(6) Å.[21] For comparison with the "long" Bi–Cl distances, a search of Bi–Cl bonds greater than 3.2 Å in the Cambridge Structural Database (v. 5.34) was performed. This search returns 10 compounds. These include a polymer with a Bi–Cl distance of 3.594(2) Å,[22] a Bi–$[AlCl_4]^-$ complex with a Bi–Cl distance of 3.351(1) Å,[23] and the anion $[Bi_8Cl_{30}]^{6-}$ with Bi–(μ_3-Cl) distance of 3.207(8) Å.[24]

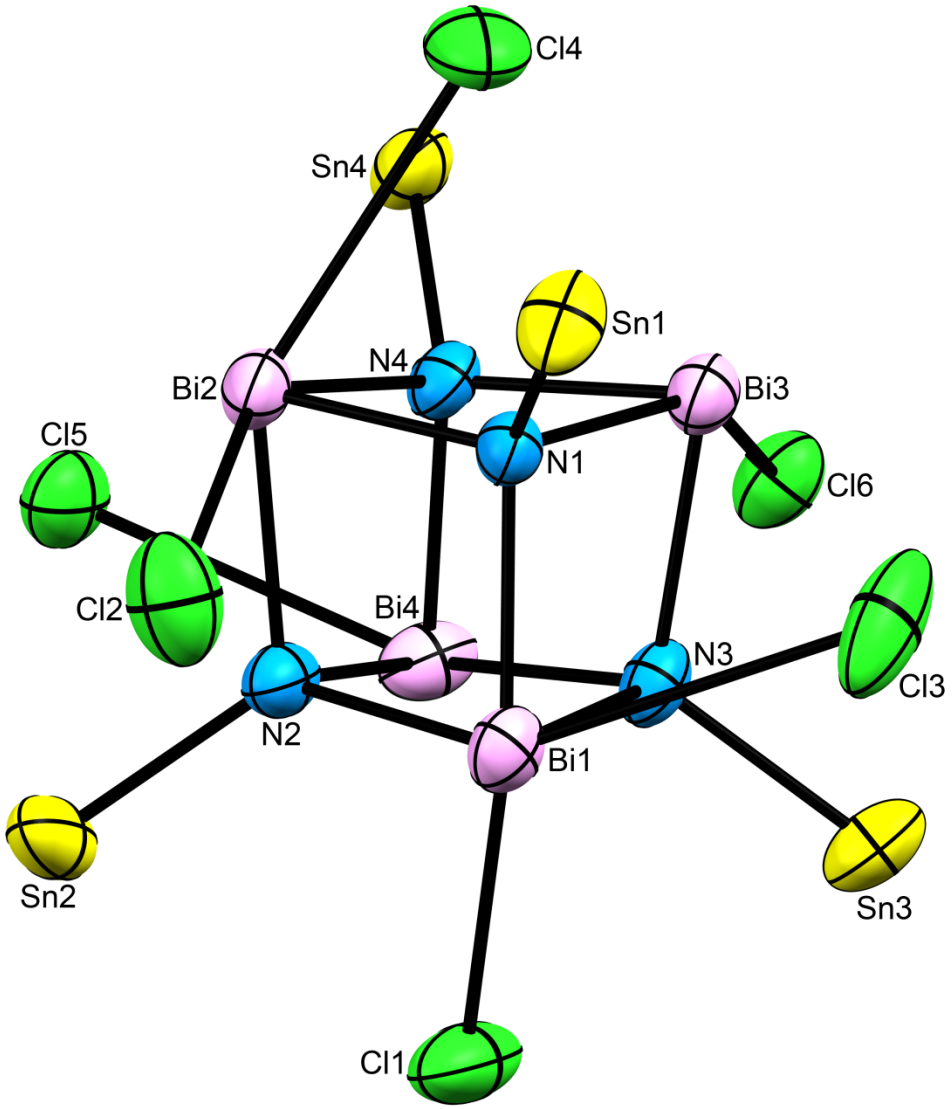

Figure 5.4. The X-ray structure of $[Bi_4(NSnMe_3)_4(\mu\text{-}Cl)_6]^{2-}$ (1) with ellipsoid probabilities set to 50%. The cations and methyl groups have been omitted for clarity. Note: the long Bi–Cl contacts are not drawn.

Table 5.2. Selected mean bond lengths (Å) and angles (°) for $(Pr^n_4N)_2[Bi_4(NSnMe_3)_4Cl_6]$, $(Pr^n_4N)_2$(1).

Bi–N	2.235(17)	N–Bi–N	79.8(6)
Sn–N	2.099(10)	Bi–N–Bi	99.4(8)
Sn–C	2.137(8)	Bi–N–Sn	118(1)
Bi–Cl (short)	3.047(35)	Bi–Cl–Bi	65.7(7)
Bi–Cl (long)	3.233(89)	N–Sn–C	109(2)
Bi–Bi	3.409(15)	C–Sn–C	110(3)
N–N	2.866(16)		

Reactivity of $BiCl_3$ versus $[Bi_2Cl_9]^{3-}$

To demonstrate the advantage of using anionic rather than neutral metal halides it is instructive to compare the reactivity of $(Pr^n_4N)_3[Bi_2Cl_9]$ with $(Me_3Sn)_3N$ to that of $BiCl_3$ with $(Me_3Sn)_3N$. The combination of MeCN solutions of $BiCl_3$ and $(Me_3Sn)_3N$ in a 1:1 ratio results in the immediate formation of an orange solution. Diffusion of diethylether into this solution afforded only a small amount of amorphous orange solid. This same reaction carried out in THF results in the immediate formation of a yellow-orange precipitate. This precipitate is quite fine and separation of the solid by filtration is problematic. Therefore the solvent was removed *in vacuo* to give a glassy orange solid. Investigation by ^1H NMR revealed that both Me_3SnCl and Me_4Sn were produced in this reaction. Reaction of $BiCl_3$ and $(Me_3Sn)_3N$ in a 1:1 ratio in diethyl ether yields an isolable yellow-orange precipitate. Investigation of the precipitate and the mother liquor reveals that Me_3SnCl was formed and some $(Me_3Sn)_3N$ was left unreacted. The electronic spectrum of the precipitate consisted of a broad absorption from 200-600 nm with a λ_{max} of approximately 320 nm. Investigation of the solubility of this precipitate found it to be insoluble in non-polar and polar aprotic solvents. A sample left in MeCN eventually turned black indicating possible reduction of Bi(III) to Bi metal. It is possible that the solid produced from this reaction in THF and Et_2O is polymeric in nature. Thus use of the anion $[Bi_2Cl_9]^{3-}$ rather than $BiCl_3$ appears to be advantageous as it allows for the easy isolation of a discrete molecular bismuth nitrogen compound.

Conclusion

We have isolated the novel Bi–N cubane compound, $[Bi_4(NSnMe_3)_4(\mu\text{–}Cl)_6]^{2-}$ (**1**), from the reaction of $[Bi_2Cl_9]^{3-}$ and $(Me_3Sn)_3N$ in MeCN. $(Pr^n{}_4N)_2$**1** was characterized by elemental analysis, X-ray crystallography, mass spectrometry, and NMR. Diffuse reflectance UV-Vis spectroscopy and IR show that **1** decomposes slowly in air. A search of the Cambridge Structural Database shows that **1** is only the second Bi–N cubane characterized, however, the previously reported compound contained organic groups bonded to N, whereas all N atoms in **1** are only coordinated by metals.

Acknowledgements

Most of the experimental work in this chapter was done by Robert Gilley (under the supervision of R.J.W.), and Nobuyuki Yamamoto. R.G. crystallized and obtained elemental analysis of **1**. Other characterization of **1** was performed by N.Y. We thank Dr. Dale Chatfield for obtaining mass spectra.

This chapter contains material which is being prepared for submission. Yamamoto, Nobuyuki; Gilley, Robert N.; Wilson, Robert J.; Bennett, Miriam V. "Unprecedented Octanuclear Heterobimetallic-Nitrogen Compounds: Synthesis and Dehalostannylation of $[Bi_4N_4(SnMe_3)_4Cl_6]^{2-}$ to Afford $[Bi_4N_4(GaCl_3)_4]\cdot 6MeCN$" *Manuscript in preparation.*

References

(1) Nitta, M.; Mitsumoto, Y.; Yamamoto, H. *J. Chem. Soc., Perkin Trans. 1* **2001**, 1901.

(2) Matano, Y.; Nomura, H.; Suzuki, H. *Inorg. Chem.* **2002**, *41*, 1940.

(3) Mitsumoto, Y.; Nitta, M. *Bull. Chem. Soc. Jpn.* **2003**, *76*, 1029.

(4) Wirringa, U.; Roesky, H. W.; Noltemeyer, M.; Schmidt, H.-G. *Inorg. Chem.* **1994**, *33*, 4607.

(5) James, S. C.; Norman, N. C.; Orpen, A. G.; Quayle, M. J.; Weckenmann, U. *J. Chem. Soc., Dalton Trans.* **1996**, 4159.

(6) Evans, W. J.; Rego, D. B.; Ziller, J. W. *Inorg. Chim. Acta* **2007**, *360*, 1349.

(7) Michalik, D.; Schulz, A.; Villinger, A. *Angew. Chem., Int. Ed.* **2010**, *49*, 7575.

(8) Edwards, A. J.; Beswick, M. A.; Galsworthy, J. R.; Paver, M. A.; Raithby, P. R.; Rennie, M.-A.; Russell, C. A.; Verhorevoort, K. L.; Wright, D. S. *Inorg. Chim. Acta* **1996**, *248*, 9.

(9) Bickley, J. F.; Bond, A. D.; Garcia, F.; Jantos, K.; Lawson, G. T.; McPartlin, M.; Steiner, A.; Wright, D. S. *J. Chem. Soc., Dalton Trans.* **2002**, 4629.

(10) Shishido, K.; Kojima, S. *J. Org. Chem.* **1964**, *29*, 907.

(11) Sheldrick, G. *Acta Cryst.* **2008**, *A64*, 112.

(12) Macrae, C. F.; Bruno, I. J.; Chisholm, J. A.; Edgington, P. R.; McCabe, P.; Pidcock, E.; Rodriguez-Monge, L.; Taylor, R.; van de Streek, J.; Wood, P. A. *J. Appl. Crystallogr.* **2008**, *41*, 466.

(13) Strohalm, M.; Kavan, D.; Novak, P.; Volny, M.; Havlicek, V. *Anal. Chem.* **2010**, *82*, 4648.

(14) Slater, J. C. *J. Chem. Phys.* **1964**, *41*, 3199.

(15) Cucka, P.; Barrett, C. S. *Acta Crystallogr.* **1962**, *15*, 865.

(16) Ciani, G.; Moret, M.; Fumagalli, A.; Martinengo, S. *J. Organomet. Chem.* **1989**, *362*, 291.

(17) Monakhov, K. Y.; Zessin, T.; Linti, G. *Eur. J. Inorg. Chem.* **2010**, 3212.

(18) Stark, J. L.; Harms, B.; Guzman-Jimenez, I.; Whitmire, K. H.; Gautier, R.; Halet, J.-F.; Saillard, J.-Y. *J. Am. Chem. Soc.* **1999**, *121*, 4409.

(19) Kohata, K.; Fukuyama, T.; Kuchitsu, K. *J. Phys. Chem.* **1982**, *86*, 602.

(20) Appel, A.; Kober, C.; Neumann, C.; Noeth, H.; Schmidt, M.; Storch, W. *Chem. Ber.* **1996**, *129*, 175.

(21) Ahmed, I. A.; Blachnik, R.; Reuter, H. *Z. Anorg. Allg. Chem.* **2001**, *627*, 2057.

(22) Frank, W.; Reiland, V. *Acta Crystallographica Section C* **1998**, *54*, 1626.

(23) Conrad, E.; Burford, N.; McDonald, R.; Ferguson, M. J. *Chemical Communications* **2010**, *46*, 4598.

(24) Zaleski, J.; Glowiak, T.; Jakubas, R.; Sobczyk, L. *Journal of Physics and Chemistry of Solids* **1989**, *50*, 1265.

Appendix A: Structures of $[Me_3SnX_2]^{1-}$ (X = Cl, Br) Salts

Background

In the course of our investigations into reactions between various anionic metal halides and $(Me_3Sn)_3N$ we have crystallized several salts of the byproducts $[Me_3SnX_2]^-$ (X = Cl (**1**), Br (**2**)). We discovered that only 18 salts of these anions have been reported, none of which included the examples produced by our research. The structural data of these byproducts is presented here.

X-ray Structure Determination

Crystals were coated in Paratone oil and mounted by mean of a glass capillary fiber on a Bruker APEX-II CCD area detector instrument operated by the APEX software package. Data reduction was performed by SAINT, absorption correction was applied using SADABS, and the space group was assigned using XPREP. Structure were solved by direct methods and refined against all data by full-matrix least squares on F_2. Hydrogen atoms were attached at idealized positions on carbon atoms and were refined as riding atoms with uniform isotropic thermal parameters. Structure solution, refinement, graphics and report generation were performed using SHELXTL[1] and Mercury.[2]

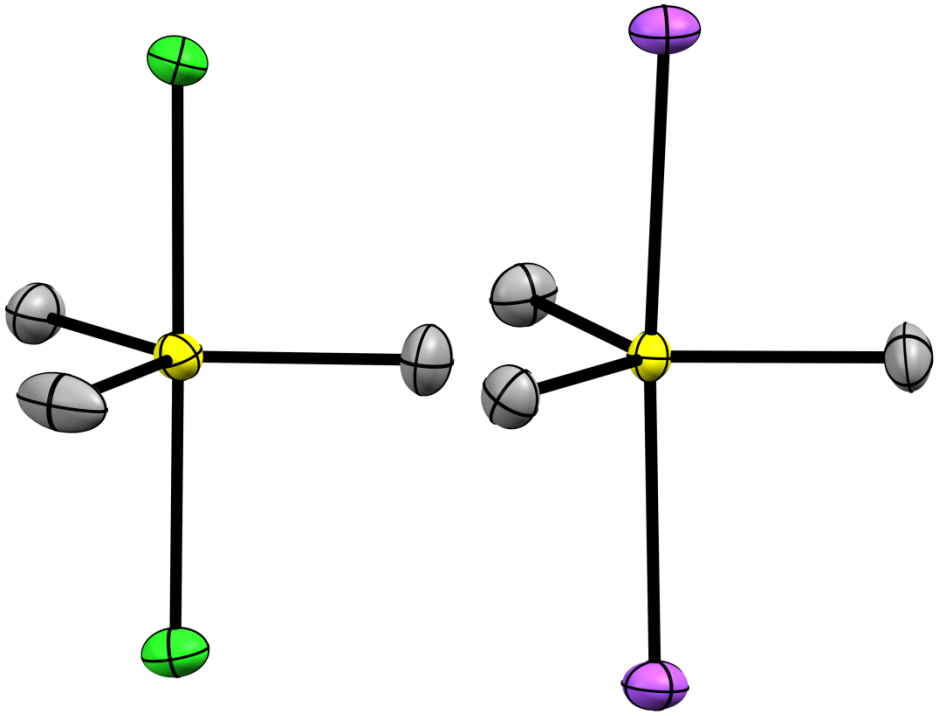

Figure A.1. Crystal structures of $[Me_3SnX_2]^-$ (X = Cl (1), Br (2)) with thermal ellipsoids set at 50% probability. The cations (Ph_4P^+ for the above examples) and hydrogen atoms have been omitted for clarity.

Table A.1. Crystallographic data for salts of $[Me_3SnCl_2]^-$ (1).

	(Et_4N)**1**	$(Bu^n{}_4N)$**1**	$(Bu^n{}_4N)$**1**· dioxane	(Ph_4P)**1**
formula	$C_{11}H_{29}Cl_2NSn$	$C_{19}H_{45}Cl_2NSn$	$C_{23}H_{53}Cl_2NO_2Sn$	$C_{27}H_{29}Cl_2PSn$
form. weight	364.94	477.15	565.25	574.06
cryst. syst.	monoclinic	triclinic	monoclinic	monoclinic
space group	*C*2	$P\bar{1}$	$P2_1/c$	$P2_1/c$
a, Å	12.373(4)	10.4380(6)	11.2059(11)	13.0799(3)
b, Å	6.691(2)	10.8593(6)	13.1746(13)	7.5669(2)
c, Å	11.614(4)	13.0913(11)	20.830(2)	26.1051(6)
α, deg	90	102.696(4)	90	90
β, deg	119.467(11)	105.888(4)	90.196(5)	90.8100(10)
γ, deg	90	111.543(2)	90	90
V, Å^3	837.1(5)	1239.50(14)	3075.2(5)	2583.48(11)
Z	2	2	4	4
ρ_{calc}, g/cm^3	1.448	1.278	1.221	1.476
2θ range, deg	3.30 to 28.26	1.73 to 28.28	3.64 to 57.4	3.12 to 52.8
GOF (F^2)	1.072	1.05	1.134	1.045
R_1/wR_2, %	1.12/2.86	2.47/5.77	3.04/5.58	2.48/5.53
largest peak/hole (e^-/Å^3)	0.256/-0.322	1.536/-0.408	0.78/-0.82	0.60/-0.37
Flack *x* parameter	0.051(15)			

Table A.2. Selected bond lengths (Å) and angles (°) for salts of $[Me_3SnCl_2]^{1-}$ (1).

	(Et_4N)**1**	(Bu^n_4N)**1**	(Bu^n_4N)**1**·dioxane	(Ph_4P)**1**
Sn1–Cl1	2.6223(9)	2.6211(5)	2.6339(8)	2.5894(6)
Sn1–Cl2	2.6223(9)[a]	2.6210(5)	2.6141(8)	2.5945(6)
Sn1–C1	2.1285(17)	2.1265(19)	2.120(3)	2.132(2)
Sn1–C2	2.129(3)	2.129(2)	2.120(3)	2.135(2)
Sn1–C3	2.1285(17)[b]	2.128(2)	2.116(3)	2.132(2)
Cl1–Sn1–Cl2	178.83(6)[a]	176.064(16)	178.12(2)	179.26(2)
C1–Sn1–C2	118.89(5)	122.51(8)	124.59(15)	117.23(12)
C2–Sn1–C3	118.89(5)[b]	118.10(9)	120.58(13)	124.34(10)
C1–Sn1–C3	122.21(11)[b]	119.39(9)	114.84(14)	118.42(12)
C1–Sn1–Cl1	89.16(5)	89.26(6)	89.73(12)	89.94(7)
C1–Sn1–Cl2	90.28(5)[a]	87.09(6)	88.47(12)	90.00(7)
C2–Sn1–Cl1	90.58(3)	89.10(6)	89.51(13)	89.95(7)
C2–Sn1–Cl2	90.58(3)[a]	91.63(6)	91.05(13)	89.42(7)
C3–Sn1–Cl1	90.28(5)[b]	91.33(8)	91.02(10)	91.13(7)
C3–Sn1–Cl2	89.16(5)[a,b]	91.75(8)	90.24(10)	89.55(7)

[a] Cl2 = Cl1′ [b] C3 = C1′

Table A.3. Crystallographic data for salts of $[Me_3SnBr_2]^{1-}$ (2).

	(Et_4N)**2**	(Ph_4P)**2**	$(MePh_3P)$**2**
formula	$C_{11}H_{29}Br_2NSn$	$C_{27}H_{29}Br_2PSn$	$C_{22}H_{27}Br_2PSn$
form. weight	453.86	662.98	600.92
cryst. syst.	tetragonal	monoclinic	orthorhombic
space group	$P\bar{4}2_1m$	$P2_1/c$	$Pbca$
a, Å	11.2378(14)	9.564(2)	16.8382(11)
b, Å	11.2378(14)	21.119(5)	14.1311(9)
c, Å	6.9226(9)	13.598(3)	41.310(3)
α, deg	90	90	90
β, deg	90	106.284(11)	90
γ, deg	90	90	90
V, Å^3	874.24(19)	2636.5(11)	9829.4(11)
Z	2	4	16
ρ_{calc}, g/cm^3	1.724	1.670	1.624
2θ range, deg	2.56 to 30.51	1.93 to 29.57	1.94 to 28.28
GOF (F^2)	1.123	1.039	1.02
R_1/wR_2, %	1.86/4.69	2.21/4.77	3.48/5.97
largest peak/hole (e^-/Å^3)	0.257/-1.179	0.663/-0.483	0.892/-0.623

Table A.4. Selected bond lengths (Å) and angles (°) for salts of $[Me_3SnBr_2]^{1-}$ (2).

	(Et_4N)**2**	(Ph_4P)**2**	$(MePh_3P)$**2**[a]
Sn1–Br1	2.8049(4)	2.7956(6)	2.7772(4)
Sn1–Br2	2.8049(4)[b]	2.7710(6)	2.7940(4)
Sn1–C1	2.120(3)	2.1389(18)	2.139(3)
Sn1–C2	2.120(4)	2.1293(19)	2.143(3)
Sn1–C3	2.120(3)[c]	2.1348(19)	2.124(3)
Br1–Sn1–Br2	179.152(19)	175.056(7)	177.051(14)
C1–Sn1–C2	119.76(13)	118.04(8)	118.45(17)
C2–Sn1–C3	120.5(3)[c]	119.86(8)	118.91(16)
C1–Sn1–C3	120.5(3)[c]	121.91(8)	122.51(16)
C1–Sn1–Br1	89.790(5)	87.21(6)	89.09(10)
C1–Sn1–Br2	89.790(5)[b]	91.66(6)	89.80(10)
C2–Sn1–Br1	90.424(9)	90.99(6)	90.21(11)
C2–Sn1–Br2	90.424(9)[b]	93.79(6)	92.72(11)
C3–Sn1–Br1	89.790(5)[c]	87.52(6)	87.14(10)
C3–Sn1–Br2	89.790(5)[b,c]	89.00(6)	91.15(10)

[a] Values for one of the two formula units present in the asymmetric unit. [b] Br2 = Br1′.

[c] C3 = C1′.

References

(1) Sheldrick, G. *Acta Cryst.* **2008**, *A64*, 112.

(2) Macrae, C. F.; Bruno, I. J.; Chisholm, J. A.; Edgington, P. R.; McCabe, P.; Pidcock, E.; Rodriguez-Monge, L.; Taylor, R.; van de Streek, J.; Wood, P. A. *J. Appl. Crystallogr.* **2008**, *41*, 466.

Appendix B: Synthesis of $[MX_4]^{1-}$ (M = Ga, In; X = Cl, Br) and $[InCl_5]^{2-}$ Salts

Background

This appendix details the syntheses of tetraalkylammonium and tetraphenylphosphonium salts of $[GaCl_4]^-$ (**1**), $[GaBr_4]^-$ (**2**), $[InCl_4]^-$ (**3**), and $[InCl_5]^{2-}$ (**4**), which were used in this research. Many of these are modifications of literature procedures. In addition we report the crystal structures of (Pr^n_4N)**1** and (Pr^n_4N)**3** which are not present in the literature.

Preparation of Compounds

Reactions requiring the use of acid were performed in open air in a fume hood. All other manipulations were carried out under a pure dinitrogen atmosphere in a glove-box. Anhydrous tetrahydrofuran (THF), purchased from EMD, diethylether (Et_2O), purchased from EMD, and acetonitrile (MeCN), purchased from Burdick and Jackson were stored over activated 4 Å molecular sieves under a pure dinitrogen atmosphere. $GaCl_3$ (Alfa Aesar, 99.999%), $GaBr_3$ (Alfa Aesar, 99.99%), $InCl_3$ (J.T. Baker, 99.99%), and $BiCl_3$ (Alfa Aesar, 99.997%) were stored under a pure dinitrogen atmosphere and used as received. The salts (Me_4N)Cl (Alfa Aesar, 97%), (Et_4N)Cl·H_2O (Alfa Aesar, 98%), (Pr^n_4N)Cl (ACROS, 94%), (Ph_4P)Cl (ACROS, 98%), (Me_4N)Br (Alfa Aesar, 98%), (Ph_4P)Br (Alfa Aesar, 98%) were dried *in vacuo* at 100 ºC before being stored under a dinitrogen atmosphere. Elemental analysis was performed at the Ecology Analytical Laboratory at San Diego State University.

(Ph_4P)[$GaCl_4$]. A solution of $GaCl_3$ (1.25 g, 7.12 mmol) in 10 mL of concentrated HCl was added to a solution of (Ph_4P)Cl (2.72 g, 7.10 mmol) in 15 mL of EtOH immediately producing a white precipitate. The mixture was placed in an ice bath and stirred for 20 minutes then collected by filtration and washed with successive aliquots of cold EtOH (3 × 10mL) followed by cold Et_2O (3 × 10mL) then dried *in vacuo* to yield 2.87g (5.20 mmol, 73%) of crude (Ph_4P)[$GaCl_4$]. Under a pure dinitrogen atmosphere, the crude product was dissolved in 16 mL of anhydrous MeCN and filtered through celite. Upon slow diffusion with Et_2O, pale cream colored, rod shaped crystals formed, which were washed with successive aliquots of Et_2O (3 x 5 mL) and dried to afford 2.18 g (3.95 mmol, 56%) of (Ph_4P)[$GaCl_4$]. Anal. Calcd (%) for $C_{24}H_{20}Cl_4GaP$: C, 52.32; H, 3.66. Found: C, 51.75; H, 3.66.

(Me_4N)[$GaCl_4$]. A solution of $GaCl_3$ (3.36 g, 19.1 mmol) in 10 mL of concentrated HCl (use caution when adding HCl to $GaCl_3$, pour slowly!) was added to a solution of (Me_4N)Cl (2.14 g, 19.0 mmol) in 20 mL of concentated HCl immediately producing a white precipitate. The mixture was stirred in an ice bath for 20 minutes, after which the precipitate was collected by filtration and washed with successive aliquots of concentrated HCl (2 × 10 mL), cold EtOH (3 × 10 mL), and Et_2O (3 × 10 mL) respectively. The white solid was dried for 12 h *in vacuo* to yield 4.47 g (15.6 mmol, 82%) of crude (Me_4N)[$GaCl_4$]. The crude product was dissolved in 12 mL of anhydrous MeCN under a pure N_2 atmosphere, filtered through celite, and recrystallized by diffusion with Et_2O. The resulting white crystals were washed with

successive aliquots of ether (3 x 5 mL) and dried to yield 3.46 g (12.1 mmol, 64%) of $(Me_4N)[GaCl_4]$. Anal. calcd for $C_4H_{12}Cl_4GaN$: C, 16.82; H, 4.23; N, 4.90. Found: C, 16.69; H, 3.99; N, 5.05.

$(Et_4N)[GaCl_4]$. A solution of $GaCl_3$ (1.78 g, 10.1 mmol) in 10 mL of concentrated HCl (use caution when adding HCl to $GaCl_3$, pour slowly!) was added to a solution of $(Et_4N)Cl$ (1.68 g, 10.1 mmol) in 10 mL of concentrated HCl immediately producing a white precipitate. The precipitate was collected by filtration and washed with successive aliquots of concentrated HCl (3 × 10 mL), cold EtOH (3 × 10 mL), and Et_2O (5 × 10 mL) respectively. The white solid was dried *in vacuo* to yield 2.57 g (7.52 mmol, 74%) of crude $(Et_4N)[GaCl_4]$. The crude product was dissolved in 6 mL of anhydrous MeCN under a pure N_2 atmosphere, filtered through celite, and recrystallized by diffusion with Et_2O. The resulting white crystals were washed with successive aliquots of Et_2O (3 x 5 mL) and dried to yield 2.28 g (6.68 mmol, 66%) of $(Et_4N)[GaCl_4]$. Anal. calcd for $C_8H_{20}Cl_4GaN$: C, 28.11; H, 5.90; N, 4.10. Found: C, 27.56; H, 5.06; N, 4.57.

$(Pr^n_4N)[GaCl_4]$. A solution of $GaCl_3$ (2.85 g, 16.2 mmol) in 10 mL of concentrated HCl (use caution when adding HCl to $GaCl_3$, pour slowly!) was added to a solution of $(Pr^n_4N)Cl$ (Acros, 94%) (3.76 g, 15.9 mmol) in 15 mL of conc. HCl immediately yielding a white precipitate. The mixture was stirred in an ice bath for 30 minutes, after which the white precipitate was collected by filtration and washed with

conc. HCl (1 × 10 mL), cold EtOH (3 × 10 mL), and cold Et_2O (3 × 10 mL) respectively. The solid was dried *in vacuo* to yield 5.55 g of crude $(Pr^n_4N)[GaCl_4]$ (14.0 mmol, 88%), which was dissolved in 10 mL of MeCN, filtered through celite, and recrystallized by diffusion with Et_2O. The resulting white crystals were washed with aliquots of Et_2O (3 × 3 mL) and dried to afford 3.06 g of $(Pr^n_4N)[GaCl_4]$ (7.68 mmol, 48%). Anal. calcd for $C_{12}H_{28}Cl_4GaN$: C, 36.22; H, 7.09; N, 3.52. Found: C, 35.91; H, 6.98; N, 3.48.

$(Et_4N)[InCl_4]$. A solution of $(Et_4N)Cl$ (0.79 g, 4.8 mmol) and $InCl_3$ (1.0 g, 4.7 mmol) in 8.9 mL of THF was stirred for 30 min then filtered through celite. Diffusion of Et_2O into the solution afforded colorless trigonal prismatic crystals of $(Et_4N)[InCl_4]$. The unit cell of the sample was matched to the literature values.[1]

$(Et_4N)_2[InCl_5]$. A solution of $(Et_4N)Cl$ (1.04 g, 6.28 mmol) in 10 mL of anhydrous MeCN was added to a solution of $InCl_3$ (0.69 g, 3.1 mmol) in 10 mL of MeCN. The resulting colorless solution was filtered through celite. Vapor diffusion with Et_2O afforded colorless block shaped crystals of $(Et_4N)_2[InCl_5]$ which were collected by filtration and washed with Et_2O (3 × 5 mL) to give 1.35 g (2.44 mmol, 79%) of product. Anal. calcd for $C_{16}H_{40}Cl_5InN$: C, 34.78; H, 7.30; N, 5.07. Found: C, 34.70; H, 7.17; N, 5.04.

$(Me_4N)[GaBr_4]$. A solution of $GaBr_3$ (1.36 g, 4.41 mmol) in 5 mL of concentrated HBr was added to a solution of $(Me_4N)Br$ (0.72 g, 4.7 mmol) in 5 mL of concentated HBr immediately producing a white precipitate. The mixture was stirred in an ice bath for 20 minutes, after which the precipitate was collected by filtration and washed with successive aliquots of concentrated HBr (3 × 5 mL) and Et_2O (5 × 10 mL) respectively. The orange solid was dried for 12 h *in vacuo* to yield 0.50 g of crude $(Me_4N)[GaBr_4]$. The crude product was recrystallized twice from MeCN by diffusion with Et_2O. The resulting white-orange crystals were washed with successive aliquots of ether (3 x 5 mL) and dried to yield 0.13 g (0.29 mmol, 7%) of $(Me_4N)[GaBr_4]$. Anal. calcd for $C_4H_{12}Br_4GaN$: C, 10.37; H, 2.61; N, 3.02. Found: C, 10.41; H, 2.61; N, 3.06.

$(Ph_4P)[GaBr_4]$. A solution of $GaBr_3$ (0.84 g, 2.7 mmol) in 5 mL of EtOH was added to a solution of $(Ph_4P)Br$ (1.1 g, 2.6 mmol) in 10 mL of EtOH immediately producing a white precipitate. The mixture was placed in an ice bath and stirred for 30 min then collected by filtration and washed with successive aliquots of cold EtOH (3 × 5 mL) and cold Et_2O (3 × 5 mL) then dried *in vacuo* and recrystallized from MeCN/Et_2O to afford 0.97 g (1.3 mmol, 50%) of $(Ph_4P)[GaBr_4]$. Anal. Calcd (%) for $C_{24}H_{20}Br_4GaP$: C, 39.56; H, 2.77. Found: C, 39.11; H, 2.77.

$(Pr^n_4N)_3[Bi_2Cl_9]$. A solution of $(Pr^n_4N)Cl$ (0.14 g, 0.45 mmol) in 2 ml of MeCN was added to a solution of $BiCl_3$ (0.11 g 0.30 mmol) in 3 ml of MeCN,

resulting in a clear solution. The solution was filtered through celite. Diffusion of Et_2O into the filtrate afforded a large amount of colorless crystals after 5 days. The crystals were collected by filtration, washed with successive aliquots of THF (3 × 10 mL) and Et_2O (3 × 5 mL), and dried *in vacuo* to afford 0.20 g of $(Pr^n_4N)_3[Bi_2Cl_9]$ (80%). ES^--MS (MeCN): *m*/*z* 888 ($(Pr^n_4N)[Bi_2Cl_9]^-$). Analysis calcd for $C_{36}H_{84}Bi_2Cl_9N_3$: C, 33.36; H, 6.53; N, 3.24. Found: C, 33.65; H, 6.29; N, 3.09.

X-ray Structure Determination

Crystals were coated in Paratone oil and mounted by mean of a glass capillary fiber on a Bruker APEX-II CCD area detector instrument operated by the APEX software package. Data reduction was performed by SAINT, absorption correction was applied using SADABS, and the space group was assigned using XPREP. Structure were solved by direct methods and refined against all data by full-matrix least squares on F_2. Hydrogen atoms were attached at idealized positions on carbon atoms and were refined as riding atoms with uniform isotropic thermal parameters. Structure solution, refinement, graphics and report generation were performed using SHELXTL[2] and Mercury.[3]

Table B.1. Crystallographic data for (Pr^n_4N)[MCl_4] (M = Ga (1), In (3))

	(Pr^n_4N)**1**	(Pr^n_4N)**3**
formula	$C_{12}H_{28}Cl_4GaN$	$C_{12}H_{28}Cl_4InN$
form. weight	397.87	442.97
cryst. syst.	100	100
space group	*Pbca*	*Pbca*
a, Å	13.5961(9)	13.6641(3)
b, Å	16.3971(11)	16.4584(4)
c, Å	17.2433(11)	17.4154(4)
α, deg	90	90
β, deg	90	90
γ, deg	90	90
V, Å^3	3844.2(4)	3916.54(16)
Z	8	8
ρ_{calc}, g/cm^3	1.375	1.503
2θ range, deg	2.48 to 28.32	2.26 to 34.97
GOF (F^2)	0.998	1.025
R_1/wR_2, %	3.24/5.26	3.03/6.89
largest peak/hole (e^-/Å^3)	0.397/-0.283	1.534/-0.538

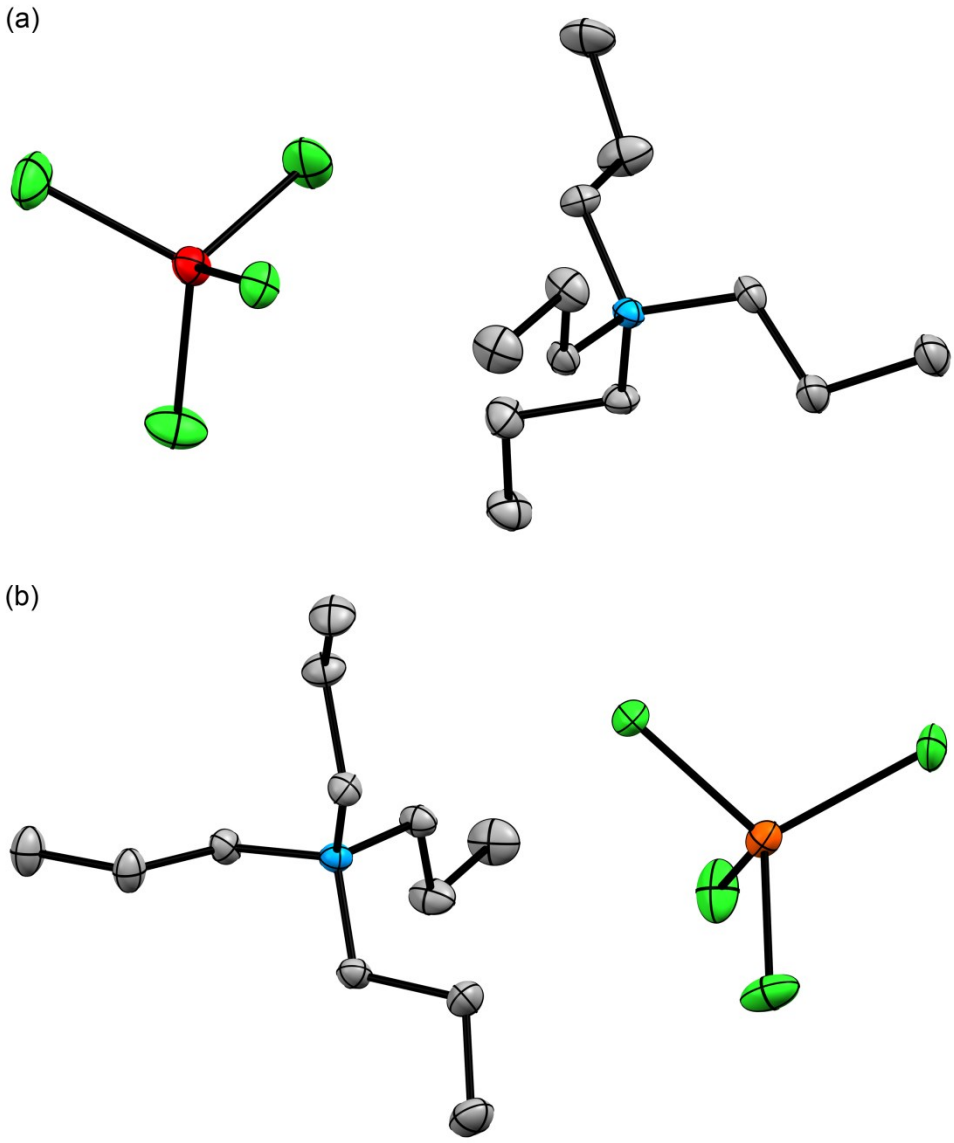

Figure B.1. Structures of (a) (Pr^n_4N)1 and (b) (Pr^n_4N)3 with thermal ellipsoids set at 50% probability; $[MCl_4]^-$ (M = Ga (1), In (3)); red = Ga, orange = In, green = Cl, blue = N, gray = C. Hydrogen atoms have been omitted for clarity.

Table B.2. Selected bond lengths (Å) and angles (°) for (Pr^n_4N)[MCl_4] (M = Ga (1), In (3)).

	(Pr^n_4N)**1**	(Pr^n_4N)**3**
M–Cl1	2.1819(6)	2.3574(5)
M–Cl2	2.1786(6)	2.3575(6)
M–Cl3	2.1721(7)	2.3776(5)
M–Cl4	2.1650(6)	2.3509(5)
M–Cl (mean)	2.174(7)	2.36(1)
Cl1–M–Cl2	107.86(3)	107.12(2)
Cl1–M–Cl3	109.34(3)	109.020(18)
Cl1–M–Cl4	110.36(2)	111.329(19)
Cl2–M–Cl3	108.71(3)	108.15(2)
Cl2–M–Cl4	109.09(3)	108.54(2)
Cl3–M–Cl4	111.40(3)	112.50(2)

References

(1) Trotter, J.; Einstein, F. W. B.; Tuck, D. G. *Acta Crystallogr., Sect. B* **1969**, *25*, 603.

(2) Sheldrick, G. *Acta Cryst.* **2008**, *A64*, 112.

(3) Macrae, C. F.; Bruno, I. J.; Chisholm, J. A.; Edgington, P. R.; McCabe, P.; Pidcock, E.; Rodriguez-Monge, L.; Taylor, R.; van de Streek, J.; Wood, P. A. *J. Appl. Crystallogr.* **2008**, *41*, 466.